الجمهورية الجزائرية الديمقراطية الشعبية
République Algérienne Démocratique et populaire
وزارة التعليم العالي و البحث العلمي
Ministère de l'enseignement supérieur et de la recherche scientifique

Université Mohamed Khider – Biskra
Faculté des Sciences et de la technologie
Département de Génie Civil et Hydraulique
Réf : ……

جامعة محمد خيضر بسكرة
كلية العلوم و التكنولوجيا
قسم الهندسة المدنية و الري
المرجع:.....

Thèse de Doctorat LMD

Spécialité : GÉNIE CIVIL

Option : MATÉRIAUX DE CONSTRUCTION

Réhabilitation et réparation des bétons après incendie

Présentée par :

DRIDI Meriem

Soutenue publiquement le : 24/09/ 2023.

Devant le jury composé de :

Dr. CHADLI Mounira	**Maitre de Conférences 'A'**	**Président**	**Université de Biskra**
Pr. HACHEMI Samya	**Professeur**	**Rapporteur**	**Université de Biskra**
Pr. BENAMARA Dalila	**Professeur**	**Examinateur**	**Université de Djelfa**
Pr. TEBBAL Nadia	**Professeur**	**Examinateur**	**Université de M'sila**

الجمهورية الجزائرية الديمقراطية الشعبية
People's Democratic Republic of Algeria
وزارة التعليم العالي و البحث العلمي
Ministry of Higher Education and Scientific Research

Mohamed KhiderUniversity – Biskra
Faculty of Science and Technology
Department of Civil and Hydraulics Engineering
Ref:……

جامعة محمد خيضر بسكرة
كلية العلوم و التكنولوجيا

قسم الهندسة المدنية و الري
المرجع :.....

Thesis presented with a view to obtaining

LMD doctorate in Civil Engineering

Option: CONSTRUCTION MATERIALS

Rehabilitation and repair of concretes after fire

Presented by :

DRIDI Meriem

Publicly supported on: 24 /09/2023.

The jury composed of:

Dr. CHADLI Mounira	**Lecturer 'A'**	**President**	**University of Biskra**
Pr. HACHEMI Samya	**Professor**	**Supervisor**	**University of Biskra**
Pr. BENAMARA Dalila	**Professor**	**Examiner**	**University of Djelfa**
Pr. TEBBAL Nadia	**Professor**	**Examiner**	**University of M'sila**

ACKNOWLEDGMENTS

*Dear **Prof. Samya Hachemi**, I would like to express my heartfelt gratitude for your guidance and support throughout my thesis journey. Your invaluable knowledge, expertise, and encouragement have played a pivotal role in my academic growth and accomplishments.*

Prof. Hachemi, I deeply appreciate your mentorship and unwavering support. Your expertise and advice have provided me with a deeper understanding of the subject matter and have instilled confidence in conducting my research.

*I would also like to extend my profound thanks to the **members of the jury** for dedicating their time to evaluate my work and provide valuable feedback. Your ideas and suggestions have shaped my thesis and enhanced my comprehension of the subject.*

*Furthermore, I am immensely grateful to the **laboratory members** and **administrative staff**, including the **department head** at the **University of Bordj Bou Arreridj**, who opened their doors to facilitate my experimental work. I would also like to express my gratitude to the staff at the **LARGHYDE laboratory** at the **University of Biksra** for their invaluable scientific assistance.*

*Once again, I want to convey my sincerest appreciation to **Professor Hachemi** for your continuous support and guidance throughout this process. Your contribution to my success will always be cherished and remembered.*
A big thank you, to my Dear PARENTS for their sacrifices and their permanent encouragement, which God protects. my dear husband and my daughter.

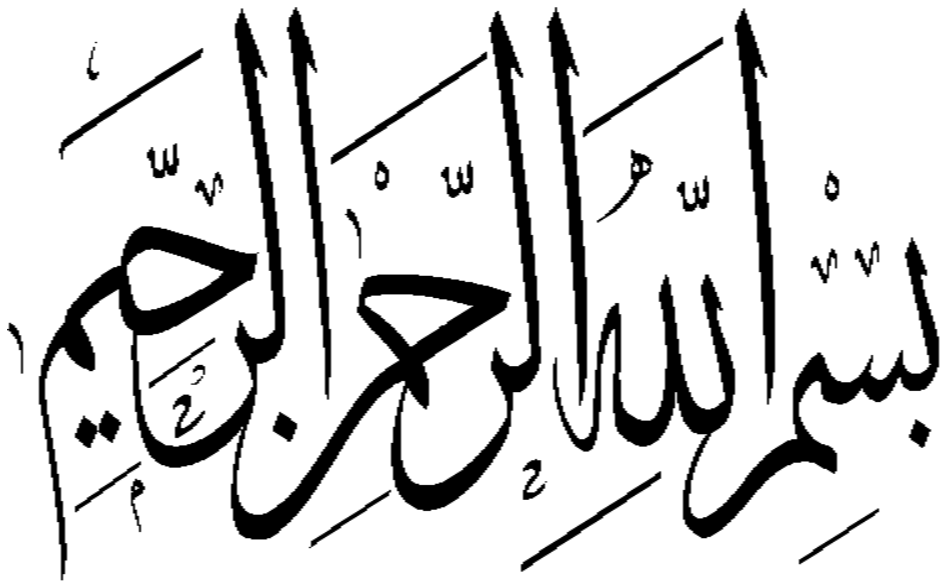
بسم الله الرحمن الرحيم

ABSTRACT

Many concrete structures have been subjected to high temperatures. If the demolition of the structure and its reconstruction can be accompanied by higher costs, reinforcement of the element is a well-known solution to maintain its operation. Mortar-polymer composites are widely used in industry for the protection and/or repair applications of concrete surfaces. Indeed, the addition of polymer in mortar formulations allows modifying the properties of these materials, particularly by favoring their adhesion while reducing their permeability. However, these materials are applied to repair much more concrete that is cracked or degraded due to chemical attack or mechanical shock. In addition, fire damage to concrete is often very detrimental, therefore requiring repair. This thesis aims to study the behavior of polymer-mortar composites applied to concrete degraded due to fire. To this end, studies were first carried out to better understand the properties of the newly prepared polymer-mortar composites. A setting retarder effect was evidenced by adding polymers to the cement paste formulation. It was partially attributed to the adsorption of polymer particles on the surface of cement grains, but mainly to the complexation of calcium ions from the interstitial solution by polymers which are then hydrolyzed. Then, the polymer-mortar composites were reinforced with different fibers (hemp and glass) to improve their mechanical and physical behavior.

Tests have shown that the presence of fibers in polymer mortars significantly increases the compressive strength, bending and adhesion. In addition, blends that contain 0.5% hemp or 0.3% glass in a matrix containing 5% of polymer (styrene-butadiene rubber) have the best physical and mechanical properties.

In the second part, studies were carried out on the repair of concrete subjected to a high temperature of 750°C. In the first case, the results show a remarkable effect of the concretes repaired by the polymer mortars made at the laboratory level. In the second case, the results showed that the concretes repaired with polymer-mortar behave similarly to marketed mortars. Through the image analysis, different zones of damage in the repaired concrete were identified, and specific colors associated with various stresses were analyzed. This analysis provides valuable insights into the strengths and weaknesses of the material, aiding in the understanding of its behavior under different loading conditions.

Keywords: reparation, high temperatures, mortar, hemp fibers, glass fibers, polymer.

RESUME

Des températures élevées ont affecté plusieurs structures en béton, et bien que démolir et reconstruire ces structures puissent être plus coûteux, le renforcement est une option courante pour préserver leur fonctionnalité. Les composites polymère-mortier sont largement utilisés pour protéger et réparer les surfaces en béton, car l'ajout de polymère aux formulations de mortier peut améliorer leur adhésion tout en réduisant leur perméabilité. Cependant, ces composites sont souvent utilisés pour réparer des bétons plus fissurés ou endommagés par une attaque chimique ou un choc mécanique. Les dommages causés par le feu au béton sont souvent graves et nécessitent une réparation. Le but de cette étude est d'examiner le comportement des composites de mortier de polymère lorsqu'ils sont utilisés pour réparer des bétons endommagés par un incendie. Des recherches ont été menées pour mieux comprendre les propriétés des composites de mortier de polymère fraîchement préparés, et il a été démontré qu'ajouter des polymères à la formulation du ciment peut ralentir la prise, principalement en raison de l'adsorption de particules de polymère sur la surface des grains de ciment et de la complication des ions de calcium de la solution interstitielle. Les composites polymère-mortier ont également été renforcés avec des fibres de chanvre et de verre pour améliorer leur comportement mécanique et physique, et les tests ont montré que ces fibres augmentent considérablement leur résistance à la compression, la flexion et leur adhésion. Les mélanges contenant 0,5% de fibre de chanvre ou 0,3% de fibres verre dans une matrice de 5% de polymère ont les meilleures propriétés. Des études ont également été menées sur la réparation de bétons soumis à des températures de 750°C, et les résultats montrent que les bétons réparés avec les composites polymère-mortier préparés en laboratoire se comportent bien, tout comme les bétons réparés avec les mortiers commercialisés.

Grâce à l'analyse d'image, différentes zones de dommages dans le béton réparé ont été identifiées, et des couleurs spécifiques associées à diverses contraintes ont été analysées. Cette analyse fournit des informations précieuses sur les forces et les faiblesses du matériau, aidant à la compréhension de son comportement dans différentes conditions de charge.

Mots clés : réparation, hautes températures, mortier, fibres de chanvre, fibres de verre, polymère.

ملخص

تتعرض العديد من الهياكل الخرسانية لارتفاع درجات الحرارة. في حالة كان بإمكان هدم الهيكل وإعادة بنائه يترتب عليه تكاليف أعلى، يُعتبر تعزيز العنصر خيارًا معروفًا وفعّالًا للحفاظ على جاهزيته واستدامته. تُستخدم مركبات الملاط المعززة بالبوليمر بشكل واسع في الصناعة لحماية الأسطح الخرسانية وإصلاحها إذا دعت الحاجة. فعلى وجه الخصوص، يسمح إضافة البوليمر إلى تركيبات الملاط بتعديل خصائص هذه المواد، بما في ذلك تعزيز قدرتها على الالتصاق وتقليل نفاذيتها.

ومع ذلك، تُستخدم هذه المواد على نطاق واسع لإصلاح الخرسانة المتضررة بسبب التشقق أو التدهور الناتج عن التآكل الكيميائي أو الصدمات الميكانيكية. بالإضافة إلى ذلك، يعتبر التلف الناجم عن الحرائق للخرسانة أمرًا خطيرًا بشكل كبير، مما يجعل الإصلاح ضروريًا. تهدف هذه الأطروحة إلى دراسة تصرف مركبات الملاط المعززة بالبوليمر عند تطبيقها على الخرسانة المتدهورة نتيجة للحرائق. ومن أجل ذلك، تم إجراء دراسات أولية لفهم خصائص مركبات الملاط المعززة بالبوليمر المعدة حديثًا بشكل أفضل. تم اكتشاف تأثير تأخير التصلب عند إضافة البوليمرات إلى تركيبة معجون الإسمنت. ورُبِط هذا التأخير جزئيًا بامتصاص جزيئات البوليمر على سطح حبيبات الإسمنت، ولكن السبب الرئيسي يعود إلى تعقيد أيونات الكالسيوم في المحلول الفواصلي بواسطة البوليمرات التي تتحلَّل بعد ذلك. ثم تم تعزيز مركبات الملاط المعززة بالبوليمر بألياف مختلفة (قنب وزجاج) لتحسين أدائها الميكانيكي والفيزيائي.

أظهرت الاختبارات أن وجود الألياف في الملاط المعزز بالبوليمر يزيد بشكل كبير من قوة الضغط والانثناء والالتصاق. بالإضافة إلى ذلك، تظهر المزجات التي تحتوي على 0.5% من ألياف القنب أو 0.3% من ألياف الزجاج والتي تحتوي ايضا على 5% من البوليمر (اللاتكس الاستريني-البيوتادايين) بأفضل الخصائص الفيزيائية والميكانيكية.

في الجزء الثاني، تمت إجراء دراسات حول إصلاح الخرسانة التي تعرضت لدرجة حرارة عالية تصل إلى 750 درجة مئوية. في الحالة الأولى، تُظهر النتائج تأثيرًا ملحوظًا للخرسانات التي تم إصلاحها باستخدام مركبات الملاط المعززة بالبوليمر المُعدة على مستوى المختبر.

في الحالة الثانية، أظهرت النتائج أن الخرسانة التي تم إصلاحها بواسطة مركبات الملاط المعززة بالبوليمر تتصرف بشكل مماثل للملاط المتوفر في الأسواق.

من خلال تحليل الصور، تم التعرف على مناطق مختلفة من التلف في الخرسانة المصلحة، وتم تحليل الألوان المحددة المرتبطة بمجموعة متنوعة من الضغوط. يقدم هذا التحليل رؤى قيمة حول مزايا وعيوب المادة، مما يساعد في فهم سلوكها تحت ظروف التحميل المختلفة.

الكلمات المفتاحية: إصلاح، درجات حرارة عالية ، ملاط ، ألياف قنب ، ألياف زجاجية ، بوليمر.

Table of Contents

CHAPTER III:

CHARACTERIZATION OF BASE MATERIALS AND TEST METHODOLOGY

Figure list

CHAPTER I: THE BEHAVIOR OF CONCRETE AT HIGH TEMPERTURES

CHAPTER II: STATE OF THE ART ON REPAIR MATERIALS CASE STUDY: CONCRETE SUBJECTED TO HIGH TEMPERATURE

CHAPTER III: CHARACTERIZATION OF BASE MATERIALS AND TEST METHODOLOGY

CHAPTER IV: RESULTS AND DISCUSSIONS

Table list

CHAPTER I: THE BEHAVIOR OF CONCRETE AT HIGH TEMPERTURES

CHAPTER III: CHARACTERIZATION OF BASE MATERIALS AND TEST METHODOLOGY

CHAPTER IV: RESULTS AND DISCUSSIONS

GENERAL INTRODUCTION

General introduction

Concrete is a prevalent construction and engineering material utilized in numerous national bridges and tunnels. Nevertheless, despite its widespread application, concrete structures are vulnerable to thermal shocks, necessitating substantial maintenance and rehabilitation expenses. Consequently, clients are actively seeking solutions to protect and repair concrete surfaces. One such solution involves the utilization of hydraulic binders, specifically mortar-polymer composite materials, which incorporate polymers in varying proportions. These materials exhibit exceptional strength and adhesion capabilities, attributable to the formation of a polymer/cement co-matrix. However, despite a comprehensive understanding of the properties of these materials, the challenges encountered on construction sites are often overlooked in the study of polymer mortar composites.

Typically, studies focusing on modified mortars primarily concentrate on specimens that have undergone mechanical or chemical degradation. However, it is important to note that these specimens can also be exposed to high temperatures during the curing process, which plays a vital role in the formation of a polymer/cement co-matrix. Unfortunately, the curing conditions experienced at construction sites may not always be ideal, resulting in premature drying and potential alterations in material properties prior to hardening. Presently, the full extent of the impact of these environmental conditions on the behavior of mortar-polymer composites remains insufficiently understood. Hence, the objective of this thesis is to delve deeper into comprehending how polymers influence the behavior of fiber-reinforced mortar-polymer composites, particularly in the context of high temperature concrete repair applications.

The primary objective of this research is to optimize the formulation of mortar-polymer composites for the repair of concrete structures subjected to thermal shock. Additionally, the study investigates the behavior of these composite materials when interacting with damaged concrete.

The laboratory tests conducted for this research are documented in the manuscript and are divided into four distinct chapters, each addressing specific aspects of the study.Chapters I and II lay the groundwork by presenting an extensive literature review on the behavior of concrete under high temperature conditions and offering an overview of repair mortars. These chapters extensively explore multiple facets, including the characteristics of concrete when subjected to elevated temperatures, the underlying mechanisms governing the interaction between mortar and polymers, and the methodologies utilized for examining and observing these materials within laboratory environments. Moreover, the study's research problem and experimental approach are introduced and thoroughly discussed, setting the stage for the subsequent chapters.

Chapter III provides a detailed account of the materials and methods employed in the study, encompassing various experimental techniques, mineral components, polymers, and fibers. The chapter delves into the comprehensive description of these elements, shedding light on their significance and relevance to the research.

In Chapter IV, the study unveils the results pertaining to the short and long-term behavior of mortar-polymer composites. This includes a thorough examination of the performance of concrete when repaired using different types of mortars, namely a newly developed laboratory-made mortar and a commercially available repair mortar. To optimize the formulation of the resin and fiber-based repair mortars, a numerical study based on factorial design will be employed.

CHAPTER I:

THE BEHAVIOR OF CONCRETE AT HIGH TEMPERTURES

I.1 Introduction

Due to its heterogeneity, when concrete is exposed to high temperatures, it undergoes physical and chemical transformations, resulting in changes in its mechanical, physical and thermal properties. This chapter aims to provide a bibliographical review of research work on the behavior of concrete at high temperatures. It is divided into three main parts; the first part focuses on the microstructure of hardened concrete (cement paste and the paste-aggregates interface), as well as the role played by water in concrete. The second part delves deeper into the effects of high temperatures on concrete and its constituents, and changes in the physical and mechanical properties of concrete with temperature, followed by an overview of thermal instability with these mechanisms.

I.2 The microstructure of hardened concrete

Hardened concrete is a highly heterogeneous mixture composed of various components, some of which are active, and others are inert. Generally, this material is composed of two phases: the cement matrix (cement paste) and aggregates (gravel and sand).

I.2.1 The microstructure of the cement paste

Cement is a hydraulic binder, i.e., able to take hold in water. It appears as a very fine powder mixed with water to form a paste that gradually hardens over time. This hardening is due to the hydration of certain mineral compounds, especially, calcium silicates and aluminates, the proportion of lime and reactive silica must be at least 50% of the mass of cement [1].

Table I. 1 Clinker minerals in portland cement [1].

Clinker minerals	Name	Abbreviated chemical désignation	Typical proportion (% by mass)	Influence on cement properties
Tricalcium silicate	Alite	C_3S	50 – 70	Rapid hydration, high hydration heat, high short-term strength, promotes the general development of strength.
Dicalcium silicate	Belite	C_2S	10 – 20	Slow hydration, low heat of hydration, high long-term strength, low short-term strength.
Tricalcium aluminate	Aluminate	C_3A	5 – 10	Rapid hydration, rapid stiffening, high heat of hydration, contributes to short-term strength, increase shrinkage, and react with sulfates.
Tetracalciumaluminoferrite	Ferrite	C_4AF	5 – 10	Dark color, slow hydration, low contribution to resistance.

In the presence of water, these constituents of cement are transformed into hydrates.

The main hydrates formed are:

- **Hydrated calcium silicate C-S-H**

In the cementitious notation convention: C: CaO, S: SiO_2, H: H_2O). This compound is often called “C-S-H gel”.

Ordinary hardened cement paste contains 50-70% of C-S-H. In the case of high-performance cement pastes, the amount of C-S-H phase is even more important. This is helped to increase the strength.

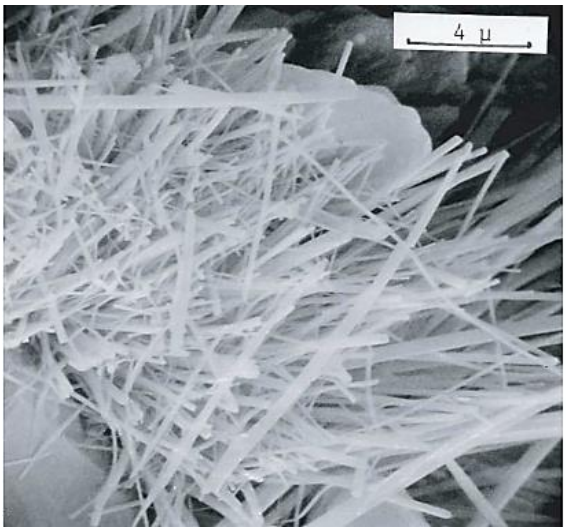

Figure I. 1 Hydrated calcium silicate image obtained with SEM [2].

- **Portlandite $Ca(OH)_2$** (calcium hydroxide)

It has 20 to 25% of the volume of the cement paste, crystallizing in hexagonal platelets. It contributes little to the strength. In addition, portlandite is easily soluble in water which reduces the durability of concrete.

Figure I. 2 Portlandite Image obtained with SEM [2].

- **Ettringite TSA** (hydrated calcium trisulfoaluminate)

Gypsum acts as a setting regulator by controlling the hydration of C_3A. The aluminates react with the sulphate of the gypsum to form ettringite ($CaO_6\ AL_2O_3\ SO_3$, $32H_2O$).This reaction is strongly exothermic.

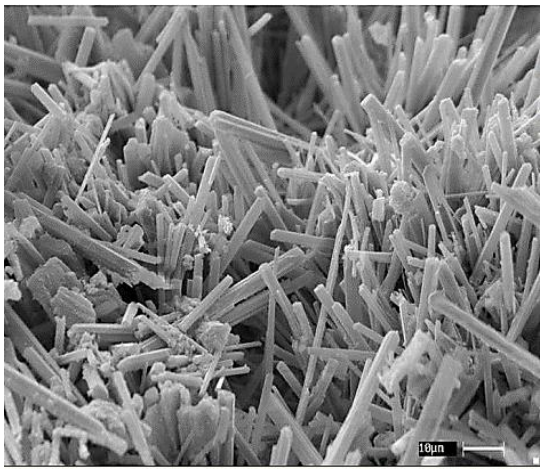

Figure I. 3 Image of ettringite crystals obtained with SEM [2].

Many models exist in the scientific literature to describe the structure and morphology of hydrated calcium silicate C-S-H which represents the structure of cement paste. The model proposed by Feldman and Sereda [3] is the best model able to justify most of the mechanical behavior of the material.

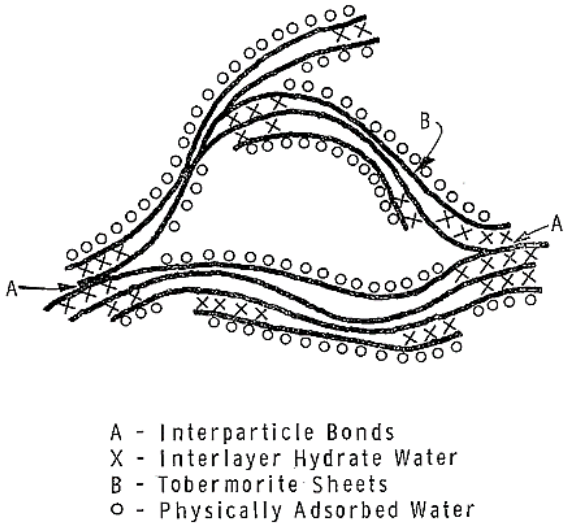

Figure I. 4 Schematic representation of the microstructure of C-S-H gel [3].

In this model, the C-S-H particles are in the form of strips. Each strip (lamella) consists of 2 to 3 single sheets. These sheets can have a relative movement between them, reversible or not during mechanical loading. Thus, the penetration or the departure of water from inter-lamellar spaces (between lamellae) and interfoliar spaces (between leaflets) are possible. These departures are the predominant phenomenon explaining the dimensional variations observable over time under various stresses [3].

I.2.2 Water in cement matrix

Water in concrete plays a dual role; on the one hand, it is necessary for the chemical reaction of the constituents of cement (cement hydration). On the other hand, water provides the workability of the concrete in a fresh state.

Water in concrete can be present in different forms:

I.2.2.1 Free and capillary water

Free water is not subjected to the forces of attraction of solid surfaces. It is mainly found in capillary pores larger than 10µm (large pores and cracks). This water is the first to drain or evaporate (between 30 and 120˚C) during drying or heating.

I.2.2.2 water adsorbed

The adsorbed water is found on the surface of the cement matrix and the surface of anysolid phase. It is due to the physical forces of Van der Waals. Under the influence of attractive forces, water molecules are physically adsorbed to the surface of solids in the hydrated

cement matrix. It can form up to 5 regular and superimposed layers[4-6].The fifth layer has a close status to condensed water. Another chemical adsorption can also appear between the water molecule and the solid. Each water molecule is linked to the hydroxyls of the hydrates between the layers by hydrogen bonds. Which are ten times more intense than Van der Waals bonds. The least bound water is adsorbed on the outer surface of the particles (interlamellar water). Either attached to a hydroxyl of the hydrates or linked to another water molecule by Van der Waals type bond. See figure I.5 démonstration the Sierra model [7].

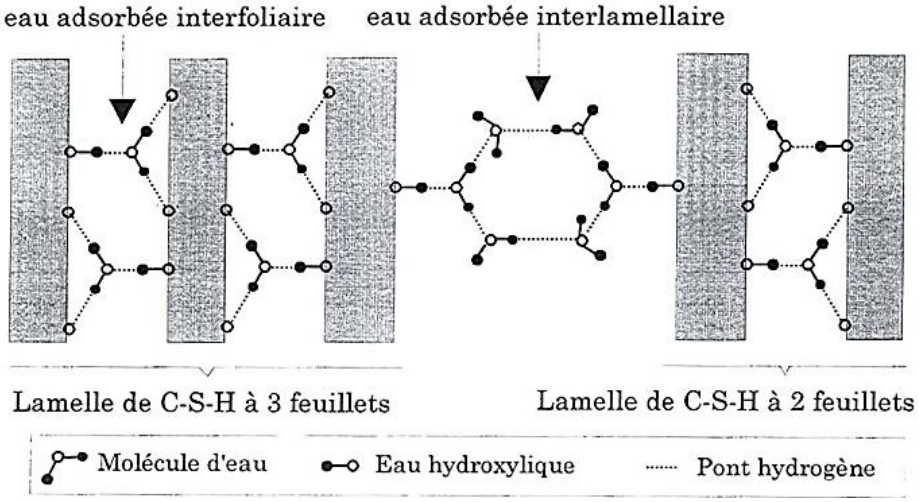

Figure I. 5 The Sierra model [7].

I.2.2.3 Chemically bound water

It is water that reacts chemically with anhydrous cement to form various hydration products such as hydrated calcium silicates C-S-H and portlandite $Ca(OH)_2$.

I.2.3 Porosity and pore distribution

Concrete is a porous material; these pores are decisive for the mechanical characteristics and durability of concrete.

Porosity is the natural cause of the excess water that is necessary for the hydration of the cement and the voids of the aggregates.

- **Capillary porosity:** or capillary pores present in the form of intergranular spaces occupied by excess mixing water which has not been consumed during the chemical reactions of hydration of cement. Therefore, this excess water is drained out of these pores over time by drying.

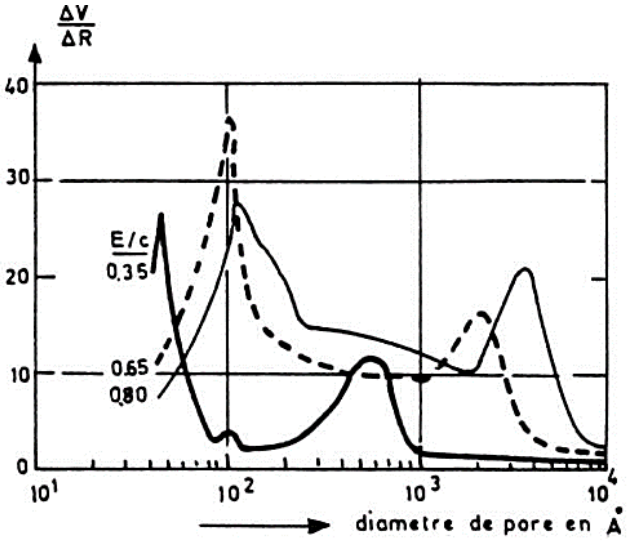

Figure I. 6 Porosimetric distribution concrete in terms of the ratio W/C [7].

- **Porosity intrinsic at C-S-H:** Or hydrate pores. The size of these pores is a few nanometers. They are independent of the formulation of the cement paste (especially the W/C ratio).

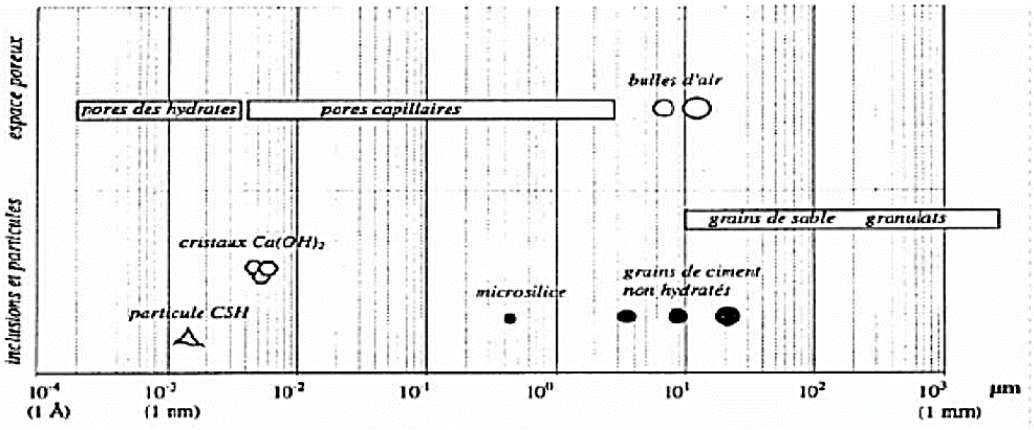

Figure I. 7 Pore sizes and solid phases present in concrete [8].

I.2.4 Microstructure of the paste-aggregate interface

In concrete, the bond which is established during hydration between the cement matrix and the aggregates that it coats, results in a particular area of paste zone called the “transition zone”. This interface has a greater porosity and a lower resistance than the rest of the matrix. It is the weak point of concrete facing mechanical or thermal stresses. The thickness of this

zone increases with the size of the aggregate and the W/C ratio. But remains in all cases less than 50 µm.

Figure 1.8 shows the model of Diamond [9]. we observe a particular hydrated paste zone around the aggregates. Its first layer is composed of portlandite crystals oriented perpendicular to the aggregates. The second layer, 0.5µm thick, is composed of C-S-H sheets. After the second layer, it is the zone of high porosity with large grains and low cohesion. This zone is a zone of weakness during mechanical stresses.

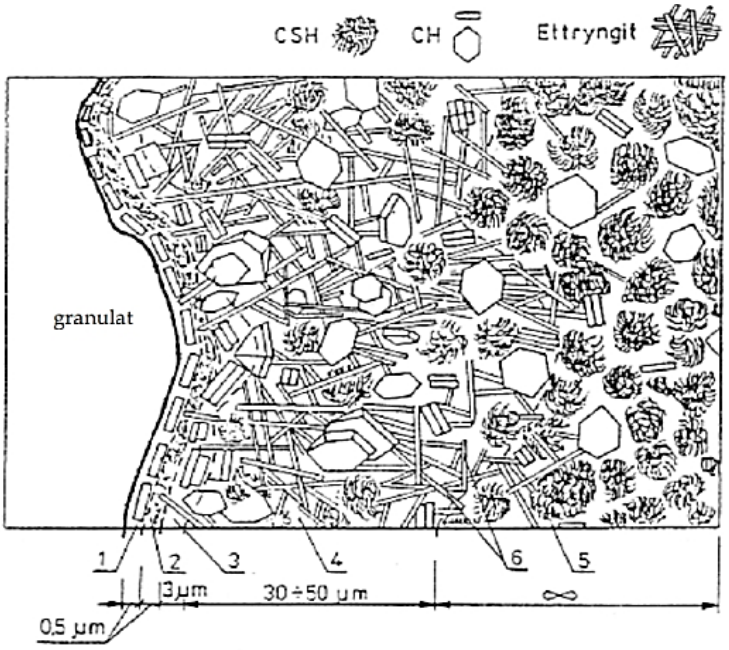

Figure I. 8 Model of the morphology of the transition zone of concrete [9].

According to Stark & Wicht [10] for high-performance concrete, there is a reduction in porosity and thickness of the transition zone (figure I.9).

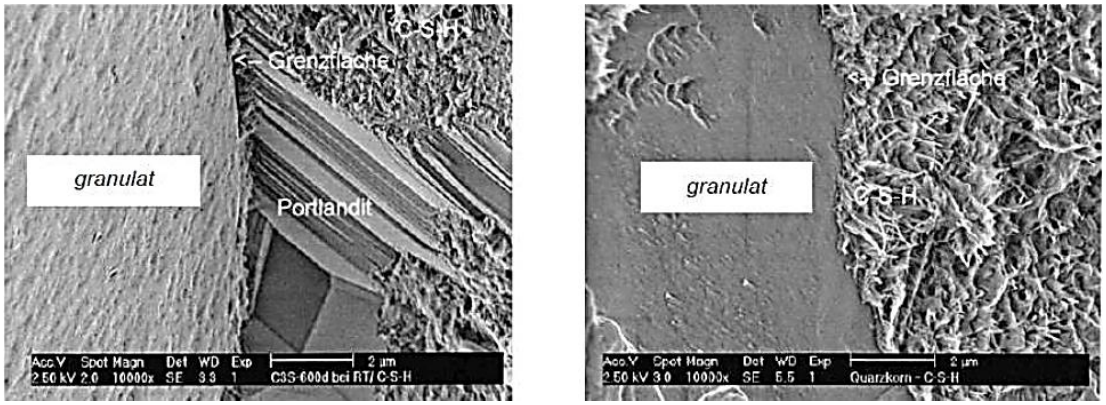

Figure I. 9 Microstructure of the contact zone between the cement paste and the aggregates, left: concrete without silica fume - right: concrete with silica fume [10].

I.3 Mechanical behavior of concrete at ambient temperature

I.3.1 Compressive strength

The resistance describes the load necessary for the breaking of the material relative to the application surface of this load. Therefore, the compressive strength corresponds to the compressive stress that the concrete can support. Compressive strength is the main if not often the only characteristic required of hardened concrete.

We can distinguish, with increasing deformation, three phases of behavior [11].

1- A phase of behavior similar to that of a homogeneous and elastic material, resulting in an approximately linear relationship between stress and strain.
2- The development phase of microcracking causes a progressive curvature of the curve until the maximum stress is reached.
3- The phase of development of fracture surfaces and more or less generalized cracking, i.e. the progressive propagation of fracture.

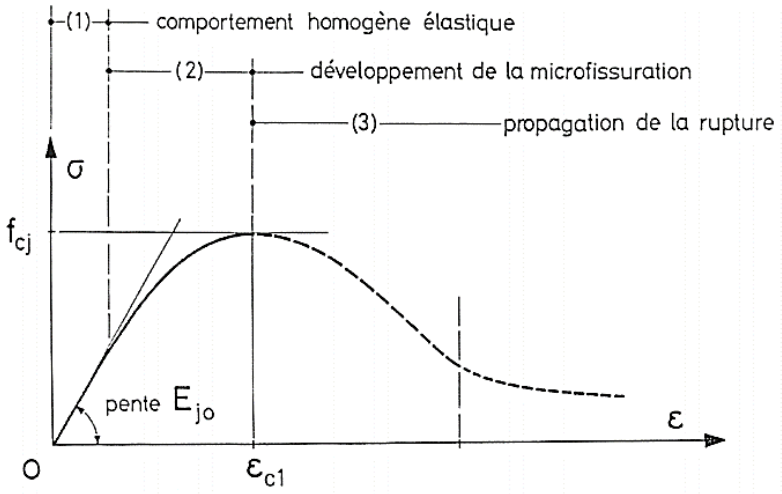

Figure I. 10 Stress-strain curve in simple compression [11].

I.3.2 Tensile strength

There is also another basic parameter, which is the tensile strength. Generally, this resistance is neglected in the calculations because concrete has very low resistance and fragile behavior in the face of tensile stress.

The tensile strength partly depends on the same influencing factors as the compressive strength.

I.4 Behavior of concrete at high temperatures

Exposure of concrete to high temperatures leads to transformations that totally or partially modify its microstructure. Among the most important mechanisms of this transformation, we find the decomposition of the cement matrix and the aggregates, also the modification of the water content (evaporation). These mechanisms cause a strong degradation of the concrete microstructure.

In the following, we are going to talk about the effects of high temperatures on the components (cement paste and aggregates), also the physical and mechanical properties of concrete.

I.4.1 Effect of high temperature on concrete constituents

I.4.1.1 Effect of temperature on cement paste

When the cement paste is subjected to high temperatures, the deformations begin with the decomposition of the C-S-H gel and the evaporation of free water.

- Between 30°C and 105°C, free water and part of the adsorbed water escape from the concrete. Unbound water would be completely removed at 120°C [12].
- Before the temperature of 100°C, ettringite decomposes [13].
- At a temperature of 100°C to < 500°C, the C-S-H hydrates begin to dehydrate followed by evaporation of water, the structure of the C-S-H breaks down progressively in this interval by a breaking of the silicon chains [14].
- From 400°C, portlandite decomposes into free lime and water which evaporates [15]. According to the following reaction

$$Ca(OH)_2 \xrightarrow{\text{température}} CaO + H_2O \quad \text{.....(I.1)}$$

Castellote et al [16] show the transformation of the main components of a cement paste under the effect of temperature variation, using the modiffractometric analysis (the neutron diffraction technique).

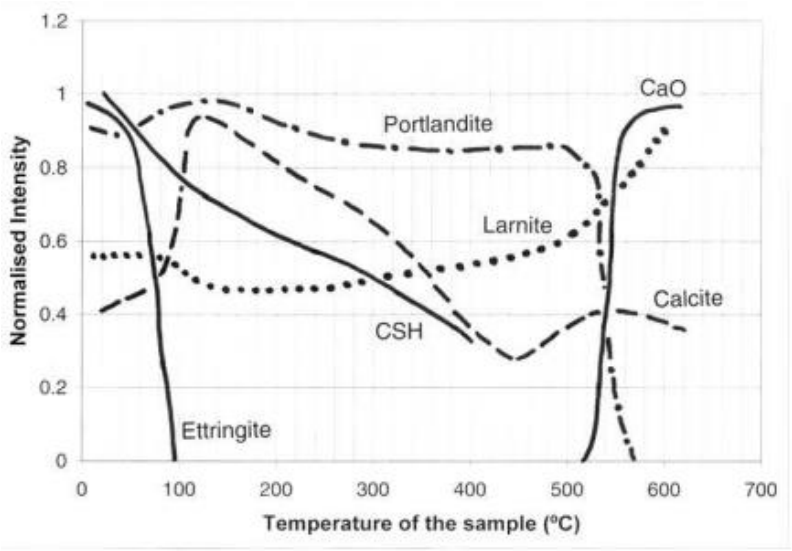

Figure I. 11 Evolution of the quantity of constituents of the cement paste during heating [16].

From the start of heating, the hydrates undergo various modifications. The disappearance of ettringite occurs at the start of heat treatment (before 100°C). The C-S-h gel is exposed to progressive dehydration before 100°C up to 400°C. At 500°C, portlandite decomposes into CaO and water suddenly, at the same time the quantity of lime CaO increases.

I.4.1.2 Effect of temperature on aggregates

Aggregates are generally inert materials added to the concrete formulation to form the granular skeleton which transmits the forces applied to the concrete. Consequently, the behavior of concrete subjected to high temperature is necessarily linked to the nature of the aggregates which constitute 70% to 80% of the total volume of the concrete.

According to Hager [17], the properties of a good aggregate used at high temperatures are :

- A low coefficient of thermal deformation.
- The absence of residual deformations after cooling.
- Thermal stability, i.e. a low number of peaks on the differential thermal analysis curves and thermo-gravimetric analysis; either little or no phase changes.
- A mono-mineral structure of the rock component of the aggregate.

With high temperatures, the aggregates undergo physic-chemical modifications. Several studies have shown that the behavior of concrete based on siliceous aggregates is worse than that of concrete based on limestone aggregates [18-20]. This is generally attributed to a high thermal expansion of the siliceous aggregates and the increase in volume due to the transformation of α quartz to β quartz at about 575°C. [17][21]

Hachemi [22] studied the influence of the nature of the sand (siliceous and limestone) on the evolution of the physical and mechanical properties of 3 types of concrete subjected to different temperatures (150°C, 250°C,400°C, 600°C and 900°C).

The author[22]showed that concrete containing calcareous sand with a high W/C ratio could be used in high-temperature applications.

I.4.1.3 Degradation of the paste-aggregate interface

The paste-aggregate interface is the weakest part of heated concrete. Generally, concrete damage is caused by cracks that occur due to incompatible thermal stresses between the aggregates and the cement matrix. Figure I.12 shows an example of concrete containing sand-lime aggregates heated to 600°C [17].

An image obtained by the SEM shows cracks crossing the cement paste and continuing to the transition zone, also cracks are going through the aggregates, and some siliceous aggregates decompose at 350°C [23].

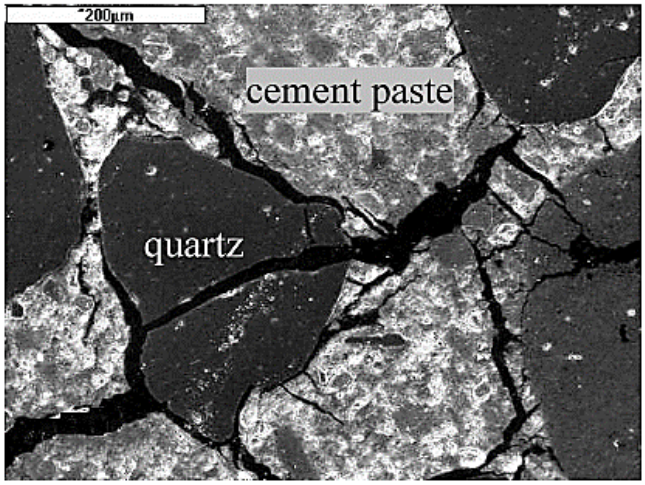

Figure I. 12 SEM image of the microstructure of concrete based on sand-lime aggregates heated to 600°C, fc = 75 MPa [23].

I.4.2 Evolution of the physical properties of concrete with temperature

I.4.2.1 Mass loss

Exposure of concrete to high-temperature results in weight loss, this loss is generally due to the evaporation of water.

Hager [17] carried out an important experimental work concerning the loss of mass, she studied three types of high-performance concrete HPC (M100C with and without polypropylene fibers, M75SC, M75C) and an ordinary concrete OC (M30C) (figure I.13).

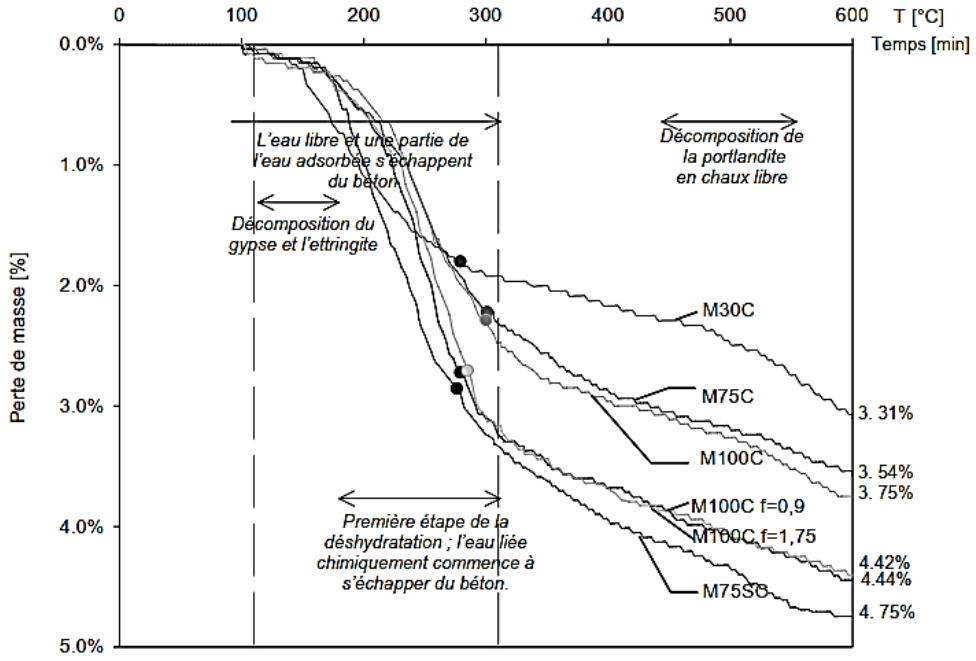

Figure I. 13 Mass loss of concrete determined during heating from 20 to 600°C at a rate of 1°C/min. the points indicate the value of the water content obtained by drying at 105°C [17].

Figure I.13 shows that the mass loss of the different concretes starts from a temperature greater than 100°C. It increases between 150°C and 200°C, the loss of mass in this temperature range corresponds to the departure of free water and part of the water adsorbed following the decomposition of gypsum and ettringite. From 300°C, the rate of mass loss slows down; however, the reduction of the pass continues because of the dehydration of the C-S-H gel and portlandite $Ca(OH)_2$.

Also, Hachemi [13]studied the evolution of the mass loss of concrete with different W/C ratios and different types of aggregates.

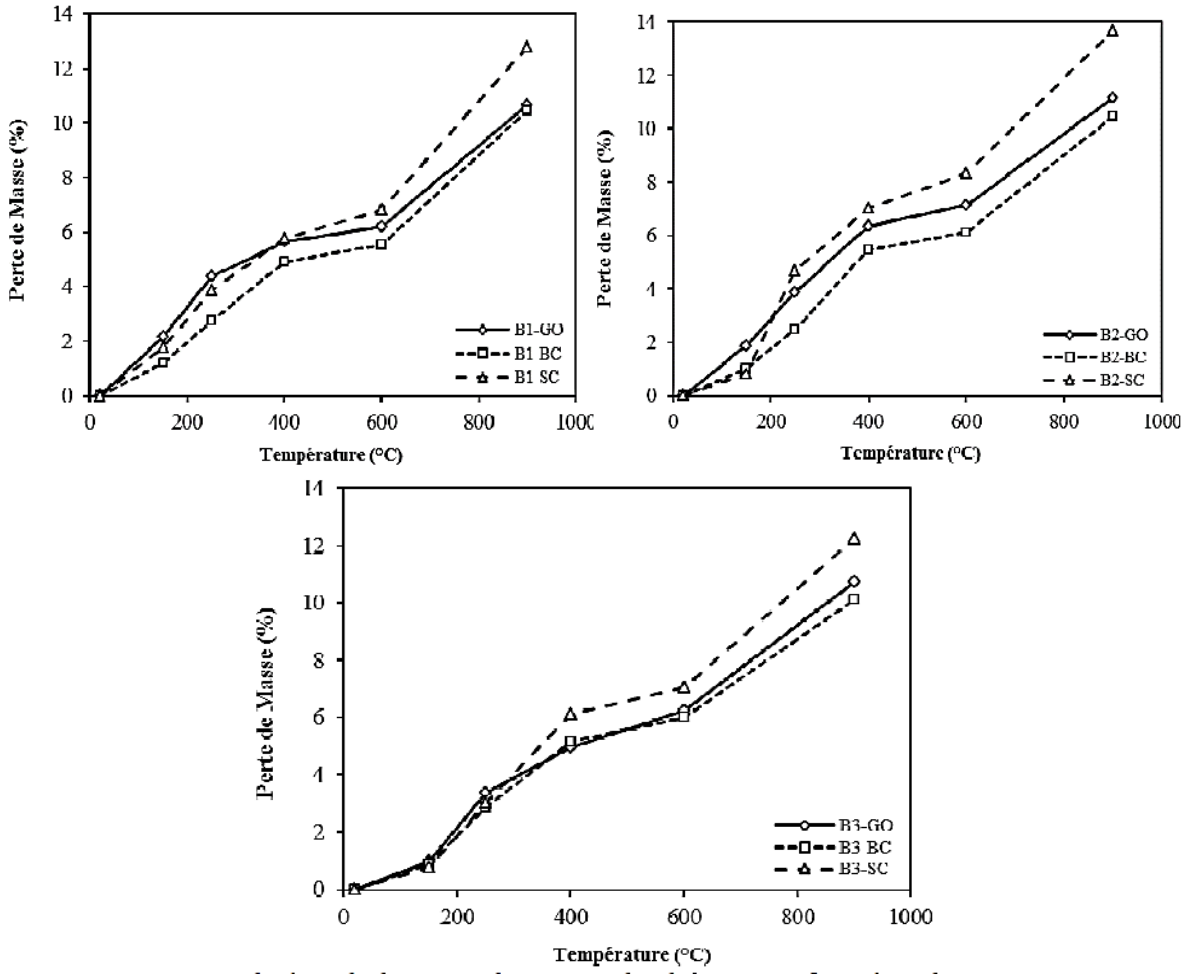

Figure I. 14 Evolution of the mass loss of the concrete tested as a function of the temperature (GO : ordinary concrete based on ordinary aggregates, SC : ordinary concrete based on limestone sand, BC : ordinary concrete based on crushed bricks) [13].

According to Figure I.14, between room temperature and 250°C, concretes with a high W/C ratio lose more of mass than concretes with a low W/C ratio. Because they contain more water and have a greater permeability than concretes with low W/C which facilitates the evaporation of water. Above 250°C, concretes containing crushed brick aggregates have the lowest mass loss compared to other concretes. From 600°C, the author [13] noticed that the greatest loss of mass of concretes based on calcareous sand can be explained by the departure of CO_2 coming from calcium carbonates which leads to an increase in the additional mass loss.

The results were led by Rafi [24] concerning the loss of mass of concrete, which has been illustrated in Figure I.15.

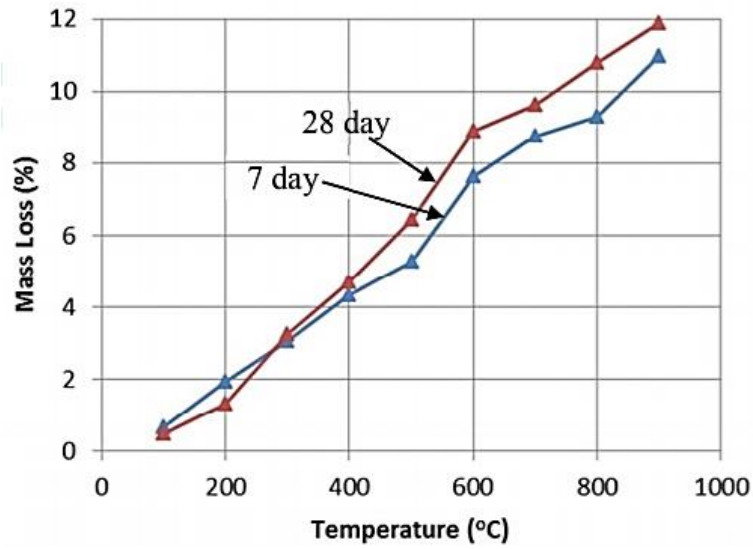

Figure I. 15 Mass loss as a function of temperature [24].

The loss of mass of the test specimens tested at 7 days and 28 days is similar from 20 °C to 400 °C, beyond this temperature, the loss of mass of the test pieces at 28 days is greater than that measured at 7 days. Figure I.15 shows that the mass loss increases almost in a quasi-linear up to 600°C. The other noted that, after heating to 900°C, the loss of mass of the test pieces tested at 7 days is approximately 11%, which is equal to 12% for the test pieces of 28 days.

I.4.2.2 Porosity

The porosity of concrete is strongly modified by the temperature, according to the research carried out by Hager [17] about the water porosity of different concretes (Figure I.16).

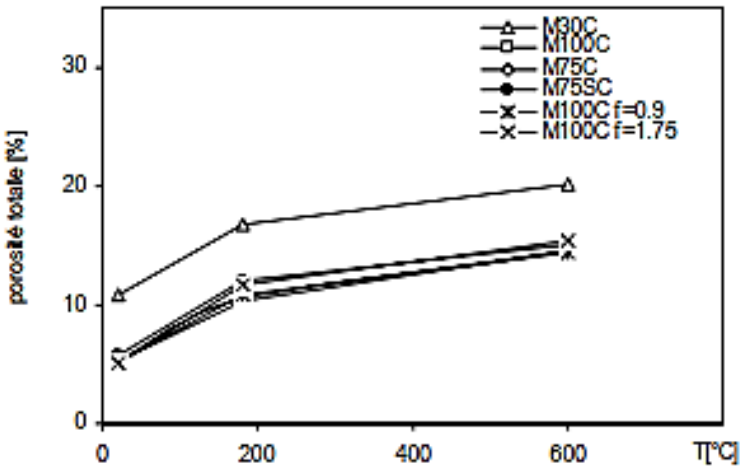

Figure I. 16 The average total porosity to the water of the concretes was studied as a function of temperature [17].

According to figure I.16, the OC (M30C) shows a greater porosity than that of the three HPC (M100C, M75C et M75SC), at room temperature (20°C) as well as at high temperature (600°C). This is explained by the presence of a greater quantity of water in the OC. In general, it can be said that an increase in temperature induces an increase in porosity and pore sizes.

Another research was carried out by Rijaniaina [25] on the behavior of natural siliceous and limestone aggregates at high temperature and their influence on that concrete. An ordinary concrete OC, high strength concrete HSC, with four types of aggregates (black limestone –N, white limestone –B, brown flint sileX–X, red granite –G) are tested. Rijaniaina [25] concludes that: OC shows less change in porosity than HSC. At 600°C, the porosity value is practically doubled for OC and is almost three times greater for HSC. The change in porosity with temperature is more pronounced after heating to 600°C for OC-X and OC-N. Concretes -N has a relatively greater increase in porosity than other concretes. Concretes -G and –X have a more or less similar evolution (figure I.17). The other [25]concluded that the thermal stability of aggregates and the W/C ratio influence the evolution of porosity and cracking of concrete when subjected to high temperature.

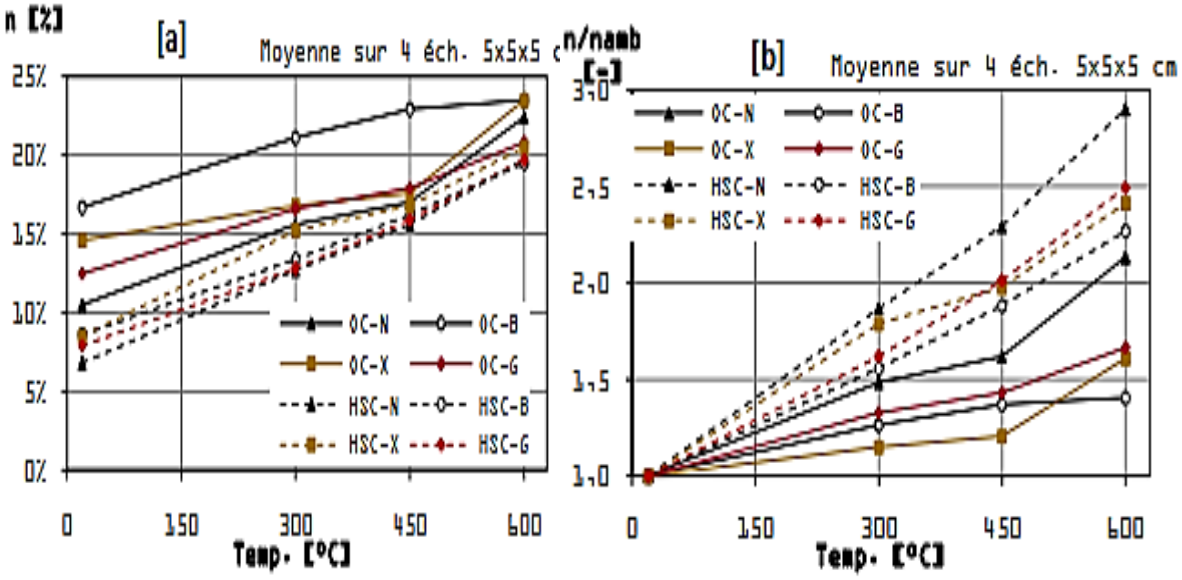

Figure I. 17 Absolute residual porosity [a] and [b] relative porosity of concrete [25].

I.4.2.3 Permeability

The permeability of a porous medium characterizes the capacity that this medium possesses to allow fluid to pass through under a pressure gradient [26].

The permeability of concrete depends on the porosity of the cement paste, this last is dependent on the W/C ratio as well as the aging of the concrete [27].

According to figure I.18, tshimanga [26] notes that the permeability of concretes decreases at 150°C to increases exceptionally for higher temperatures. He attributes the drop in residual intrinsic permeability at 150°C to the presence of water in liquid form in the pores. The increase in permeability observed after heating to 300°C is attributed to an enlargement of the capillary pores while that observed between 300°C and 450°C is due to a deterioration of the cement matrix.

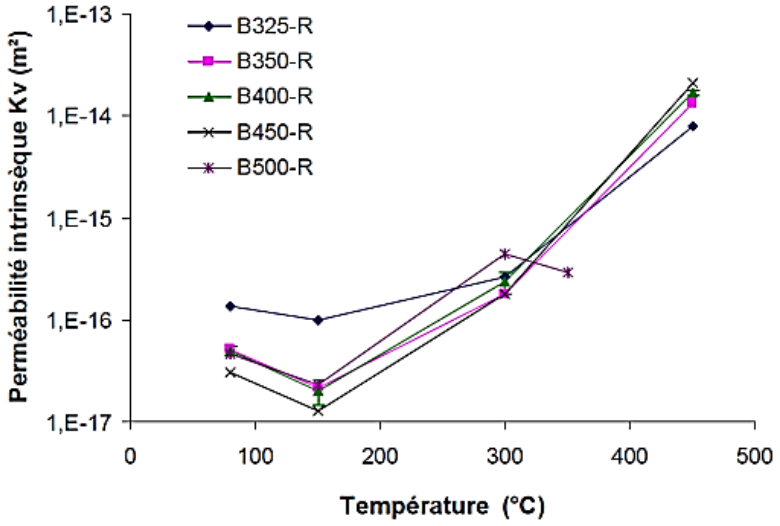

Figure I. 18 Evaluation of the residual intrinsic permeability of concrete as a function of temperature [26].

Results conducted by Haniche [28] concerning the influence of polypropylene fibers on the permeability of OC and HPC with different percentages of fibers are presented in the figure I.19.

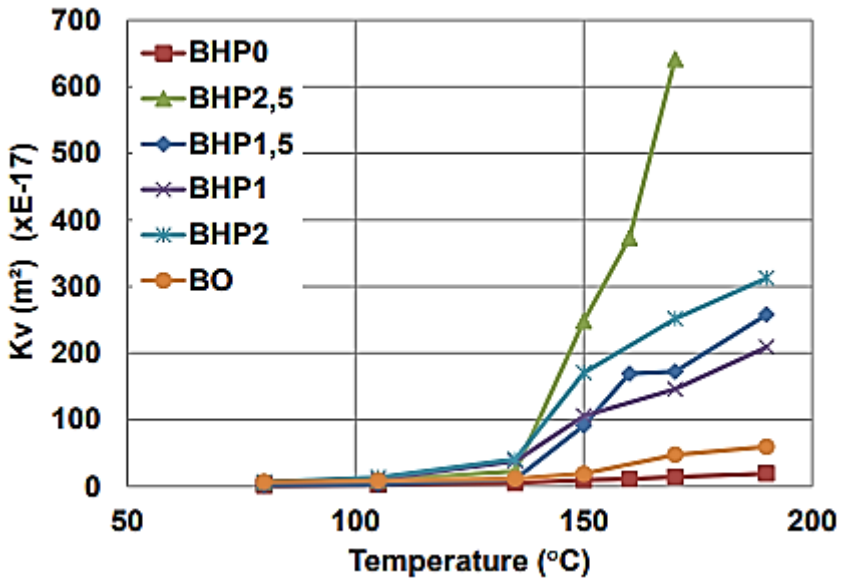

Figure I. 19 The variation of the intrinsic permeability of OC and HPC with different proportions of polypropylene fibers depends on the temperature [28].

These results show that the intrinsic permeability of ordinary concrete BO is higher than that of high-performance concrete without fibers BHP0. For temperatures below 135 °C, the permeability of concrete with fibers is slightly higher than that of concrete without polypropylene fibers. This increase can be explained by the evaporation of water (free and chemically bound) existing in the porous network. On the other hand, for temperatures greater or equal to 150 °C, a significant increase in the permeability of HPC with fibers was observed. When the fiber content increases, the permeability increases. The increase in permeability is linked to the fusion of the fibers which begin to melt at 150 °C (fibers are melted at 165 °C) which creates additional connections causing an increase in the porous network of the material.

I.4.3 Evolution of the mechanical properties of concrete with temperature

More and more concrete has become a very necessary material in our life. On the mechanical properties side, concrete is characterized by compressive strength, tensile strength and elasticity modulus (Yong modulus). During a fire, the high temperature causes physic-chemical modifications in the concrete, which influence the evolution of these properties.

I.4.3.1 Evolution of compressive strength

Compressive strength is the ability of a material to withstand uniaxial loads during crushing. It is a key value to characterize the evolution of the mechanical properties of concrete subjected to high temperatures.

Hachemi [29] studied the effect of high temperature on the evolution of the compressive strength of three types of concrete (OC, HSC, HPC).

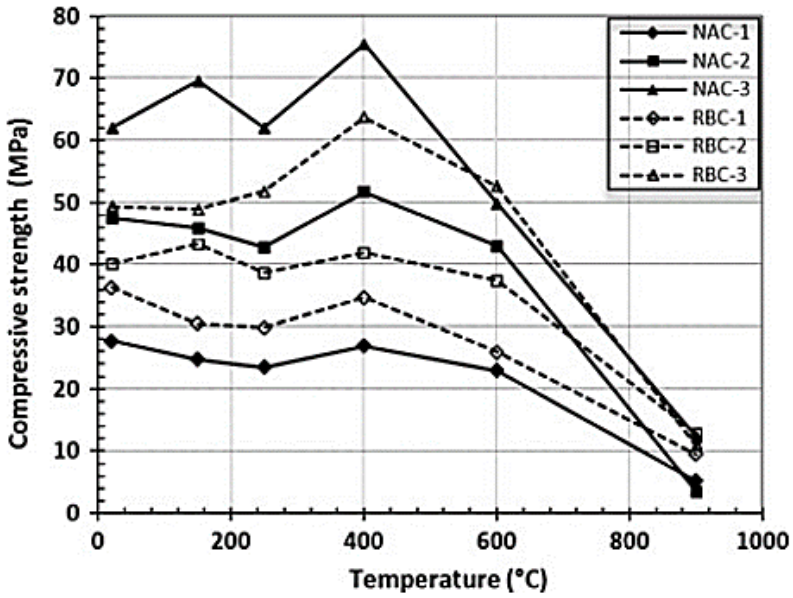

Figure I. 20 The evolution of the compressive strength of concrete with temperature (NAC: concrete made with natural aggregates, RBC: concrete made with 20% of crushed brick aggregates) [29].

From the results obtained, the author [29] found that the compressive strength undergoes a slight variation (decrease or increase) in the temperature range from 20°C to 250°C. Around 400°C, the compressive strength increases slightly, beyond this temperature, it gradually decreases.

From figure I.20, we can note a better evolution of the residual strength of HPC (NAC-3 and RBC-3) and HSC (NAC-2 and RBC-2) up to 400°C and a less good development for the BO (NAC-1 and RBC-1). Beyond this temperature, the curves of the compressive strength would join.

Several hypotheses have been proposed in the literature to explain the increase in compressive strength at 400°C. it is assumed that removing moisture from the intermediate layers of C-S-H gel would reduce the disjoint pressure and increase the attractive forces between the hydrate particles and hence the compressive strength of the concrete [30].

Also, Tufail [31] studied the effect of high temperatures on the mechanical properties of concrete with limestone, quartz, and granite aggregates. Figure I.21 shows the results:

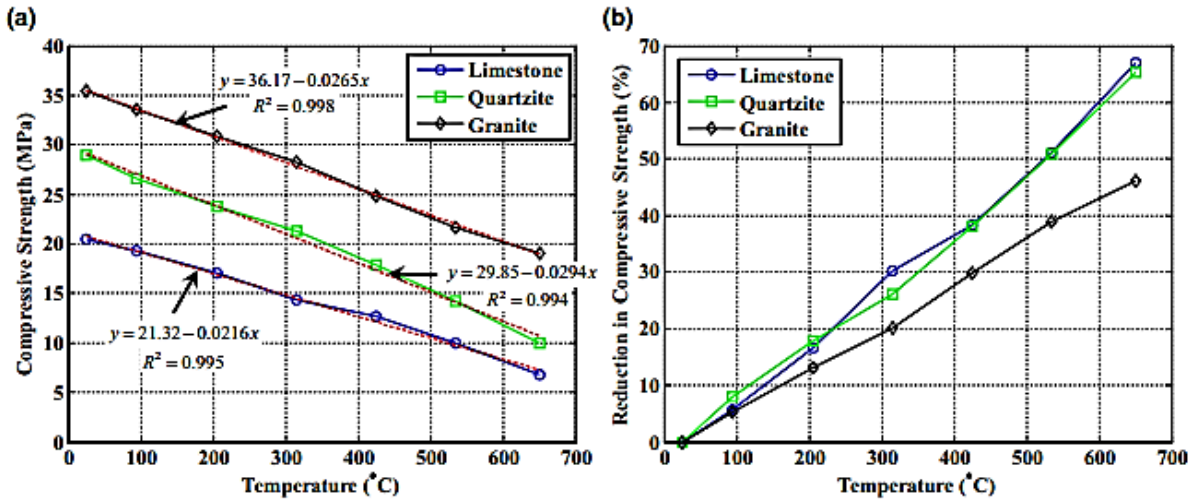

Figure I. 21 (**a)**The compressive strength of concrete tested at different temperatures. (**b)** the percentage change in compressive strength with temperature [31].

The compressive strength of concrete samples subjected to high temperatures is reduced at 650°C by 6,77MPa, 10MPa, and 19,08MPa respectively for limestone, quartz, and granite concrete (figure I.21 (a)).

The percentage loss compared to the initial strength of the concrete is shown in figure I.21 (b). Concrete with granite has higher compressive strength at room temperature and retains superior strength at increasing temperatures compared to concrete with quartz and limestone.

Figure I.22 collects the work of several researchers concerning the evolution of residual compressive strengths of self-compacting concrete [27], ordinary concretes and high-performance concretes [32][33][34] as a function of temperature. The analysis of the evolution curve makes it possible to group the resistance behavior into two domains [35].

- The first area (domain), from room temperature to 300 °C-400 °C, is characterized by a slight decrease, maintenance, or increase in resistance. The drop in resistance is observed around 100 °C - 150 °C according to the authors. This slight drop in resistance is linked to the departure of the water, when the temperature rises, expands, and causes the gel sheets to move apart. This spacing thus causes a drop in the cohesion forces. Up to 300 °C- 400 °C, a gain in resistance is noticed and can be delayed with the HPC given their low permeability which slows the departure of water [36][37].

The second area, beyond temperature 300 °C - 400 °C, is characterized by a continual decrease in compressive strength linked to different physic-chemical transformations [38].

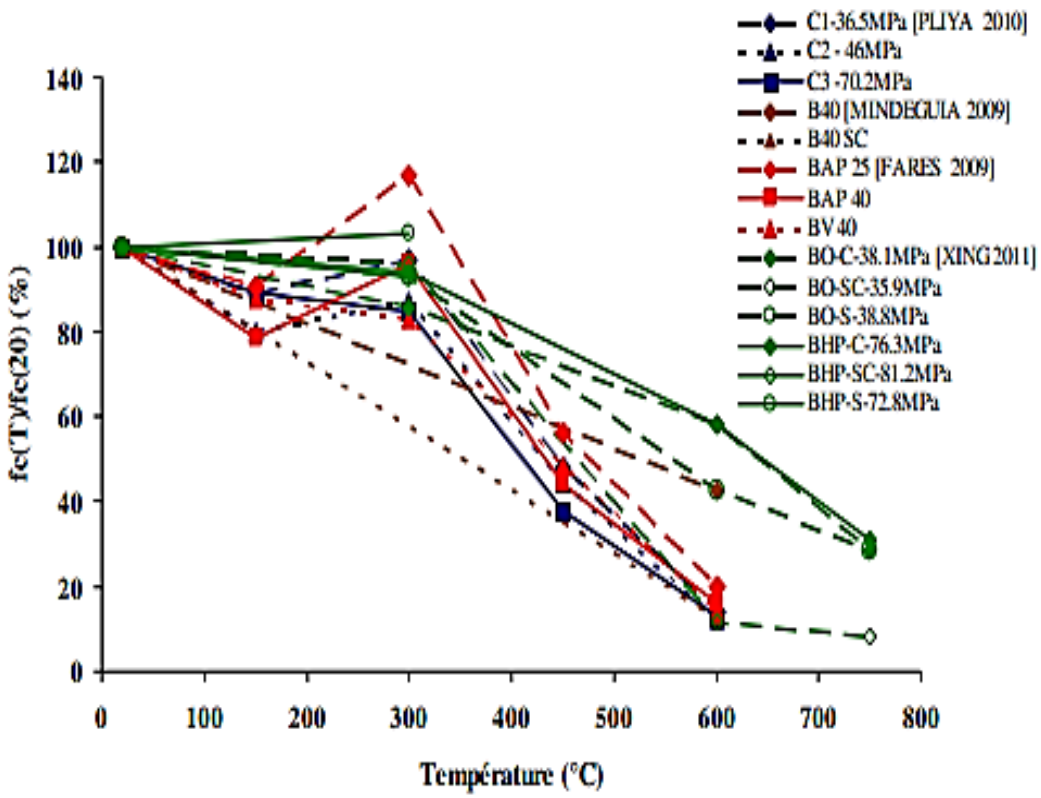

Figure I. 22 Evolution of the residual relative compressive strength of OC and HPC [32][33][34].

I.4.3.2 Evolution of tensile strength

In the literature, given the difficulty of performing direct tensile tests, few studies have been carried out to determine the tensile strength at high temperatures.

Kanema [39] studied the evolution of residual tensile strength of concrete with different cement dosages (B325 (fc = 39 MPa), B350 (fc = 45 MPa), B400 (fc = 53 MPa), B450 (fc = 60 MPa) et B500 (fc = 72 MPa) (Figure I.23). concretes with a low W/C ratio (B450 and B500) exhibit a greater reduction in their tensile strength compared to concrete with a high W/C ratio (B325). The decrease in resistance results from a restructuring of the cement matrix and more particularly from the dehydration of the transition zone with the increase in temperature. The author [39] concludes that the decrease in the residual tensile strength of concrete depends on the initial W/C ratio and the thermal stress imposed.

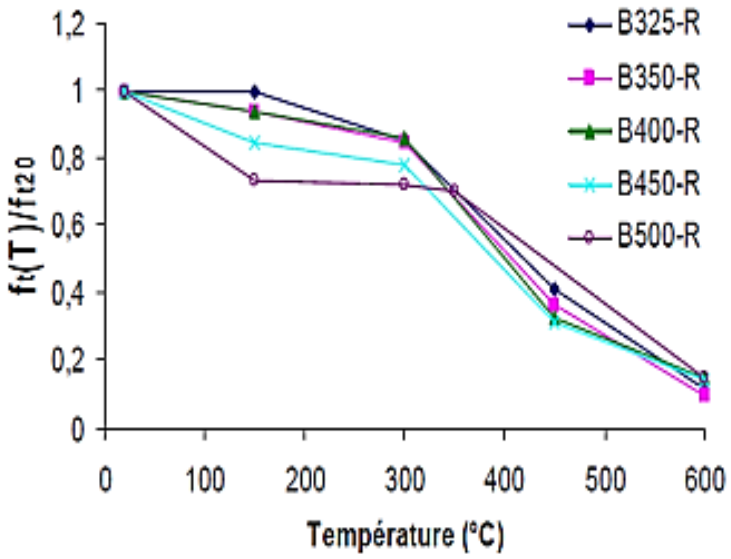

Figure I. 23 Evolution of the residual relative tensile strength of concrete heated with a heating rate of 1 °C/min [39].

Also Anand and Arulraj [40] do tests to understand the behavior of self-compacting concrete SCC beams exposed to high temperatures (900 °C). The following figure shows the percentage reduction in tensile strength.

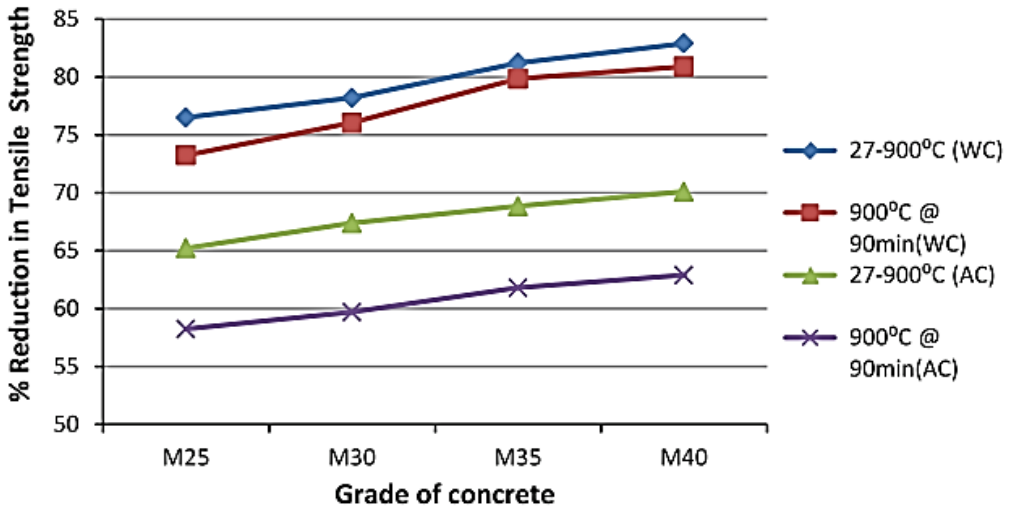

Figure I. 24 The percentage reduction in tensile strength of concretes depending on the temperature [40].

According to the results, the authors [40] observed that samples have been kept at 900 °C for 90min and cooled in the air marking the minimum values of tensile strength. indicating that the reduction in compressive, tensile, and flexural strengths of concrete exposed to higher temperatures increases as the quality of the SCC increases.

Other studies made by Md. shamim al razib [41] to understand the effect of plasticizer setting retardant type (PAZZOLITH CRP4) on the evolution of tensile strength by splitting of concrete subjected to high temperatures.

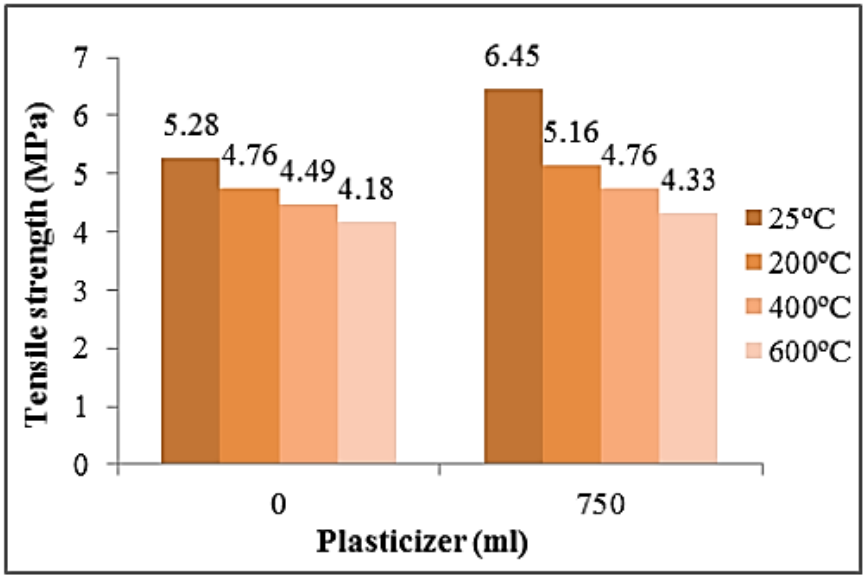

Figure I. 25 Variation of the tensile strength by splitting of concrete with and without setting retardant plasticizer with different temperatures [41].

As figure I.25 shows, the tensile strength by splitting varies with the use or not of the adjuvant and with the variation of temperature. The tensile strength by splitting varies from 5.28 MPa to 4.18MPa for concrete without admixture and from 6.45MPa to 4.33MPa for concrete with plasticizer setting retardant according to the different temperatures (25 °C, 200 °C, 400 °C, and 600 °C).

According to the results, the tensile strength splitting of concretes with admixture is superior to that of concrete without admixture. With increasing temperature, the loss of strength is increased for both types of concrete, but the loss is greater for concrete with admixture plasticizer setting retardant.

Several researchers like [30], [33] and [28] found that polypropylene fibers improve the residual tensile strength by splitting high-performance concrete from 300 °C.

Fares et al [42] collected many results from several researchers about tensile strength for different polypropylene fibers contents.

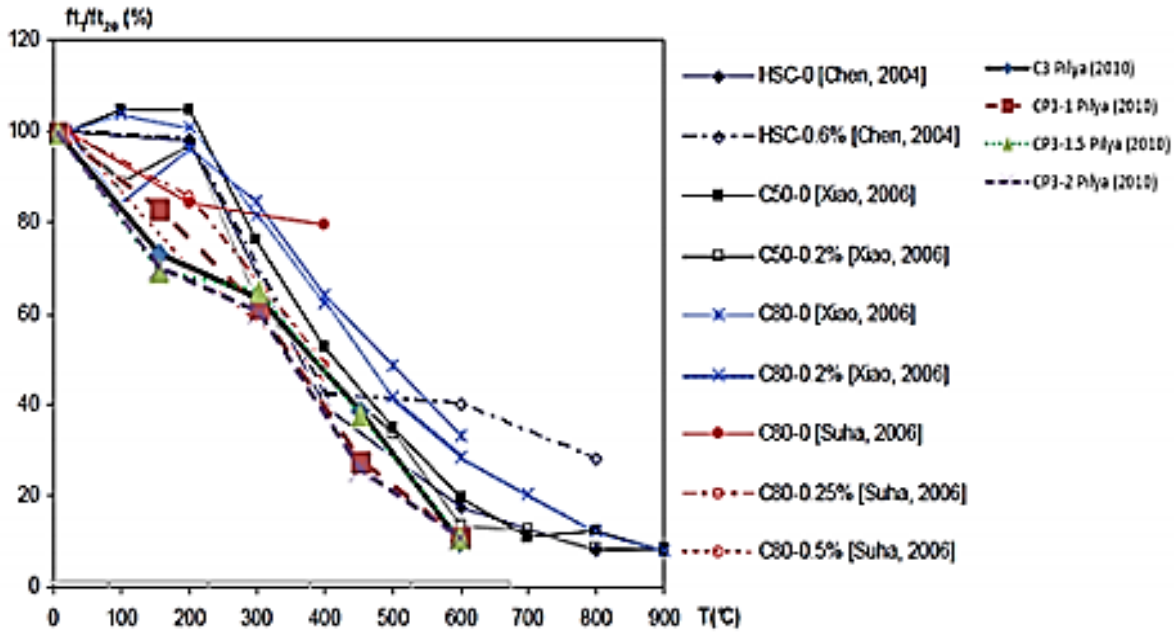

Figure I. 26 Evolution of residual tensile strength of concretes with polypropylene fibers depending on the temperature [42].

I.4.3.3 Evolution of the modulus of elasticity of concrete

The modulus of elasticity expresses the stiffness and rigidity of concrete. This is strongly affected by temperature rise. Many experimental studies have shown a gradual decrease in the modulus of elasticity with temperature. These variations depend on the one hand, on the microstructure of the cement paste and the composition of the concrete, and the other hand, on experimental parameters (water content, nature of aggregates, etc.).

The work of [17], [39], and [33] shows that the W/C ratio had no significant influence on the evolution of the modulus of elasticity, and that the residual modulus of elasticity decreases progressively and identically as a function of temperature (Figure I.27).

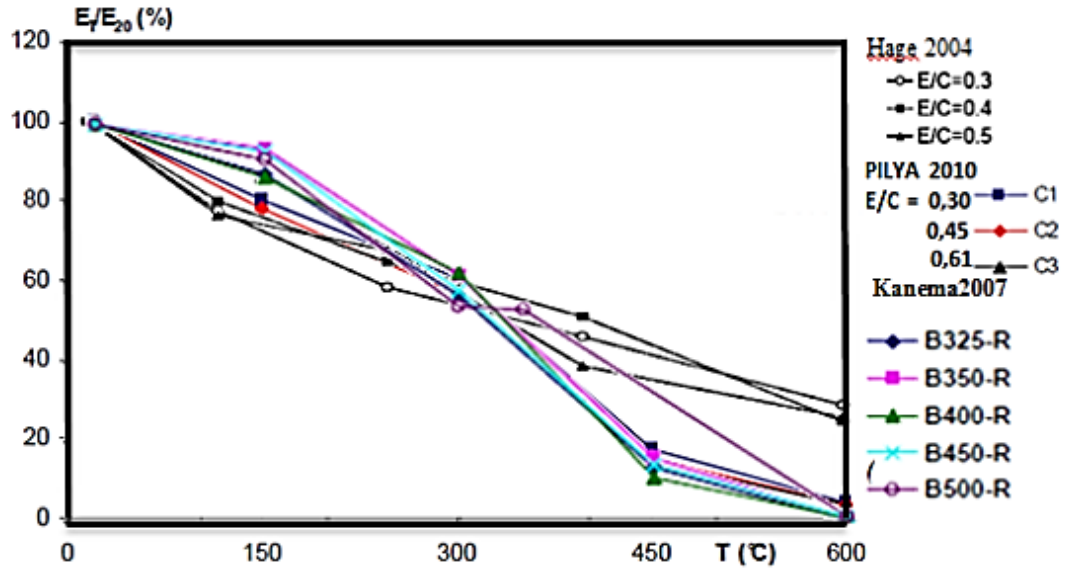

Figure I. 27 Change with the temperature of the relative apparent modulus of elasticity of concrete as a function of the W/C ratio [17], [39] and [33].

An important study was carried out by Yermak [43]on the behavior at high temperatures of concrete with added fibers. Figure I.28 shows the evolution of the relative residual modulus of elasticity of the reference concrete ($C_{réf}$) and CPPS0.75-60 (cocktail concrete of polypropylene fibers with 0.75kg/m^{3}and metal fibers of 60kg/m^3) depending on the temperature, he notes a progressive connection of Young's modulus, which indicates that the concrete suffered damage from the start of heating. The percentage improvement in the residual modulus of elasticity of concretes CPPS0,75-60 compared to $C_{réf}$ concretes is about 8% on average up to 750 °C.

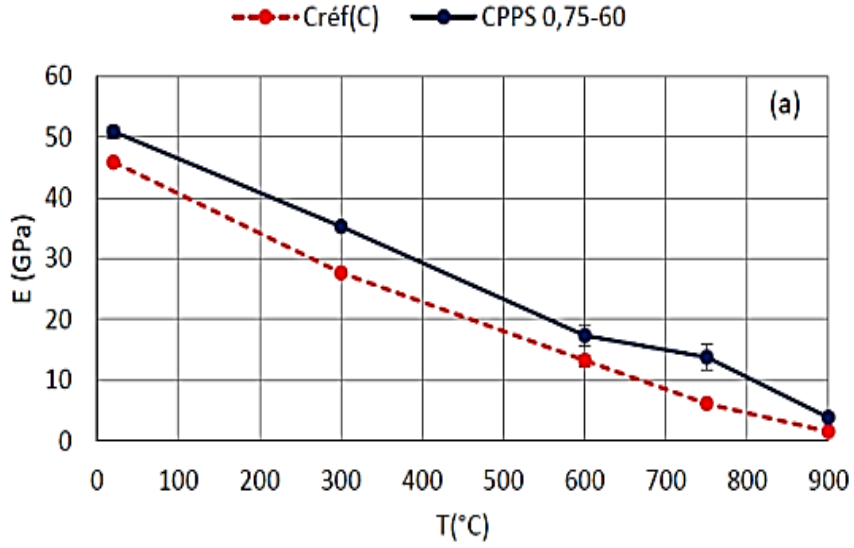

Figure I. 28 Evolution of the relative residual modulus of elasticity of $C_{réf}$ and CPPS0.75-60 depending on the heating-cooling cycle [43].

The scanning electron microscopy (SEM) images [43] (figure I.29) also show the appearance of cracks between the paste and the metal fiber following the differential thermal deformations. This incompatibility causes cracking at 500 °C, which is not observed at 200°C.

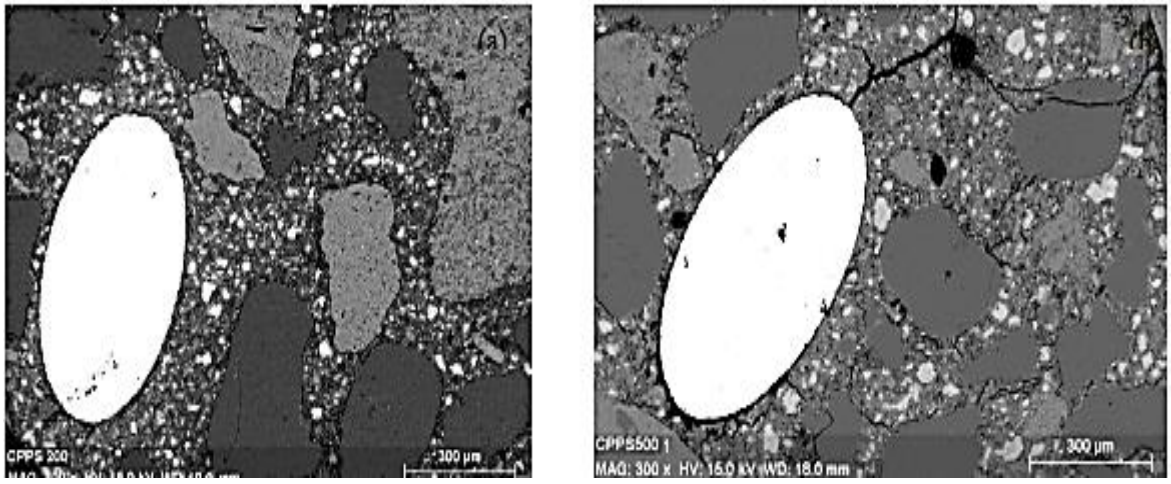

Figure I. 29 Scanning electron microscopy (SEM) images, paste/metal fiber interface in heated concrete (a) at 200 °C and (b) at 500 °C [43].

I.5 Thermal instability of concrete

Concrete is recognized as one of the best fire-resistant building materials. However, this property still has limitations; repeated fires have shown the unstable nature of concrete. Several studies have been carried out to understand the phenomenon of "thermal instability".

I.5.1 Different types of thermal instability of concrete

The thermal instability of concrete can take different forms [44]:

- Explosive spalling: It's a very violent explosion. This type can occur at a temperature above 100°C during the first thirty minutes of the fire. It is characterized by a sudden detachment of small and large pieces of concrete.
- Surface spalling: (écaillage in French) Surface spalling is characterized by a progressive detachment of materiel by small fragments (up to about 20mm) of the facing exposed to the fire; it is less violent than explosive spalling. The surface spalling is probably caused by water migration [45].
- Aggregate spalling: this phenomenon is superficial; it is caused by the thermal expansion of aggregates close to the surface due to the temperature rise.

- Corner spalling: it's a nonviolent type of spalling, it is observed when the concrete is weakened due to the high temperature, and cracks develop due to tensile stresses along the corners of the structure.
- Spalling by a detachment of aggregates: with the temperature rise, the microstructure of the cement paste changes, and internal cracks develop due to the differential thermal expansion between the cement paste and the aggregates.
- Spalling during cooling: this type is caused by the presence of limestone aggregates and the rehydration of lime during the cooling phase.

I.6 Conclusion

The objective of this chapter was to better understand the behavior of concretes subjected to high temperatures. According to the research cited above, concrete subjected to high temperature undergoes microstructural transformations (evaporation of water, dehydration of the C-S-H gel, and decomposition of portlandite). These transformations cause a significant reduction in the mechanical properties of the concretes.

CHAPTER II

STATE OF THE ART ON REPAIR MATERIALS CASE STUDY: CONCRETE SUBJECTED TO HIGH TEMPERATURE

II.1 Introduction

The second chapter of this manuscript is devoted to a bibliographic review, the aim of which is to identify the physical and chemical problems encountered in concrete in both the short and long term. Thus, it will be interesting in understanding the use of cementitious materials for the protection and restoration applications of concrete structures and buildings. The first part is dedicated to the pathology of concretes, containing various degradation mechanisms of reinforced concrete. The second part consists of mortar-polymer composites as materials for the protection and restoration of concrete buildings. This part brings together the knowledge acquired on the behavior of these materials, from their formulation to their implementation, as well as their properties' evolution over time. The third part of this thesis focuses on the interaction between protective and repair materials with concrete subjected to high temperatures. In this section, we will discuss the main methods for reinforcing concrete exposed to fire. Finally, a synthesis of all the collected information is made to identify the main areas of study that will be pursued in the remainder of this thesis. It is noteworthy that this bibliographical synthesis brings together different topics, often very disparate. The aim was to identify strong concepts that would enable us to set up a comprehensive study taking into account elements previously overlooked in laboratory studies. With this in mind, the work of researchers from various fields, including materials science, chemistry, and structural engineering, has been analyzed and synthesized.

II.2 General information on the repair of concrete structures

During the design and construction of a civil engineering structure, one of the key requirements is the expected service life. The durability of reinforced concrete structures, which can be defined as their ability to meet this service life, is a very important characteristic as it ensures increased safety and longevity. This durability also provides considerable savings in the long run, as such works will require minimal or no repairs, thus avoiding costly repair expenses which can often exceed the initial construction costs. It is therefore essential to understand the behavior of different repair materials in both the short and long term.

II.2.1 Main causes of concrete deterioration

Although this section focuses on the materials used for repair or reinforcement, it is beneficial to provide a brief overview of the mechanisms of deterioration of reinforced concrete, corrosion of its reinforcements, and some visible defects.

II.2.1.1 Pathologies of chemical origin

- **Carbonation**

The penetration of CO_2 from the air into concrete causes a chemical reaction [46]. The reaction involves small amounts of CO_2 from the atmosphere dissolving in water and forming the acid H_2CO_3. This acid then reacts with portlandite (calcium hydroxides) to form calcium carbonates and water, according to the following formula:

$$Ca(OH)_2 + CO_2 + H_2O \rightarrow Ca^{2+} + CO_3^- + 2H^+ + 2OH^- \rightarrow CaCO_3 + 2H_2O^1 \ldots \text{(II.1)}$$

The presence of portlandite helps maintain a high pH, which protects concrete reinforcement and hinders the growth of microorganisms. When portlandite is no longer sufficient to regulate the pH, the environment becomes acidic and the reinforcement can corrode [47].

- **Penetration of chlorides**

Chloride ions in concrete can come from its components like sand, cement, and mixing water, but most often from external sources such as seawater or de-icing salts. These ions enter the concrete through diffusion or capillary absorption [48]. Low chloride concentrations form FeOOH, which decreases the pH by consuming hydroxyl ions. This leads to the formation of electrochemical batteries on the reinforcement, causing its decomposition in the anodic zones and resulting in visible corrosion of the reinforcement over time [49].

- **Reinforcement corrosion**

During the pouring of concrete, the mixing water reacts with the steel and creates a protective coating made of iron [$Fe(OH)_2$] and calcium [$Ca(OH)_2$] hydroxides, which results in a high pH (around 13) of the interstitial solution. However, when the interstitial solution is no longer favorable for strong concrete, such as due to carbonation or penetration of chlorine ions, the protective layer disintegrates. This causes the accumulation of oxides and hydroxides from the oxidation at the steel's surface, leading to swelling and eventually cracking of the coating [50].

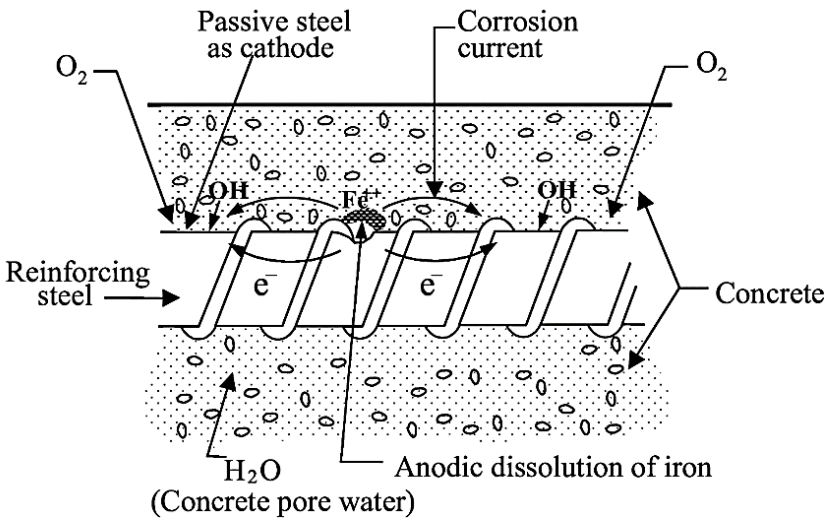

Figure II. 1 Mechanism and consequences of reinforcement corrosion in concrete [50].

- **Sulfate attack**

The phenomenon of this pathology has been widely researched in the literature, however, it is commonly portrayed as intricate and influenced by various intrinsic factors of the material and its surrounding environment, since these parameters affect the processes and outcomes of SEA [51]. Sulfates can come from groundwater [52], soils (such as gypsum or pyritic soils), river water, or seawater. It is noteworthy that dry salts do not affect concrete. The solution's presence of sulfate is crucial for the transfer of SO_4^{2-} ions into the cement matrix [53].

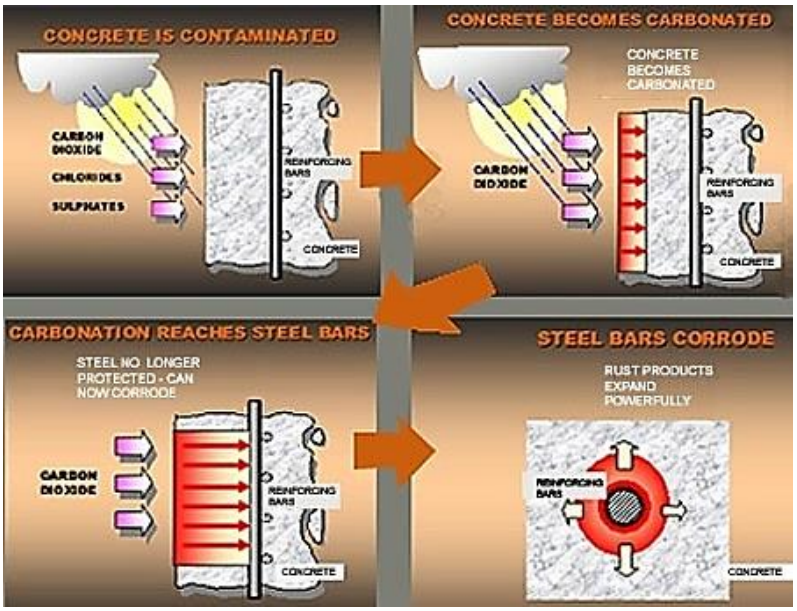

Figure II. 2 Different external attacks on reinforced concrete [53].

II.2.1.2 Pathologies of physical origin

- **Shrinkage**

Shrinkage is a systematic and prevalent physicochemical phenomenon that occurs in concrete at different stages, from setting to aging. It is a multi-faceted process that can be categorized into four types: plastic, drying, thermal, carbonation, and endogenous [54].

- **Freeze-thaw**

Water has a larger volume in its solid form than in its liquid form (for a given mass). In solid water, the molecules arrange in hexagonal mesh formations, creating more space between them. The mass stays unchanged during solidification, but its volume increases by around 10%. The durability of concrete in harsh winter conditions is determined by the material's physico-chemical characteristics and the extent of frost exposure (minimum temperature, water saturation, frequency of spreading melting salts) [55]. Freeze-thaw cycles can result in two forms of concrete deterioration: internal cracking and surface scaling in the presence of melting salts. These two deteriorations are caused by separate processes and may not occur simultaneously. By linking the liquid phase's thermodynamic properties, the hydrated cement paste's porous structure properties, and the environmental exposure characteristics, models were developed to explain, predict, and quantify freeze-thaw damage to concrete [56]. Results from many lab experiments and in-situ concrete behavior studies allowed for understanding the impact of concrete composition parameters on its freeze resistance, particularly the crucial role of entrained air bubble network characteristics. This knowledge forms the foundation for developing test methods, technical guidelines, and normative requirements for building concrete structures that are durable in harsh winter conditions [57].

Figure II. 3 Photo of the concrete bridge subjected to spalling [57].

- **Fires**

The fire resistance of concrete is influenced by its composition, permeability, water content, and mechanical strength [58], it also depends on the fire's temperature rise speed, maximum temperature and exposure duration. A fire can cause a gradual loss of mechanical strength and surface spalling in concrete, which varies based on the type of concrete used. High-performance concrete is more susceptible to spalling if not formulated properly. Understanding the physical, chemical, and mechanical processes that occur in concrete during high temperatures helps explain its behavior under fire stress. Recent studies have evaluated the role of concrete composition parameters and the effectiveness of polypropylene fibers in preventing spalling. This information improves the ability to build fire-resistant concrete structures [59].

II.2.2 Method of repairing reinforced concrete structures

II.2.2.1 Introduction

The repair of a structure, after proper diagnosis, restores not only the original steel and concrete sections but also the mechanical properties of the elements. It allows the structure to take on forces as well as it can [60]. Reinforcement or repair involves adding material in areas where sections are overstretched or degraded. Protection of the structure may be necessary to seal or limit corrosion, depending on the case. The goal of repair is to restore the structure's initial load-bearing capacity and rigidity, and possibly reinforce it to enhance performance or prolong its life. Various technologies for repairing and maintaining structures have been used for years [61, 62]. Different methods exist for repairing cracks, including those for active or stable cracks, and those that improve mechanical strength or appearance [63].

II.2.2.2 Surface repair

- **Reinforcement clearance**

The surface preparation before repair is crucial for the repair's longevity. The first step is to remove all areas of weak cohesion. If the reinforcement is corroded, it's important to expose healthy steel; various techniques can be used to confirm the corroded areas are reached (chiseling, transplanting, bush-hammering, water jet,

sandblasting) [64]. To ensure a successful repair, the concrete surface should be cleaned of all dust and dirt. If the steel loss is significant, replacement of the reinforcement may be necessary, such as sealing or welding. The leveling method involves restoring the reinforcement coating manually using a repair mortar with specific properties that will be discussed later [65]. To prevent corrosion in the repaired areas, the mortar's formulation can include corrosion inhibitors.

The mortar should have these properties:

- Good vertical holding without formwork
- Quick strength gain and greater mechanical strength than the concrete support
- Adhesion equal to or greater than the support cohesion
- Water and aggressive agents impermeability
- Thermal expansion and elastic modulus match the concrete support.

- **Reinforced concrete lining**

The reinforced concrete lining involves adding extra reinforcement and a new concrete layer on top of the existing element, to increase its section size (as shown in Figure II.4). The formwork for the new concrete layer must be created first for proper anchoring [66, 67].

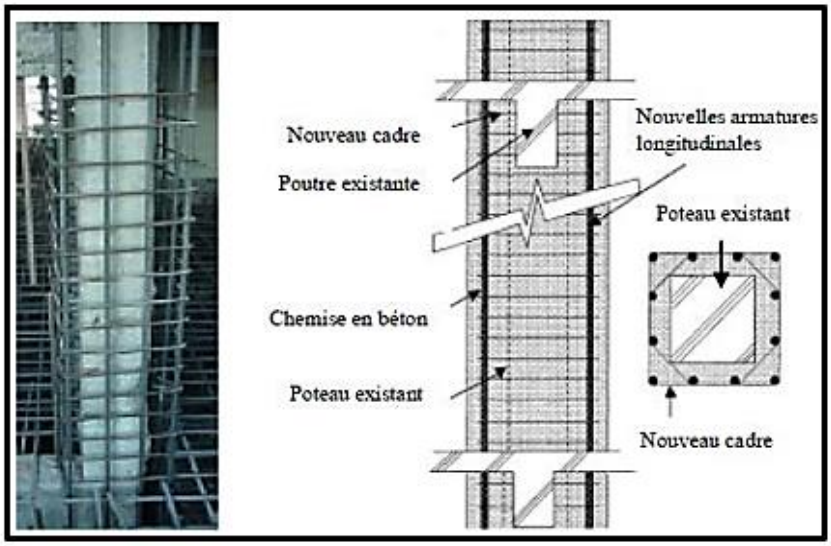

Figure II. 4 Concrete lining method [67].

II.2.2 Behavior of repair materials

II.2.2.1 Polymer materials

Engineers who specialize in repair and restoration must be knowledgeable about how polymers behave in cement-based materials. This study will focus on mortars that are modified by adding polymers, which are commonly used for protecting and repairing structures and buildings. To gain a better understanding of these materials, it's crucial to examine their properties from creation (fresh state) to installation (solid state and durability) [68].

Figure II.5 present a schematic illustration of the effect of the epoxy resin on cementitious mortars.

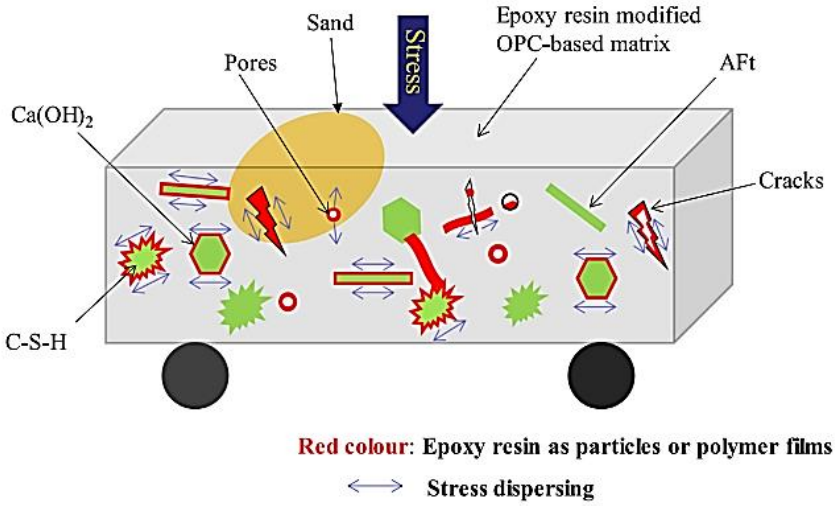

Figure II. 5 The schematic illustration of the toughening effect of the epoxy resin on the OPC-based mortars [69].

- **Definition**

Polymer-based cementitious mortars (PCM) are normal mortars that contain a new polymer component added to the water in the formulation, with a content of 10% to 60% by weight of cement. The polymers used are polymer dispersions, redispersible polymer powders, water-soluble polymers, liquid resins, and monomers. The process by which these monomers link together to form polymer chains is called polymerization[70, 71]. This process is similar to the formation of polyethylene, polystyrene, and polypropylene. Polymer composites consist of three phases: a dispersed phase made of aggregates and reinforcements, a continuous phase made of the binder matrix (cement and/or polymer), and defined by particle size or porosity imposed by the manufacturing process [72], see figure II.6. An infinite number of

mixtures can be made based on the chemical nature, content, and manufacturing method of the components.

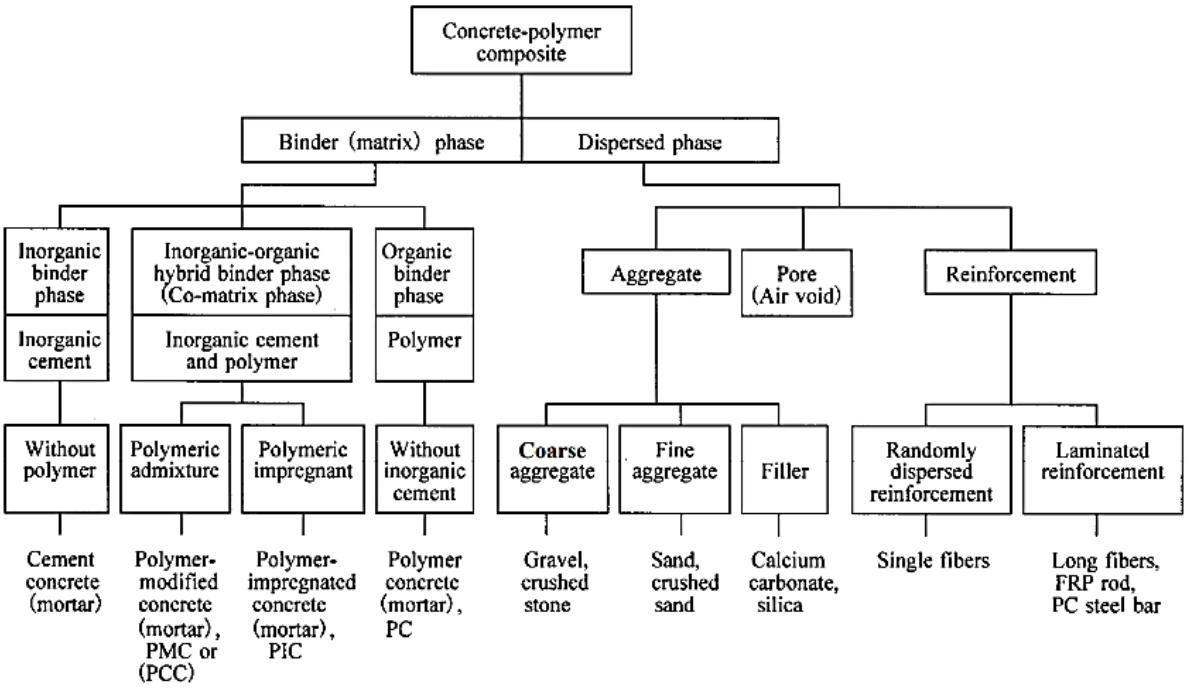

Figure II. 6 System of classification of concrete-polymer composites [73].

Polymer-based cementitious mortars (PCM) have been used in construction, repair, protection, drainage, and adhesive applications since the 1940s. There has been extensive research on PCMs by various experts, including Dhir et al.[74], Rixom, Mailvag- anam [75], Lovell and El-Aasser [76] from the UK, Lovell, El-Aasser and Fowler [77] from the US, van Gemert from Belgium [78], and Ohama from Japan[73]. PCMs are formed by partially or completely replacing the cement matrix, mortar, or concrete with a polymer to reinforce them [79, 80]. They consist of a granular skeleton and a polymer binder, but lack a hydrated cement phase. PCMs can be called resin or polymer mortar when the reinforcements are smaller sized sands or inclusions [81][72]. The polymers used can be either thermoplastic or thermosetting. Figure II.7 lists the most widely used commercial resins in cementitious composites [82]. The role of the polymer binder in modified cement technology is to bind aggregate particles, reduce moisture uptake by filling voids, and provide a workable fluidity in the mixture [72].

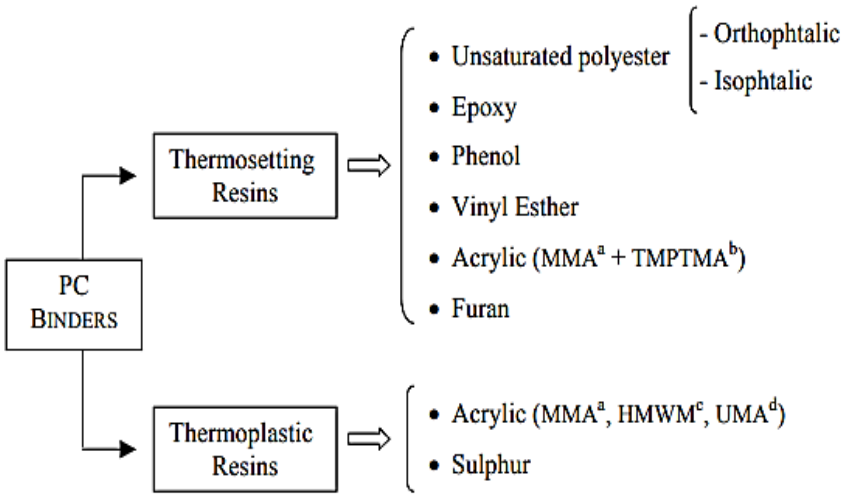

a) MMA -Methyl methacrylate; b) TMPTMA -Ttrimethylol propane trimethacrylate; c) UMA -Urethane methacrylate; d) HMWMA –High molecular weight methacrylate.

b)

Figure II. 7 Commercially available resins currently used as binders in PC materials [72].

- **Fresh properties**

The addition of polymers affects the fresh properties of mortar, improves its workability, extends the setting time and results in higher air content without the use of defoamers [68] (figure II.8). According to Wang et al. [83] survey, the addition of SBR latex reduces the water content of cement slurry mix and the efficiency of water reduction increases with more latex. Barluenga et al's [84, 85] findings concluded that the fluidity of mortar increases proportionally with the SBR latex content. Ohama [86] suggests that this is due to the action of air bubbles and surfactants in the polymer, which lower surface tension through adsorption. Ohama et al [87] explained that the increase in fluidity is due to the dispersion of polymer particles in water, reducing the blockage of the flow of cement hydration products. The presence of SBR latex in cement paste provides excellent workability as it brings air into the paste, reducing the friction resistance of cement molecules [85]. Goto [88] showed from a rheological perspective that the presence of polymers results in an increase in yield point.

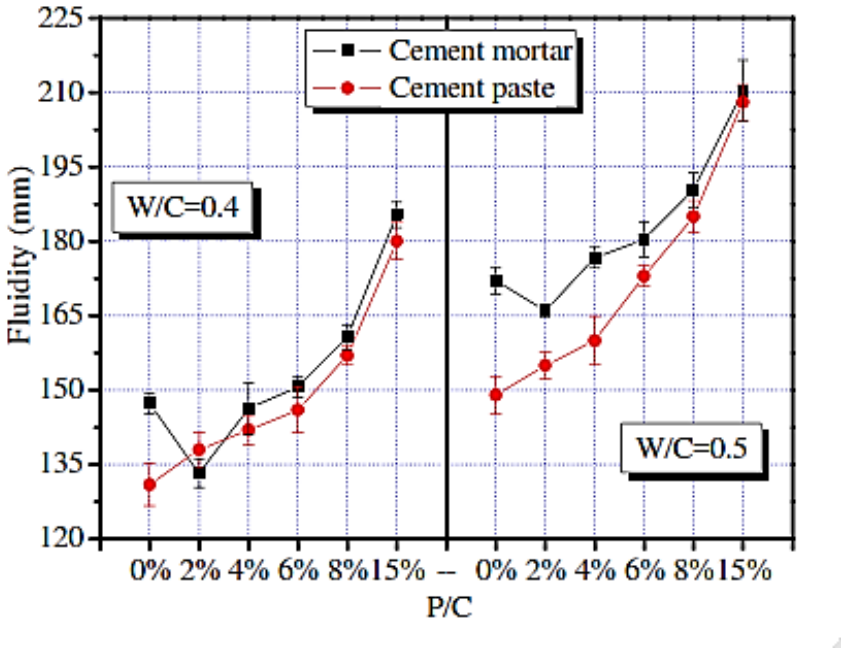

Figure II. 8 Effect of SBR content on the fluidity of mortars and modified cement pastes[84].

- **Properties in the hardened state**

The specific properties of each type of polymeric binder have been shown to greatly influence the properties of hardened mortar. Therefore, the characteristics of the most commonly used polymers in polymeric materials are described in this paragraph. The addition of polymers has been reported to improve several properties in the hardened state of mortars, such as higher tensile and flexural strengths, adhesion, impermeability, and chemical resistance. However, it has also been noted that the addition of polymer can result in a decrease in compressive strength [68]. Ramli et al [89] found that the porosity of a cement mortar containing 15% SBR was at least 5 times lower than that of an ordinary Portland cement mortar after 18 months of hardening. Wang et al. [90] reported that the lowest porosity of mortar was obtained with the addition of 5% SBR latex. The optimal content of SBR latex has been concluded to improve pore structure and durability.

Several studies have reported that the addition of latex polymers to mortars can increase their flexural strength [91, 92]; however, not in compression [93]. On the other hand, reductions in both properties have also been found to occur, depending on the nature and composition of the materials used (polymer, cement, aggregates) and the curing method applied [86, 91, 92]. Li et al [94] found that SBR latex-modified

cement mortar showed the best performance in terms of flexural and compressive strength, weight loss, and capillary adsorption compared to SAE. The effectiveness of the introduction of polymers in repair mortars for fluidity, toughness, and reduced water absorption has been demonstrated by Shi et al. [95]. This is due to the film-forming agent filling the spaces between the substrates, leading to increased adhesion and cohesion of cement mortar and concrete [68, 96-98]. It is known that the properties of polymer mortars (PM) are also influenced by factors such as the type and content of the polymer, the water/cement ratio, and the curing environment [99].

The addition of latex has been found to have various effects on the properties of mortars in their hardened state, including decreasing the dynamic modulus of elasticity and increasing deformation at rupture, damping capacity, and toughness to shocks. Wong et al. [100] showed that as styrene-acrylic ester (SAE) polymer latex was added to the cement at increasing rates, the dynamic modulus of elasticity and rate of propagation decreased, but the impact strength and ductility increased, making these materials useful in structures that must withstand dynamic loads. The addition of PA (polyacrylate) and PU/PA (polyurethane modified by PA) type latexes in mortars with a ratio of E/C=0.5, as reported by Ma et al. [101], resulted in a decrease in the modulus of elasticity for different ages. According to d'Eren et al. [102], the fluidity and mechanical resistance of mortars based on SBR latex were improved by using two different types of latex (styrene acrylate rubber (SAR) and styrene butadiene rubber (SBR)) and five different contents in the formulation of polymer mortars. The bond strength of PCM on clay bricks and cement substrates was found to depend on the polymer-cement ratio[99, 103], and Benali et al. [99] concluded that replacing cement with styrene-butadiene rubber (SBR) improved the fluidity and adhesion of mortars. The specific properties of each type of polymeric binder have a significant influence on the final properties of the hardened mortar, and therefore the main characteristics of the most commonly used polymers in polymeric materials are described here. While the addition of polymer can lead to improvements in several properties of mortars in the hardened state, such as higher tensile and flexural strengths, adhesion, impermeability, and chemical resistance, it also causes a decrease in compressive strength [68]. Finally, Ramli et al. [89] demonstrated that the porosity of a cement mortar containing 15% SBR was at least 5 times lower than that of an ordinary Portland cement mortar after 18 months of hardening.

Wang et al. [90] reported that the addition of 5% SBR latex resulted in the lowest porosity of mortar. It was concluded that an optimal content of SBR latex can improve the pore structure and durability. Several studies have shown that latex polymers can increase the flexural strength of mortar [91, 92], but not compression [93]. However, it was found that the nature and composition of materials used and the curing method applied can lead to a reduction in both properties [86, 91, 92]. Li et al. [94] found that SBR latex-modified cement mortar outperformed SAE in terms of flexural and compressive strength, weight loss, and capillary adsorption. Shi et al. [95] demonstrated that the introduction of polymers in repair mortars improves fluidity, and toughness, and reduces water absorption, leading to increased adhesion and cohesion of cement mortar and concrete [68, 96-98]. It should be noted that the properties of polymer mortars (PM) are influenced by various factors, including the type and content of the polymer, water/cement ratio, and curing environment [99].

The addition of latex is known to decrease the dynamic modulus of elasticity and increase the deformation at rupture of mortars, damping capacity, and toughness to shocks. Wong et al. [100] found that the addition of styrene acrylic ester (SAE) type polymer latex to cement decreases the dynamic modulus of elasticity and the rate of propagation while increasing the impact strength and ductility of the material, making it widely used in structures that must withstand dynamic loads. Ma et al. [101] demonstrated that the addition of polyacrylate (PA) and polyurethane modified by PA (PU/PA) latexes to mortars with a ratio (E/C=0.5) decreases the modulus of elasticity for different ages.

d'Eren et al. [102] improved the fluidity and mechanical resistance of SBR latex-based mortars by using two different types of latex (styrene acrylate rubber (SAR) and styrene butadiene rubber (SBR)) and five different contents in the formulation of polymer mortars. The bond strength of PCM to clay bricks and cement substrates was shown to depend on the polymer to cement ratio [99, 103]. Benali et al. [99] concluded that replacing cement in mortars containing styrene-butadiene rubber (SBR) improved their fluidity and adhesion. Eren et al. [104] found that the use of two different types of latex (styrene acrylate rubber (SAR) and styrene butadiene rubber (SBR)) with five different dosages in the preparation of latex-modified mortars improved their wet properties and mechanical performance. The adhesion strength of PCM to clay bricks and cement substrate was highly dependent on the polymer-

cement ratio, as widely recognized from previous studies, and increased with an increase in the polymer-cement ratio.

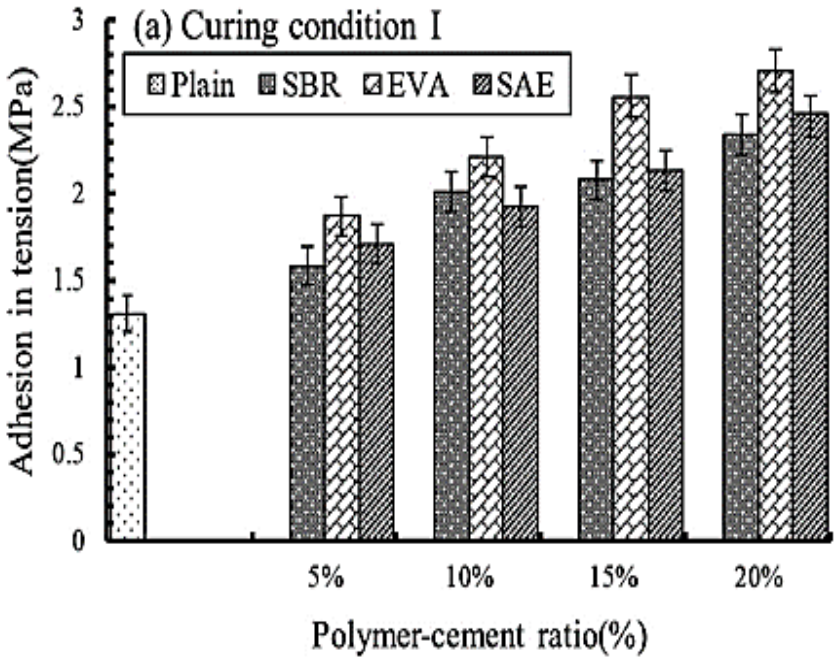

Figure II. 9 Effect of type and dosage of polymer on adhesion [104].

- **Durability**

It was found that polymeric mortars have a high degree of mechanical properties compared to ordinary cement mortar, and that they also exhibit exceptional durability in terms of resistance to freeze-thaw, chloride ions, carbonation, and chemicals, as stated in [105, 106]. The durability of PCM is improved due to the introduction of polymers into the cementitious mortar, resulting in a longer service life, as reported in [107]. It has been shown in previous studies that the resistance of hardened mortar and concrete to chloride ion penetration was increased when SBR latex was introduced into fresh cement mortar, as demonstrated in [108, 109].

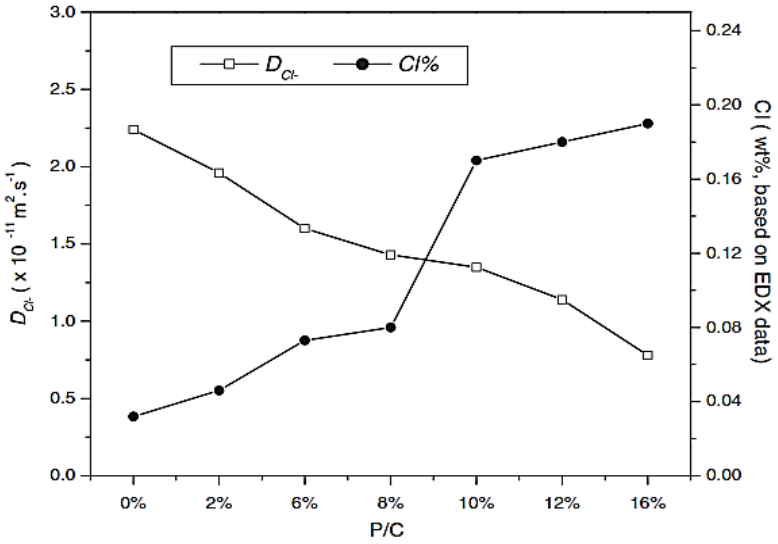

Figure II. 10 Relationship between P/C Ratio and Apparent Chloride Diffusion Coefficient (Left) and Average Chloride Content (Right) [109].

The exact mechanisms underlying the observed improvements in the properties of mortar and concrete due to the addition of SBR (styrene-butadiene rubber) have yet to be fully elucidated. One theory suggests that the polymer films that form in the structures may inhibit cement hydration [110, 111]. However, when tested in isolation, these films did not prove effective in preventing chloride transport, highlighting the need for a more comprehensive understanding of the role of SBR in reducing chloride permeability in concrete and mortar [112, 113].

Several studies have investigated the effect of polymers on the permeability of concrete and mortar to water vapor and liquid water, with consistent findings [114, 115][113, 116]. Polymer films present in the porosity of mortar-polymer composites have been found to slow down the diffusion of harmful substances, such as chloride ions, resulting in greater resistance to penetration [117]. Aggarwal et al. demonstrated that acrylic polymer-containing samples exhibited a reduction in the chloride ion penetration front after immersion in a 2.5% sodium chloride solution for 7 days, and this improvement was found to be correlated with the polymer content [118].

In addition, SBR-modified cement mortars have been shown to possess better resistance to CO_2 penetration than SAR-modified mortars [102]. Li et al. and Lu et al. investigated the sulfate resistance of SAE-modified latex cement and found that it promoted greater impermeability and sulfate resistance in cement mortar [119, 94].

II.2.3 Fiber reinforced composite material

II.2.3.1Definition

FRP composites are synthetic materials consisting mostly of fiber reinforcements held together by a matrix binder [120]. The behavior of these composites depends mainly on the fiber content and the mechanical properties of the materials. The fibers impart highly directional properties to the composites, resulting in anisotropic, linear elastic behavior until failure. Fiber-reinforced polymer technology is a highly effective way to enhance the strength of load-bearing structures. Its application is easy, convenient for users, and not very labor-intensive, making it a desirable alternative for strengthening existing structures. The non-corrosive and chemical-resistant characteristics of carbon fibers give the reinforcement system a longer life than traditional materials like steel, providing long-term economic value [121]. FRP composites are often referred to as "fiber reinforced composite material," "enhanced composite," or "fiber reinforced polymer" and consist of synthetic fibers like fiberglass, carbon fiber, and aramid fiber embedded in a matrix such as epoxy resin or vinyl ester. These composites offer higher strength-to-weight ratios and excellent corrosion resistance compared to conventional construction materials like steel, leading to increased use in civil construction [122]. Research and development efforts (both experimental and numerical) have demonstrated the potential of FRP composites to reinforce existing concrete structures, as seen in various studies (F. Elgabbas et al. 2010, A.S. Mosallam 2000, S S J Moy et al. 2015, C. Gheorghiu et al 2006, Bahira Abdul-Salam 2016, David E et al 1998, R. Madi 2009, Zakia DRAIDI 2005, Bediar Hakim 2003) [120, 123, 124].

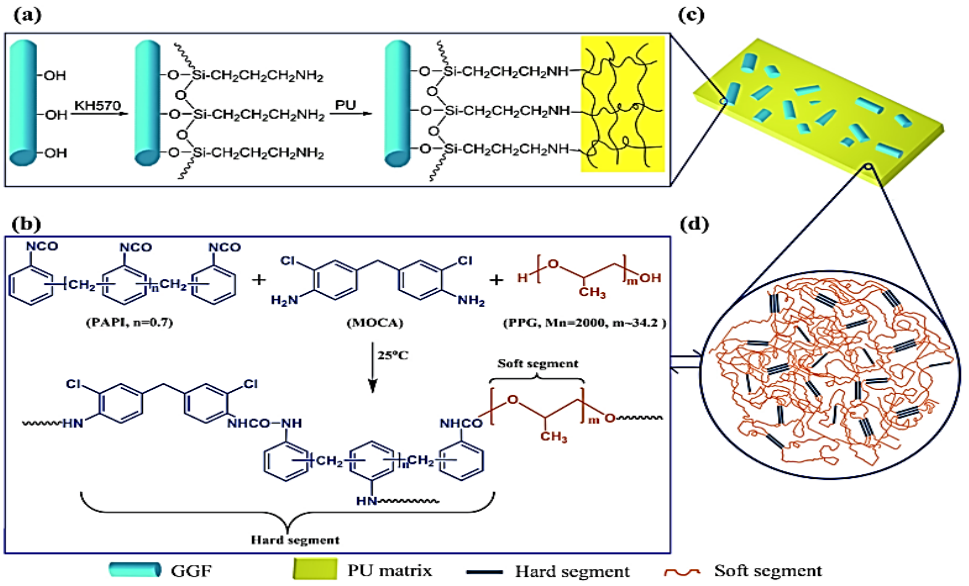

Figure II. 11 Schematic Illustration of GGF Particle Surface Treatment, Potential Interaction with PU, Synthetic Pathway for PU Matrix, Random GGF Particle Distribution, and Microphase Separation in PU Matrix [97].

II.2.3.2 State of the art on polymer composites

Various types of fibers, such as metallic, organic (polypropylene, glass), and plant fibers (e.g., hemp, sisal, and date palm), have been studied for their potential use in reinforcing composites[125]. Studies conducted by Xu et al. [126] and Yang et al. [127]have demonstrated that the addition of 1% polypropylene fiber and 20% SBR latex to cement mortar significantly improves its flexural strength, brittleness index, and abrasion resistance. This is attributed to the formation of a strong bond between the polymer matrix and fibers, which is achieved through the thin polymer films filling the gaps between particles in the composite[125]. The incorporation of glass fibers into polymer mortars has been found to increase their tensile, flexural, and compressive strength by around 8-10% [128-131]. The addition of natural fibers, such as sisal and bamboo, to polymer mortars has also been shown to improve their tensile, flexural, and compressive strength [131, 96, 137]. Furthermore, the use of processed pineapple fibers and wood ash has been found to enhance the bending and compression resistance of polymer mortars, providing good thermal insulation [137, 138]. Plant fibers are compatible with polymers and have good bonding properties, as evidenced by various studies [125, 137, 139, 141]. Finally, the use of commercial acrylic latex in the cementitious matrix has been shown to enhance the bond between chemically treated hemp fibers and the matrix, resulting in a decrease in the water

porosity of the composite [139, 140]. Ferreira et al. [140] found that the incorporation of plant fibers (Curaua, jute, and sisal) with SBR enhanced their bond with the cementitious matrix, increasing tensile strength. However, due to the high cost and CO_2 emissions associated with their production, as well as the use of non-renewable resources, the construction industry is seeking alternative materials [130, 133][134-136]. In 2016, the annual production of natural fibers exceeded 100 million tons, highlighting their economic and ecological significance [137].

II.3 Repair of concrete exposed to high temperature

The exposure of many concrete structures, both residential and industrial, to high temperatures, has been a matter of concern. While demolishing and reconstructing the structure can be costly, reinforcing the element is a well-known method for maintaining its functionality. The behavior of structures reinforced with fiber composite materials at high temperatures has been the subject of extensive study by various researchers [142-144]. The available literature on the repair of post-heated concrete with fiber-reinforced polymer (FRP) is limited. Yaqub et al. [145, 146]investigated the repair of reinforced concrete columns that had been heated to 500°C, examining their uniaxial and cyclic behavior with square and circular sections. Danie Roy et al. [147]exposed short columns to temperatures of 300, 600, and 900°C and repaired them using GFRP, ferrocement (FC), and high-strength fiber-reinforced concrete (HSFRC) sheaths. Haddad et al [148]repaired heat-damaged RC slabs with CFRP, GFRP, and fiber-reinforced concrete (FRC) after heating them to 200°C for 1 minute and then to 600°C for 16 minutes. The study concluded that FRP improved the strength and stiffness of repaired slabs, while FRC improved only stiffness. Haddad et al. [149]evaluated the bond-slip behavior of FRP to heated concrete through shear tests. The concrete was heated to temperatures of 200, 300, 400, 500, and 600°C and repaired with 0.17mm thick CFRP sheets. The results showed that slip increased with temperature, while bond strength was not significantly impacted up to 300°C, but decreased as the temperature increased up to 600°C. Roy et al. [150] evaluated the behavior of GFRP-concrete bonds with different bond lengths through simple shear tests. The concrete was exposed to temperatures of 200, 400, 600, and 800°C and then reinforced with 0.324mm thick FRP sheets. The results revealed that anchorage strength decreased considerably when temperatures exceeded 400°C. Jadooe et al

[151]studied the adhesion behavior of NSM to heated concrete, showing a decrease in anchorage resistance with increasing temperature, but with a reduction of less than 10% when exposed to 200°C for 1 hour. Amiret al [152]investigated the bonding behavior of polymer composite sheets with carbon fibers (FRP) to heated concrete by heating concrete blocks to 300, 400, and 500°C and then reinforcing them with FRP sheets. The results showed that exposing the concrete to high temperatures before FRP installation increased the strength of the anchor, and slippage and effective bond length increased with preparation temperature, resulting in increased anchorage strength (figure II.12 and II.13).

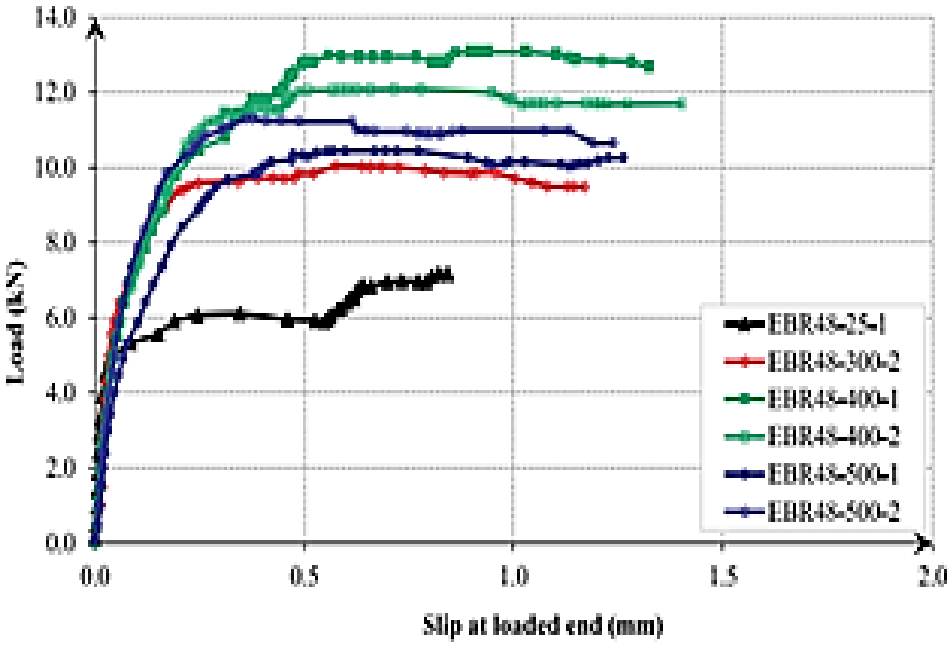

Figure II. 12 Load-slip behavior of tested specimens.

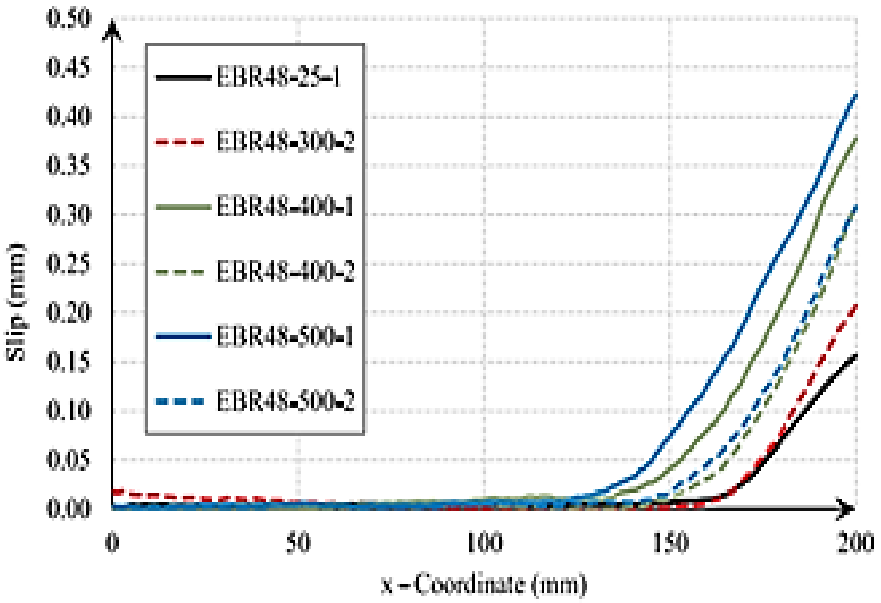

Figure II. 13 Slip distribution along the bond length.

Milad Nimafar et al [153] conducted a study on the use of bacteria to repair concrete damaged by high temperatures. Cylindrical and cubic concrete specimens were exposed to temperatures of 600°C and 800°C for an hour in an oven. Two types of bacteria, Pasteurii and Sphaericus, were then applied externally at a cell concentration of 10 cells/mL to repair the thermal cracks and improve the mechanical properties and durability of the damaged concrete. The effectiveness of the bacterial sanitization technique was evaluated by testing the compressive strength, ultrasonic pulse velocity (UPV), and electrical conductivity on control samples and those exposed to high temperatures, with or without bacterial healing.

The study found that specimens exposed to temperatures of 600 °C and 800 °C experienced a decrease in compressive strength ranging from 31% to 44% compared to control samples. However, specimens repaired with Pasteurii and Sphaericus showed a significant increase in compressive strength ranging from 31% to 93% compared to the damaged specimens (figure II.14). This increase was attributed to the precipitation of calcium carbonate in the deep and superficial cracks and pores of the damaged samples. The ultrasonic pulse velocity of the specimens subjected to bacterial remediation was found to increase significantly by approximately 1.65 to 3.47 times compared to the damaged specimens (figure II.15). In addition, a decrease

of 22-36% in electrical conductivity was noted in the repaired specimens compared to the damaged specimens.

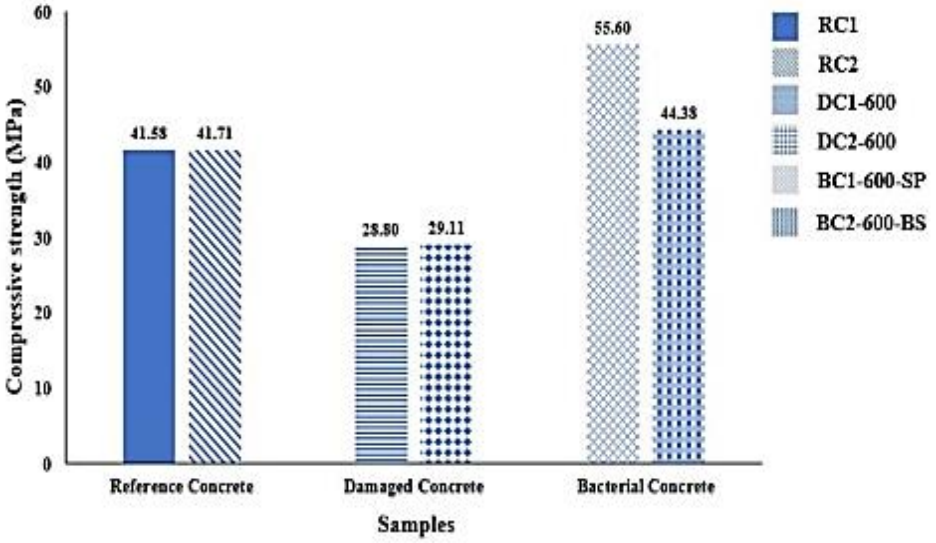

Figure II. 14 Comparing Compressive Strength Results for Control Samples, Samples Damaged at 600°C, and Samples Repaired with Type I and II Bacteria.

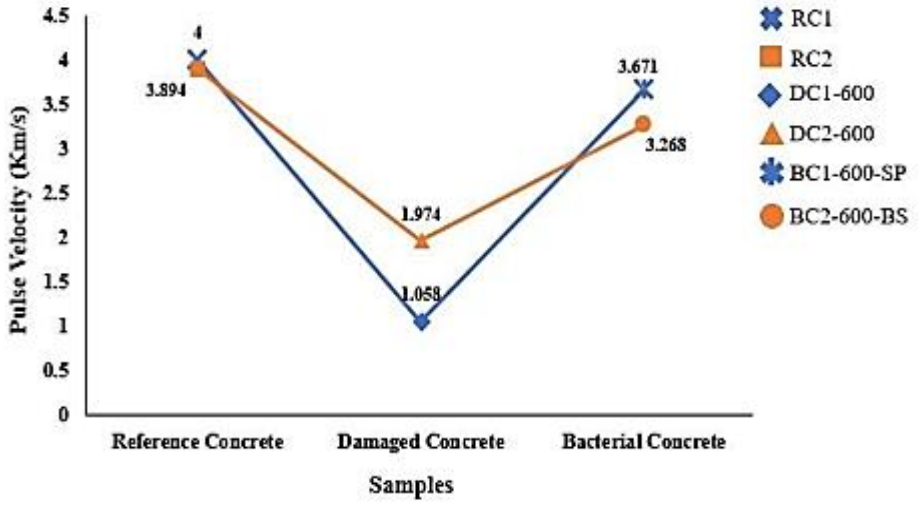

Figure II. 15 Comparing Ultrasonic Pulse Velocity Results for Control Specimens and Specimens Damaged at 600°C: An Analysis of Concrete Structural Integrity.

II.4 Conclusion

The examination of the mechanisms of degradation of reinforced concrete, the corrosion of reinforcements, and some visible flaws have been briefly conducted in this chapter. The purpose of repairing a structure is not only to restore the original sections of steel and concrete but also to revive the mechanical properties of the related elements, allowing the structure to withstand applied loads as best as possible. Among the repair materials, mortar-polymer composites stand out and are widely used for the repair and protection of concrete surfaces. The inclusion of a polymer in the mortar formulation results in enhanced properties such as increased mechanical strength and durability indicators, as well as improved adhesion and reduced permeability.

However, the use of polymer-modified cement mortars has some drawbacks, including longer setting times and low ductility that results in reduced resistance to crack propagation. To address these issues, researchers have focused on incorporating fibers into mortars and concrete to enhance their properties and ductility [154]. Many residential and industrial concrete structures have been exposed to high temperatures, and while demolition and reconstruction can be costly, reinforcing the elements is a common solution to maintain functionality. Although post-heated concrete repair is not widely studied, few studies have been conducted to assess the repair of concrete heated to high temperatures and the problems encountered, such as the bond between repair materials and the heated substrate.

The study presented in this manuscript will be conducted using the experimental approach outlined in Figure II.16 and will be divided into three chapters. In Chapter III, the selection of study materials will be justified, presented, and characterized, and the formulation parameters will be detailed. Chapter IV will focus on the properties of polymer-modified cementitious materials, with the first part examining the fresh-state characteristics of fiber-reinforced mortars incorporating polymers, and the behavior of the hardened state of the mortars at early and long-term ages, while taking into account the influence of fiber type with an investigation using a factorial design approach for statistical analysis. The second part of the chapter will study the repair of substation concrete heated to high temperatures using fiber-reinforced polymer-mortar composites, investigating the influence of the nature of the repair material and method

of repair. Finally, a general conclusion will be made on the entire study, and future research perspectives will be proposed.

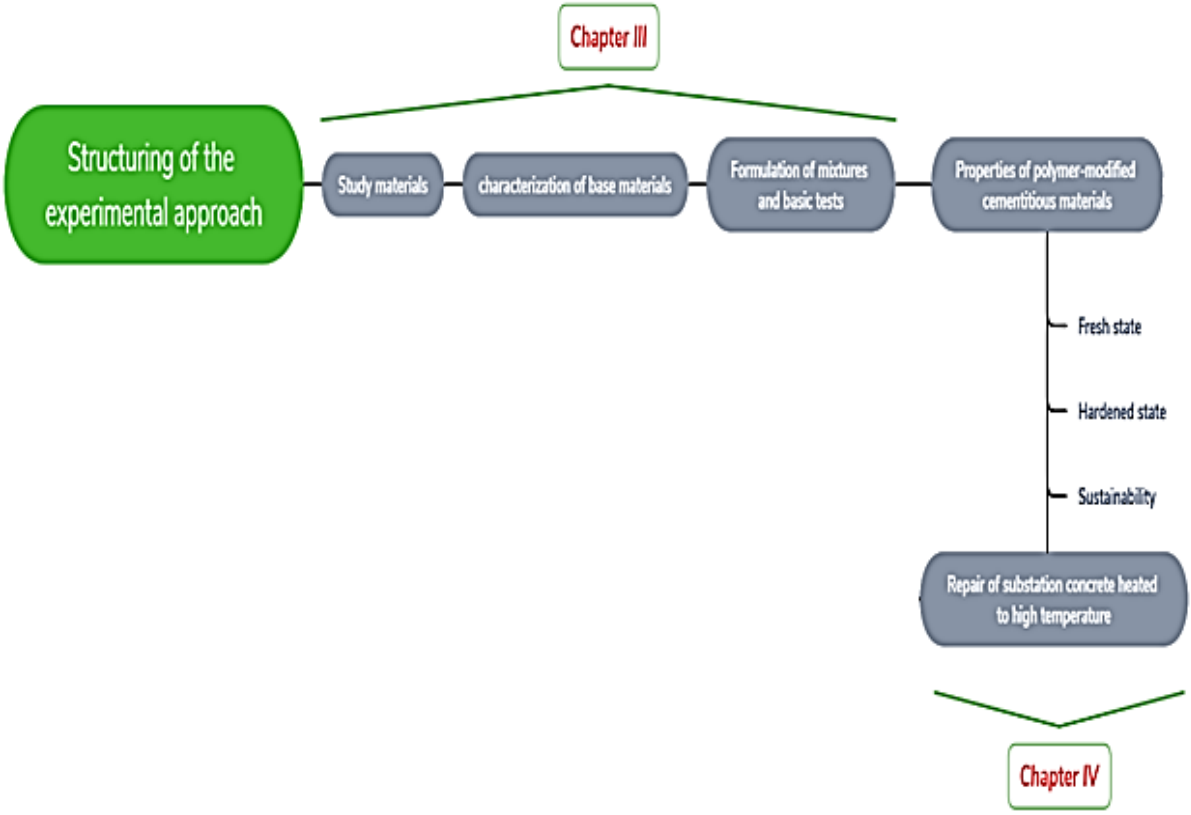

Figure II. 16 Structure of the experimental approach.

CHAPTER III:

CHARACTERIZATION OF BASE MATERIALS AND TEST METHODOLOGY

III.1 Introduction

A bibliographical synthesis was conducted to uncover the main known characteristics of mortar-polymer composite materials, the methods of repair, and general information on the behavior of concrete subjected to fire. By the end of Chapters I and II, a study project was formulated. As a reminder, fiber-reinforced polymer-mortar composites consist of cement, sand, and water to which polymers and fibers are added. To perform the study, it was first necessary to select and characterize the study materials. In this chapter, the materials and the experimental protocols used for conducting the experimental program are presented. Successively, the presentation of tests and procedures, the identification of basic materials used, and the characterization of the produced materials will be carried out. A variety of widely used and locally available constituents are utilized in the production of polymer mortars. The different constituents used are:

- CEM I/42.5
- Silica Fume
- The sand of Oued Souf,
- Tap water from urban networks,
- Hemp vegetable fibers
- Organic fiber (glass).
- “Styrene butadienes” resin from SIKA

III.2 Basic materials

III.2.1 Characteristics of aggregates

It is demonstrated by the standard (NF P18-541) that sand can possess characteristics that make it suitable for the production of mortars. The quality and specific characteristics required for each use in building and civil engineering works must be met by the aggregates used. The determination of its characteristics through various laboratory tests is necessary. The sand used was obtained from Oued Souf deposit, located 620 km southeast of Algiers, which is a natural dune sand primarily composed of small silica particles with clean, generally isometric and rounded grains with dimensions ranging from 0.08 to 3 mm. The coarse aggregates used were of natural origin, crushed limestone from Bordj Bou Arreridj quarry. Two granular classes were

obtained from this quarry, with the trade names of Gravel 5/15 and 15/25. The particle size analysis was used to determine the size and respective weight percentages of the different grain families composing the sample. The results of the test performed on the aggregates used are presented in Figure III.1.

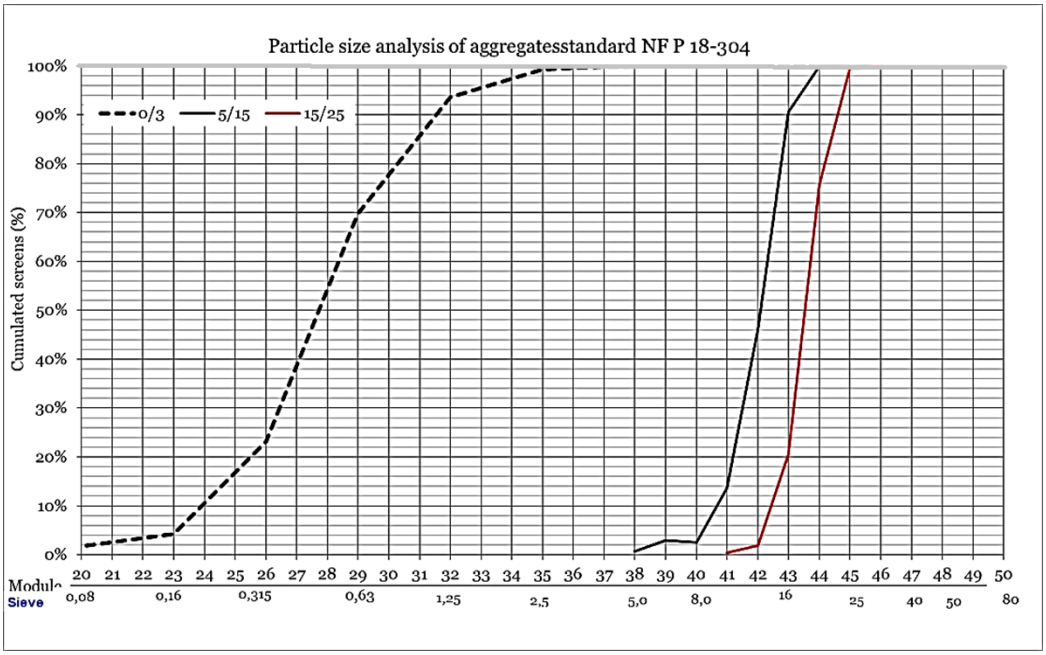

Figure III. 1 Granulometric curve of the aggregates used.

The physical characteristic of density is deemed to be a crucial aspect influencing the behavior of fresh concrete and, as a result, its performance after hardening. Various definitions of densities can be assigned to aggregates, such as apparent and absolute densities (NF EN 1097-3). The equivalent of sand is a parameter that characterizes the cleanliness of the sand and indicates the presence of fine elements, mainly of clay, vegetable, or organic origin, on the grain surface. The physical and chemical characteristics of the various aggregates used are displayed in Table III.1.

Table III. 1 Physical and chemical properties of the aggregates used.

	Absolute density (kg/m^3)	**Apparent density(kg/m^3)**	**ESP The equivalent of sand (%)**
Sand	2608	1617	87
Gravel	2650	1600	/

III.2.2 Cement

The use of CEM I/42.5 type cement was carried out. The technical sheets provided by the cement factory were utilized to establish the various chemical, physical and mechanical characteristics of the cement used. The results of these characteristics of the cement used are presented in Table III.2.

Table III. 2 Chemical and physical characteristics of the type of cement used.

Element	CEM I/ 42.5
CaO	61,60
SiO_2	20,40
Na_2O	/
MgO	1,73
Al_2O_3	5,53
K_2O	/
P_2O_5	/
Fe_2O_3	3,54
SO_3	2,29
Absolute density (kg/m^3)	3100
Apparent density (kg/m^3)	/
Fineness (cm^2/g)	3600

III.2.3 Mineral additions

The mineral addition utilized in this study was characterized by particle size smaller than 80 µm and is sourced from GRANITEX. The main characteristics of these silica fumes are displayed in Table III.3.

Table III. 3 Chemical and physical composition of silica fume.

Element	Silica fume
CaO	0.995
SiO_2	88.60
Na_2O	0
MgO	0,2
Al_2O_3	0.9649
K_2O	0.398
P_2O_5	/
Fe_2O_3	/
SO_3	/
Absolute density (kg/m^3)	2.24
Apparent density (kg/m^3)	1.4
Fineness (cm^2/g)	30000

III.2.4 Mixing water

The use of water in the study was facilitated by tap water that was supplied by the civil engineering laboratory at the University of Bordj Bou Arreridj.

III.2.5 Resin

The selection criteria for the polymers utilized in the study were based on their nature. In civil engineering applications, monomers such as acrylates, styrenes, vinyl acetates, and ethylenes are frequently utilized in latex formulation. The selection of polymers capable of forming continuous films at room temperature was deemed essential. This is because the formation of a high-quality cement-polymer matrix is necessary to achieve the desired properties. A styrene-butadiene resin from SIKA (figure III.2) was used produce the various repair mortars, and its physical and chemical characteristics are presented in ANNEX A.

Figure III. 2 Photo of resin used.

III.2.6 Fibers

In the study, both hemp and glass fibers were used. Hemp, which grows to a height of 1 to 3 meters and is grown in China, Canada, and Europe [139, 155], was used for its high tensile strength ranging from 600 to 1100 MPa, making it suitable for use in industries such as the paper industry and the reinforcement of cementitious materials like concrete. With a length of approximately 1.5 cm, the fibers were utilized in the study.

To enhance the adhesion of the fibers to the polymer matrix, a 5% sodium hydroxide solution was used to treat the hemp fibers for 2 hours at 20°C. This chemical treatment was carried out to eliminate the lignin and waxy substances that coat the

outer surfaces of the fiber cell walls, thereby improving the fibers' adhesion to the matrix. The fibers were then dried at 40°C in front of a radiator. Sodium hydroxide (NaOH) is commonly utilized as a chemical for cleaning and/or bleaching plant fiber surfaces [130].

The processed hemp and glass fibers are displayed in Figure III.3, and the physical, chemical, and mechanical properties of both fibers are presented in Table III.4. The glass fibers, with a length of 1.5 cm, were also used in the study.

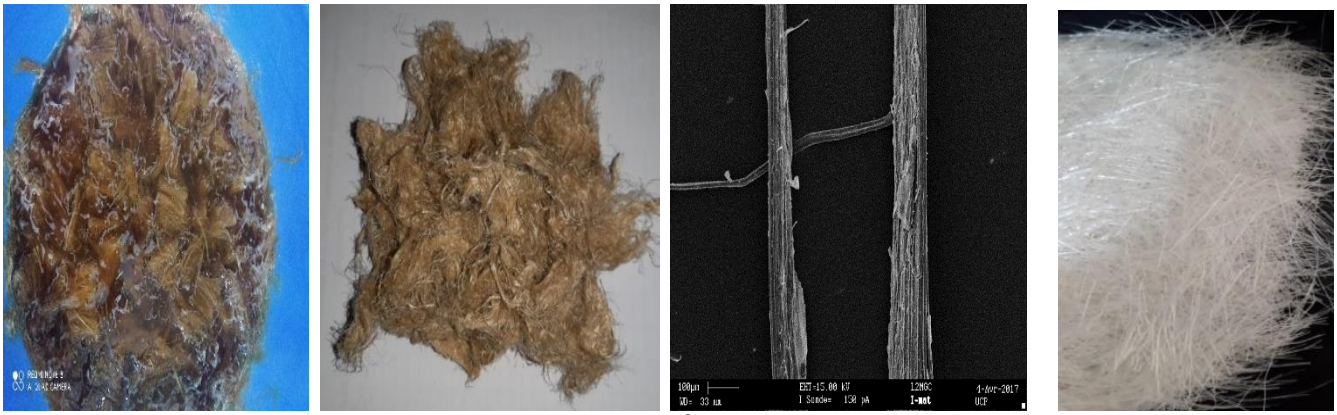

Hemp immersed in 5% NaOH solution | Hemp after treatment | Fiberglass

Figure III. 3 Hemp and glass fibers used.

Table III. 4 Physical, chemical, and mechanical characteristics of hemp and glassfibers.

Fiber properties	**Glass [120]**	**Hemp [157]**
Absolute density (kg/m^3)	2600	1580
Lignins (%)	/	6
Cellulose (%)	/	56.1
Hemicelluloses (%)	/	10.9
Ash (%)	/	/
Tensile strength (MPa)	3400	619.2
Maximum training (mm)	/	0.682
Absorption of water (%)	/	158
Diameter (µm)	13−15	110
Length (cm)	1.5	1.5

III. 3 An investigation using a factorial design approach for statistical analysis

Factorial design is a statistical technique that can be effectively used to organize experimental studies, enabling an optimal evaluation of main and interaction effects among independent variables known as factors 'xi', and outcome variables known as responses 'Y'. By employing a full factorial design, it becomes possible to construct an empirical model, enhance and optimize process factors, and examine the interactions between various parameters.

To assess the physical and mechanical properties of mortars, an experimental factorial design was employed. This design aimed to explore the impact of the fiberglass content and SBR content on compressive strength, flexural strength, water absorption, and total shrinkage. The effects of the considered factors and their interactions were analyzed using Analysis of Variance (ANOVA). The obtained results were evaluated and analyzed using JMP16 software.

III.3.1 Approach to Experimental Design Development

To model the responses (compressive strength, flexural strength, water absorption, and total shrinkage), the following steps were undertaken:

The first step involved identifying the influential factors and establishing a mathematical model to predict the experimental values of the responses based on the effect variables.

Next, an analysis of variance was conducted to differentiate the effects of the factors on the obtained responses.

The mathematical models were then employed to generate iso-response curves.

In this study, a factorial equation based on a second-order model with a two-factor interaction was utilized and can be expressed as follows:

$$Y = \beta 0 + \beta 1A + \beta 2B + \beta 12AB \quad \text{.....(1)}$$

Here: Y: represents the predicted response, β0: denotes the constant coefficient to offset terms, A and B: refer to the independent factors, with B representing Fiber glass content (%) and A indicating SBR content (%) respectively, β1 and β2: represent the coefficients for the linear effect factors, β12: signifies the coefficient for the interaction effects.

III.4 Composition of different cementitious mixtures

III.4.1 Polymer mortar

This study involved incorporating different amounts (0.1%, 0.3%, and 0.5% based on the total volume of the mortar) of hemp and glass fibers into a mortar that contained 5% styrene-butadiene rubber (SBR) latex. The optimal content, determined in the laboratory, was established to be the amount that provided good compressive and flexural strength. The results were compared with two reference mortars: one contained only cement as the binder and the other contained only 5% SBR latex. The cement-to-sand ratio was set at 1:3 by weight, and the water-to-cement ratio used to prepare the control mortar was 0.5. The water-to-cement ratio of the polymer mortar was adjusted by reducing the amount of water based on the presence of SBR.

Since latexes are polymers suspended in an aqueous phase, the polymer content of latexes is a crucial piece of information for determining the formulation of cement pastes or mortars. In this study, the initial quantity of water in the samples subjected to controlled drying was fixed, and the polymer content was determined by evaporating the aqueous phase of a known mass of latex at room temperature. The ratio between the final mass, obtained after 24 hours, and the initial mass is the polymer content of the latexes. The results showed that the SBR latex had a polymer content of approximately 45%.

The mortars were made according to the EN 196-1 method for making polymer-modified mortars containing fibers. Fresh mortars were cast in metallic molds, covered with a film, and stored in the laboratory for 24 hours. They were then stored in water at 20 ± 2°C for 6 days and outdoors at 20 ± 3°C and 55 ± 10% relative humidity for 7, 28, and 60 days. This curing mode was determined to be the most suitable for polymer-modified mortars in terms of mechanical and physical properties, according to references [104] and [99]. The samples used to determine adhesion to cementitious supports were kept in water at 20 ± 3°C until the test day. The different compositions of the mixtures are listed in Table III.5.

Table III. 5 The compositions of the different mixtures of mortars used for $1m^3$.

Designation mixtures	Cement (kg/m^3)	SF (kg/m^3)	Sand (kg/m^3)	SBR (Kg/m^3)	Water (Kg/m^3g)	Fiber (kg/m^3)
CM	527,34	58,6	1757,81	0	0.33	0
M5R	527,34	58,6	1757,81	0.065	197.5	0
M5R-0.1H	527,34	58,6	1757,81	0.065	0.25	1.74
M5R-0.3H	527,34	58,6	1757,81	0.065	0.25	5.25
M5R-0.5H	527,34	58,6	1757,81	0.065	0.25	8.73
M5R-0.1G	527,34	58,6	1757,81	0.065	0.25	3.04
M5R-0.3G	527,34	58,6	1757,81	0.065	0.25	9.19
M5R-0.5G	527,34	58,6	1757,81	0.065	0.25	15.32
M10R	527,34	58,6	1757,81	0.13	0.22	0
M10R-0.1G	527,34	58,6	1757,81	0.13	0.22	3.04
M10R-0.3G	527,34	58,6	1757,81	0.13	0.22	9.19
M10R-0.5G	527,34	58,6	1757,81	0.13	0.22	15.32

III.4.2 Ordinary concrete

Dreux-Gorisse method was utilized for formulating the concrete. This method enables the determination of a suitable concrete composition that meets the required resistance and workability based on the specific characteristics of its constituents, such as cement and aggregates. 36 cubic specimens measuring 10x10x10 cm^3, meant for high temperatures applications, were cast. After 28 days, compression tests were performed on these cubic specimens using a 3000 KN compression machine and it was determined that a strength of 43 MPa was achieved.

Table III. 6 The composition of concrete.

	Cement (Kg/m^3)	Sand (0/5) (Kg/m^3)	Gravel 5/15 (Kg/m^3)	Gravel 15/25 (Kg/m^3)	Water (Kg/m^3)
Quantities for $1m^3$ of concrete	375	636.28	332.13	854.07	190

III.5 Experimental techniques

As mentioned above, the components, preparation method, and preservation method are discussed (composition of different cementitious mixtures). Now, we are reviewing the aforementioned in Figure III.4 and Figure III.6.

III.5.1 Preparation of polymer mortar samples

Figure III.4 shows the main procedures used to make different mortars.

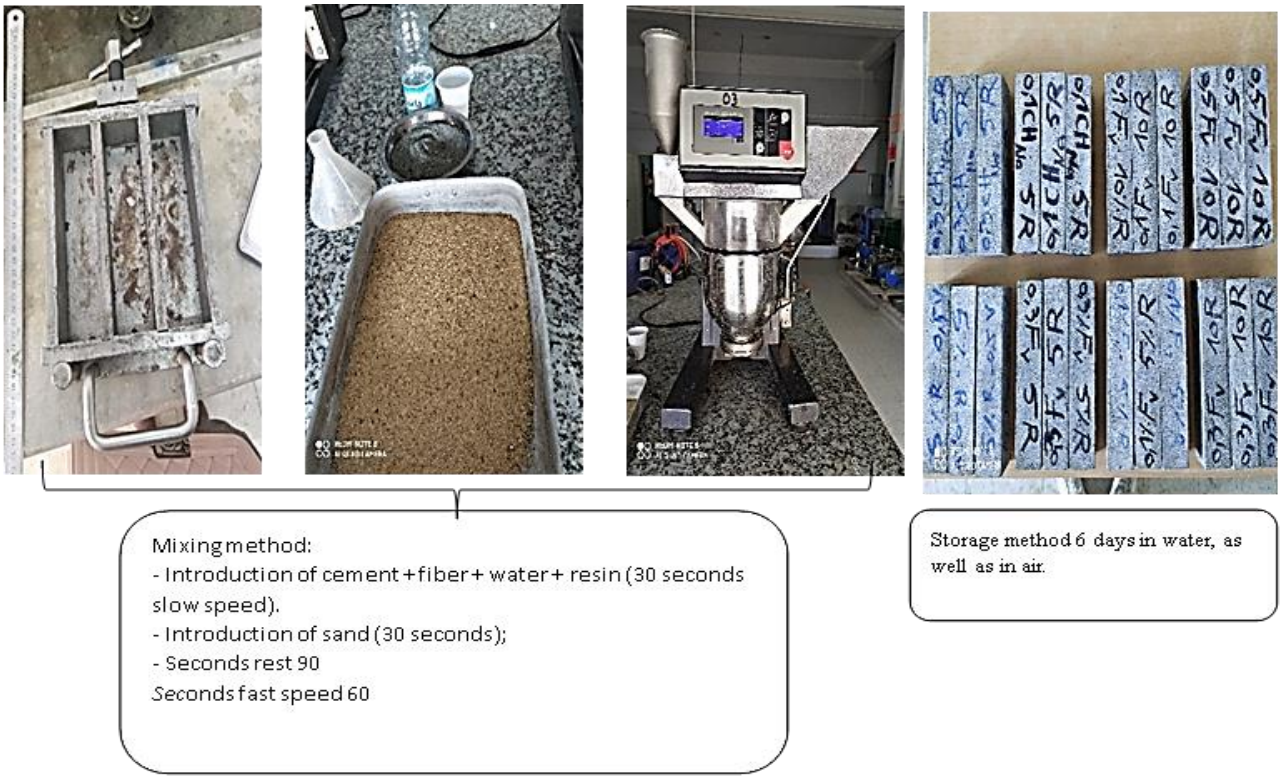

Figure III. 4 Mixing process and how to store polymer mortars.

Figure III. 5 Preparation of substrate mortar and polymer mortar test specimens for adhesion testing.

III.5.2 Concrete preparation

Figure III.6 shows the main procedures used to make ordinary concrete.

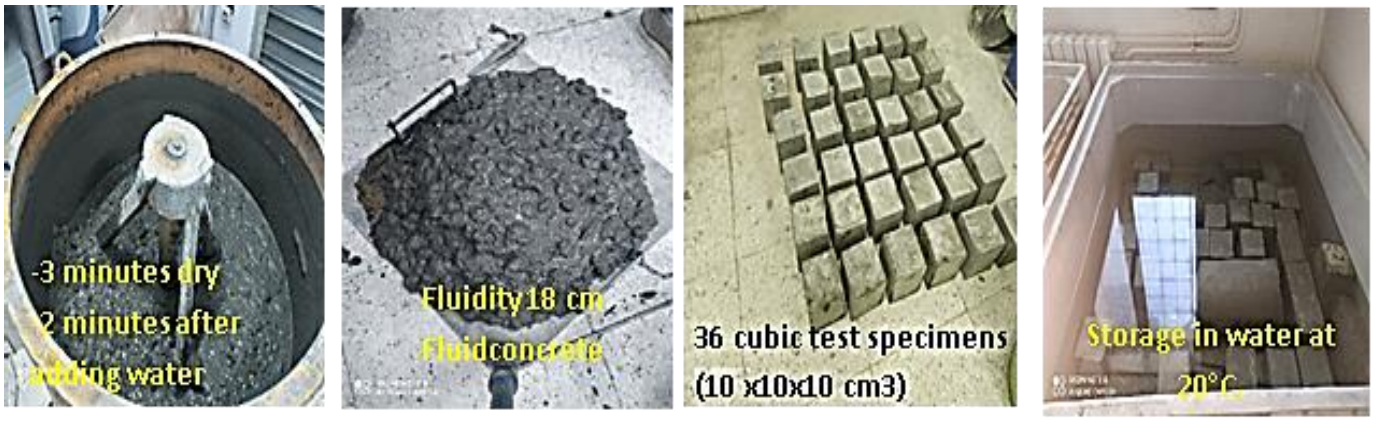

Figure III. 6 Method of mixing and preserving ordinary concrete.

III.5.3 Tests of polymer mortars in the fresh state

The fluidity of cement-based materials is a widely utilized property in construction for determining their rheological behavior and consistency. The fluidity test is conducted using the vibrating table test following ASTM C 1437-20 [157] using a conical mold that meets the standard's specifications (70 and 100 mm in diameter, 50 mm in height). Each composition is tested three times to ensure the reliability of the results. The wet density of the mortars was determined by using a cylindrical container with a volume of 83 cm^3. This method allows for the determination of the bulk density of the

cured product, which is calculated as the mass of a sample with dimensions of 4x4x16cm^3.

Figure III. 7 The flow test of polymer mortars.

III.5.4 Mechanical performance of polymer mortars

III.5.4.1 Compressive and flexural strength

Compressive and flexural strength of polymer mortars was performed following the standard EN 196-1 [158], with samples of dimensions (4x4x16 cm^3) being evaluated at 7, 28, and 60 days.

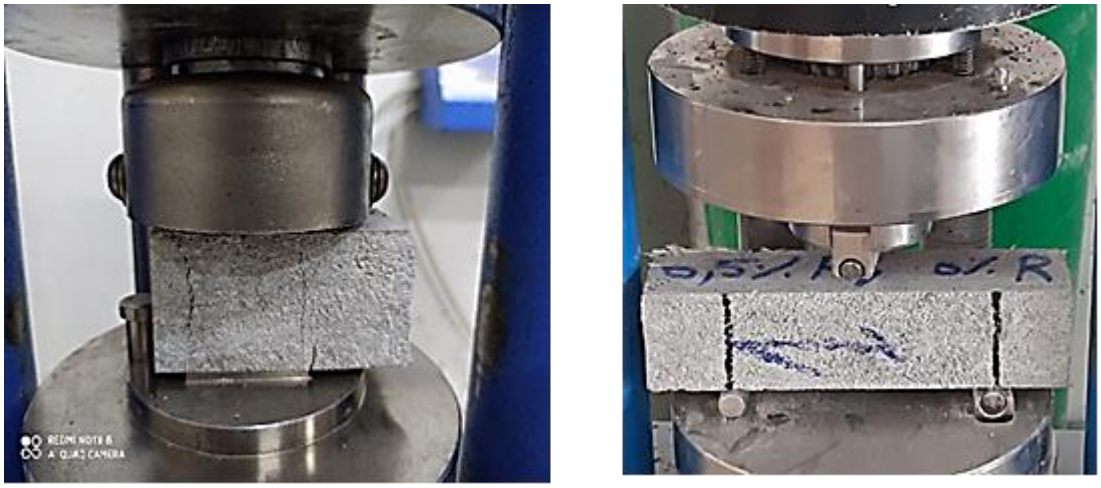

Figure III. 8 Compressive and flexural strength of polymer mortars test.

III.5.4.2 Adhesion test

The use of polymers in cement mixtures is often proposed by researchers as a means to enhance the adhesive properties and longevity of the mixture. The successful preservation and repair of structures are largely dependent on the method of conservation, as noted in references [99, 159, 160]. In this study, the bond strength was evaluated through a bending-tensile method (as illustrated in Figure III.9). To optimize adhesion and prevent water absorption in the fresh mortar, it is recommended to maintain a substrate saturation level between 50% and 90%, following the guidelines provided in reference [161]. The tested mortars underwent evaluation after undergoing 28 days of hardening.

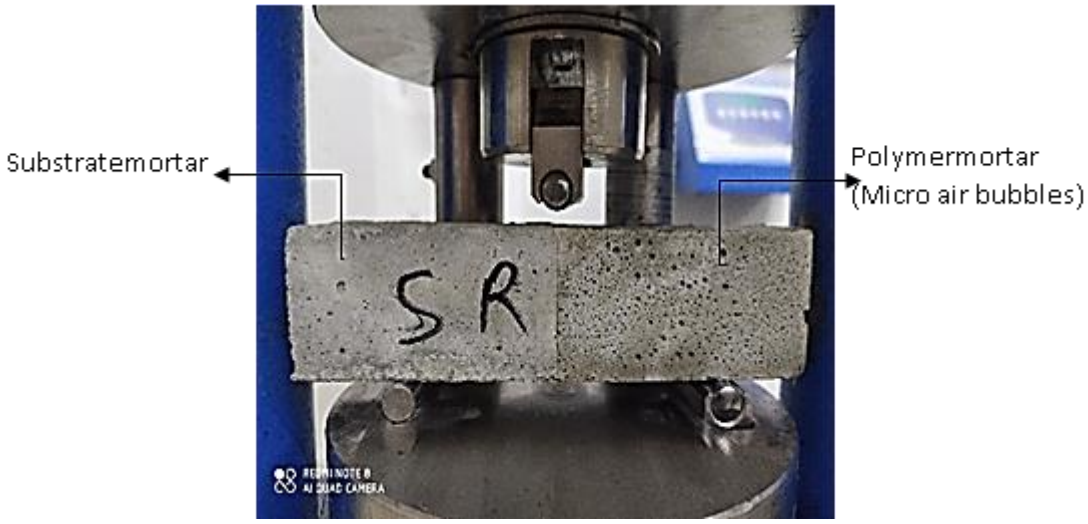

Figure III. 9 The evaluation of the adhesion between the polymer mortar and the substrate mortar.

III.5.5 Physical performance of polymer mortars

III.5.5.1 Dimensional variations (shrinkage)

In this study, the shrinkage of each mixture was evaluated using 4x4x16 cm^3 prismatic test specimens, which are measured longitudinally. The measurements are taken using a refractometer with an accuracy of ± 0.001 mm, as depicted in Figure III.10. The test specimens were kept in an open-air environment with a temperature of 20 ± 2°C and a relative humidity of 55% ± 5%.

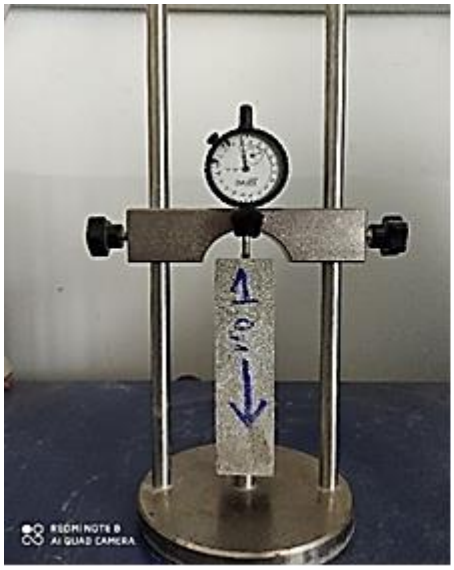

Figure III. 10 Dimensional variation measurement(shrinkage).

The shrinkage formula is interpreted by the relative variation in length. It is generally denoted by ε and calculated as follows:

$$\varepsilon(t) = \frac{L(t)-L(t_0)}{L} \qquad \text{(III.2)}$$

Where: L: the length of the standard rod l = 160 mm.

L(t): the length of the specimen at time t

$L(t_0)$: the length of the specimen at time t_0 chosen as the origin. In general, this origin is taken at the time of demoulding, i.e. 24 hours after the manufacture of the test specimens.

III.5.5.2 Capillary porosity

The transfer of liquid within a porous material due to surface tensions in its capillaries is referred to as water absorption. This transfer mechanism is influenced not only by the porous structure but also by the relative humidity of the mortar. The absorptivity or the amount of water absorbed inside the dry mortar through capillary rise depends on its open porosity and porous networks, as stated in reference [162]. This test aims to observe the mass of water absorbed by fiber-reinforced mortars over time and to determine any differences in their open porosity. Following regulations outlined in reference [163], a test to determine the water absorption by capillarity can also be conducted at 28 days. For each mixture, two prismatic specimens were prepared. The

capillary coefficients were determined by using samples that were preconditioned and dried in an oven at approximately 105 ± 5°C. The test sample was placed in a mold and exposed to water through a 40x40 mm^2 cutting plane, with the water level in the tank maintained at around 1cm above the bottom of the test tube. The sample surfaces below the water level were covered with self-adhesive aluminum foil to ensure unidirectional flow. The capillary absorption coefficient (C), expressed in (kg/mm^2), was calculated for the following time intervals: 0.15, 0.3, 1, 2, and 24 hours. The calculation was based on the following relationship:

$$Ab = \frac{M_0 - M_i}{A} \qquad \text{(III.4)}$$

Mi, M_0, A: are the initial mass, the mass measured over time, and the surface in contact with water in mm^2 respectively.

Figure III. 11 Capillary absorption tests.

III.5.6 Scanning Electron Microscopy (SEM) Analysis

Scanning Electron Microscopy is a technique for observing matter using an electron beam after the sample has been placed in a vacuum. Primary electrons from the electron gun strike the surface of the sample, and they are scattered both elastically and inelastically. The influenced area takes the shape of a pear.

Scanning Electron Microscopy (SEM) was employed to analyze the morphology and microstructure of mortar samples at room temperature.

Figure III. 12 Scanning Electron Microscopy (SEM).

III.5.7 Thermogravimetric analysis (TGA)

Thermogravimetric analysis (TGA) involves measuring the mass variation during heating. The samples were crushed into powder form. Each sample was subjected to heating at a rate of 10 °C/min up to 900 °C under an Argon atmosphere. The derivative of the thermogravimetric curve was used to determine the temperature of phase changes.

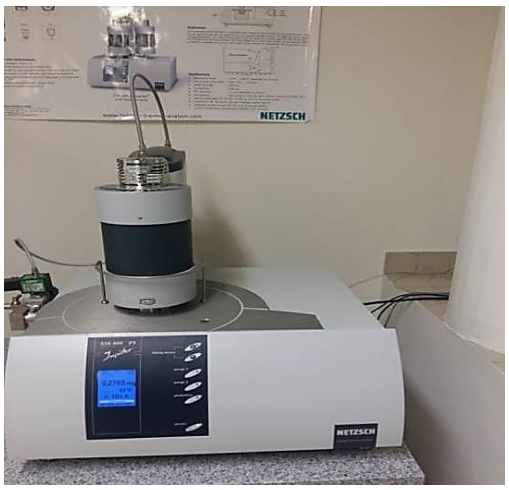

Figure III. 13 Thermogravimetric analysis apparatus.

III.5.8 Heating test

In order to study the effect of repairing concrete that has been subjected to fire, cubic test specimens measuring 10x10x10 cm^3 made of ordinary concrete are first subjected to a temperature of 750°C using a programmable oven. The specimens are heated to this temperature over 1 hour with a ramping speed of 3.5°C per minute. This process aims to simulate the conditions that concrete may encounter in real-world fire scenarios, providing valuable insights into the repair and preservation of concrete structures that have been affected by the fire. Figure III. 14 shows the specimens in the oven.

Figure III. 14 Photos of the test specimens in the ovens.

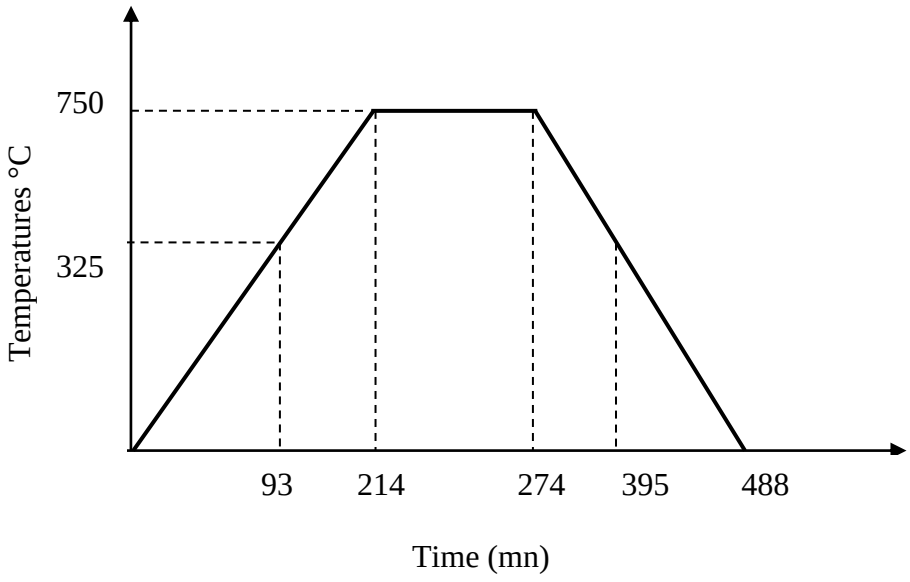

Figure III. 15 Heating-cooling cycles (heating rate 3.5°C/min).

Figure III. 16 Storage of heated test specimens.

III.5.8.1 Compressive strength test of heated concrete

After the concrete heating stage, we have deduced the compressive strength.

The application of the mechanical load is carried out with a hydraulic press of capacity 3000 KN. The loading speed is kept constant throughout the test using a hydraulic press rate meter (5 KN/s). Compressive load is applied until the specimen ruptures. The maximum load reached is recorded and the stress of rupture is obtained by the following formula:

$$fc = \frac{Fmax}{S} \qquad \text{(III.4)}$$

F_{max} denotes the breaking load in compression and S is the cross-sectional area of the test piece.

Figure III. 17 Apparatus for measuring the compressive strength of heated concrete.

III.5.8.2 Ultrasonic Pulse Velocity (UPV)

This non-destructive test allows determining the propagation velocity of longitudinal (compressional) waves. Measuring the speed of sound wave propagation offers a significant advantage by providing information about the interior of a concrete element. The test is therefore used to assess material homogeneity and detect cracking, voids, and fire-induced deteriorations. Consequently, the primary objective of this method is to obtain maximum information about the quality of concrete subjected to temperature elevation.

The principle of the method consists of measuring the time taken by a wave, which gives its name to the method, to travel a known distance. The apparatus includes sensors in contact with the concrete, a wave generator, a time measurement circuit, and a digital display of the time taken by the longitudinal waves to traverse the concrete between the transducers. The standard P 18-418 [NF P 18-418] describes the testing method.

The velocity of the waves, V, is calculated by the formula:

$$\mathbf{V}=\frac{\boldsymbol{l}}{\boldsymbol{t}}\ (\text{m/s}) \qquad \text{(III.5)}$$

Where: $\boldsymbol{l}$: is the distance between the transducers (m).

$\boldsymbol{t}$: is the propagation time (s).

In the case of concrete subjected to fire, the temperature elevation causes a physicochemical modification of the material. Sonic inspection, based on travel time measurements, is a particularly well-suited method for this type of investigation [162].

Figure III. 18 UPV measuring device.

III.5.8.3 Modulus of elasticity and damage coefficient

The dynamic elastic modulus (Ed) is a key parameter for structural analysis of concrete under dynamic conditions such as seismic loads. It is not accurately determined directly from standard cylinder compression tests. It is obtained from non-destructive testing, specifically the ultrasonic pulse velocity (VP), which is widely used to calculate Ed.

$$E_d = \frac{(1+\upsilon)(1-2\upsilon)}{(1-\upsilon)}\gamma.V \qquad \text{(III.6)}$$

Where: $\boldsymbol{\upsilon}$**:** Poisson's ratio =0.2

$\boldsymbol{\gamma}$**:** absolute density

$\boldsymbol{V}$**:** ultrasonic pulse velocity.

When concretes were exposed to high temperatures, the evolution of damage could be described by a Weibull distribution model [99] . This model is expressed by equation:

$$D_V^T = 1 - (\frac{\rho^T}{\rho^{20}}) \times (\frac{V^T}{V^{20}})^2 \qquad \text{(III.7)}$$

where $D_V^T, \rho^T and\ V^T$ represent the damage coefficient, absolute density, and impulse velocity at a given temperature, respectively. ρ^{20} and V^{20} represent the absolute density and impulse velocity at 20°C.

III.5.8.4 Surface preparation

Cleaning the surface is essential for the removal of debris and dust, enabling the attainment of a pristine surface. This, in turn, facilitates optimal adhesion between the repair material and the existing concrete substrate.

To initiate the repair procedure, the surface was thoroughly cleansed using a cloth to eliminate any residues and dust present on the samples. Subsequently, a hand saw was employed to carefully remove the severely damaged top layer of concrete, measuring approximately 2cm in depth (refer to Figure III.19). Finally, before commencing the repair, the interface was meticulously cleaned once again to ensure optimal conditions.

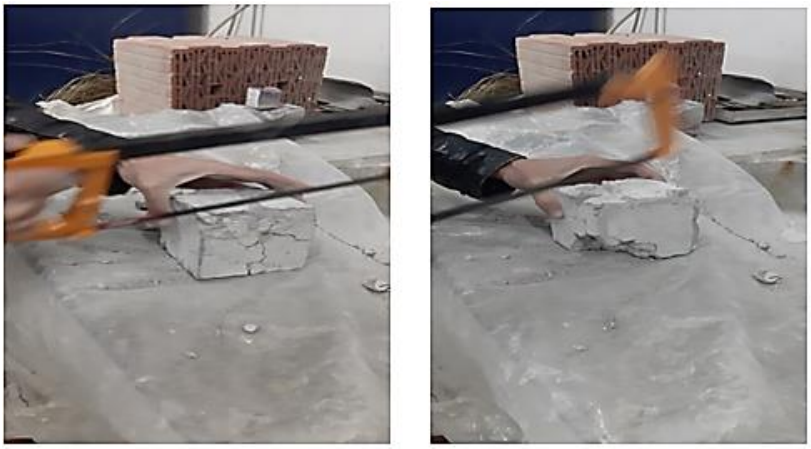

Figure III. 19 Elimination of the uppermost deteriorated layer of concrete.

III.5.8.5 Repair method

In order to repair concrete that has been damaged due to high temperatures exposure, the most effective polymer mortar that provides strong adhesion resistance was used.

After recovering the undamaged part of the concrete, we put it in a mold that measures 15x15x15cm^3. Then, both our prepared repair concrete and a commercially available repair mortar were introduced into the mold, as illustrated in the figure III.20. After the repair process is completed, the repaired specimens will be placed in

an open-air cure for a maximum of 28 days. Additionally, our new repair mortar will be compared to the commercially available product known as Sika.

Figure III. 20 Repair procedures for specimens heated to 750°C with both our prepared repair concrete and a commercially available repair mortar.

Figure III. 21 The repaired specimens after demolding.

III.6 Digital image correlation GOM of repaired concrete

Image correlation analysis using GOM software refers to a method used to measure and quantify deformations, movements, or shape changes of an object based on the analysis of variations in digital images. GOM (Gesellschaft für OptischeMesstechnikmbH) is a company specialized in the development of metrology software and optical measurement techniques.

Image correlation analysis using GOM software is based on the principle of digital image correlation. It involves comparing two images of the same object, one being a reference and the other being the deformed or modified image. The GOM software utilizes sophisticated algorithms to align the images, detect variations, and calculate the displacements or deformations that have occurred.

This technique is often used in fields such as mechanical engineering, automotive industry, aerospace, and other areas where precise measurement of deformations or movements is essential. Image correlation analysis using GOM software provides detailed information about an object's deformations, which can be used for material fatigue analysis, design optimization, validation of numerical simulations, and more.

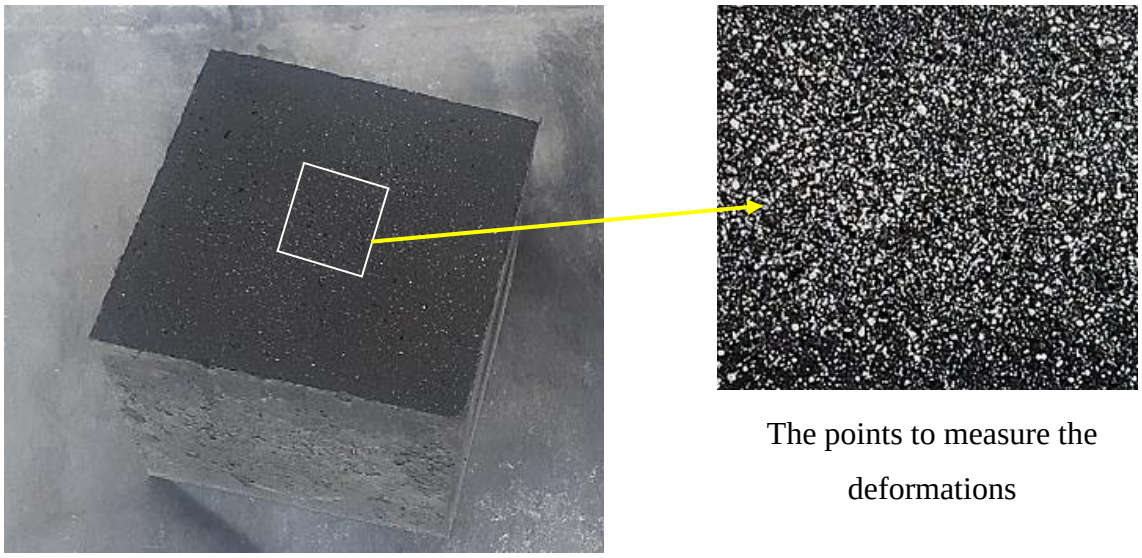

Figure III. 22 Test specimen for the digital image correlation test.

Figure III. 23 Device for image correlation.

III.7 Conclusion

In this chapter, the experimental techniques used in this work were described in the first part. In the second part, the mineral components were analyzed and characterized. The selection of Portland cement as the cement type was made as it is a commonly used material in the formulation of polymer mortar composites. Silica fume was chosen to reduce the alkaline environment of the cement. Sand with a grain size of 0/3 mm was also selected and the constituents meet the standards and recommendations for their use in hydraulic mortars. This makes it easier for us to choose an appropriate formulation approach. With these intrinsic properties of the different components, we can understand the impact of different stresses on the performance of the various mixtures. Furthermore, in this chapter, we subjected the concrete to a high temperature of 750°C, and we also prepared and applied the repair concrete.

CHAPTER IV:

RESULTS AND DISCUSSIONS

IV.1 Introduction

This thesis has the objective of investigating the behavior of mortar-polymer composites for the protection and repair of concrete surfaces. To ensure proper hydration of the cement and optimal performance of the repair mortars, it is crucial to examine both the fresh and hardened state properties of this type of mortar as well as the optimal curing method.

The chapter dedicated to the study of the properties of mortar-polymer composites is focused on those based on styrene-butadiene. To accomplish this study, two interrelated factors are analyzed: the impact of polymers on cement behavior and the behavior of mortar-polymer composites incorporating different fibers. To maintain consistency, the water/(cement+polymer) mass ratio is kept constant at 0.5 throughout all the formulations studied in this chapter. A range of polymer/cement ratios are evaluated, including 0 (reference unmodified material) and 0.05.

The chapter is divided into two parts. The first part focuses on an examination of cement mortars containing polymers in order to gain insight into the effect of polymers on cement hydration. The second part consists of a comparative study of the repair method for ordinary concrete subjected to high temperatures (750 °C), with the first repair using the polymer mortar manufactured in the laboratory and the second repair using commercially available mortar.

IV. 2 Results and discussion

IV.2.1 The statistical analysis of mortar with SBR resin

IV. 2.1.1 Analysis and Results of Variance Model

An analysis of variance was conducted to assess the contribution of the effect factors on the responses, as presented in Table IV.1. All the models employed in this study exhibited relatively high correlation coefficients ranging from 0.89 to 0.95. This indicates a strong correlation between the experimentally obtained responses and the model predictions.

Consequently, it can be inferred that the established models accurately predict the influence of glass fibers and SBR resin content on the mechanical and physical behavior of mortars. Furthermore, these models enable the creation of iso-response curves based on different effect factors.

Additionally, Table IV.2 presents the analysis of variance (ANOVA) for each of the modeled responses. The significance of the established models in this study was assessed using the Fisher test distribution. For a 90% confidence interval, the Fisher ratios for FS28, CS28, WA28, and SH were found to be 2.45, 2.46, 2.46, and 2.40, respectively. These ratios indicate a significant level of importance. Moreover, the probability values (Prob.> F) for all models were less than 5%, confirming the presence of at least one significant effect factor in each model.

Table IV.3 illustrates the contribution of each factor (GF %) and (SBR %), along with their interactions, on the examined responses. The criterion $P \leq 0.05$ was employed to determine the significance of each coefficient. It is evident that the effects of these factors, as well as their interaction, have a highly significant impact on the responses.

Table IV. 1 Summary of Fit.

	FS_{28}	CS_{28}	ABS_{28}	SH_{30}
R^2	0,943485	0,911672	0,906297	0,850877
Adjusted R^2	0,922292	0,878549	0,871158	0,794956
RMSE	0,261096	3,416372	0,750297	33,98002
Mean of response	10,55708	30,73383	4,357	1051,354

Table IV. 2 Analysis of variance (ANOVA) for derived models.

	Source	Degree of freedom	Sum of squares	Mean square	F -ratio
FS_{28}	Model	3	9,1046520	3,03488	44,5185
	Error	8	0,5453709	0,06817	Prob. > F
	Total	11	9,6500229		<,0001*
CS_{28}	Model	3	963,7400	321,247	27,5238
	Error	8	93,3728	11,672	Prob. > F
	Total	11	1057,1128		0,0001*
ABS_{228}	Model	3	43,558308	14,5194	25,7919
	Error	8	4,503560	0,5629	Prob. > F
	Total	11	48,061868		0,0002*
	Model	3	52706,099	17568,7	15,2157
SH_{30}	Error	8	9237,134	1154,6	Prob. > F
	Total	11	61943,233		0,0011*

Table IV. 3 Effect test.

	Model term	Estimation	Standard Error	t ratio	Prob. > |t|
FS_{28}	Intercepts	10,612359	0,076008	139,62	<,0001*
	FG (%)	0,5527542	0,098126	5,63	0,0005*
	SBR (%)	0,9340254	0,093091	10,03	<,0001*
	FG (%) × SBR (%)	0,0277542	0,120179	0,23	0,8232
CS_{28}	Intercepts	30,645339	0,994544	30,81	<,0001*
	FG (%)	-0,884944	1,283951	-0,69	0,5102
	SBR (%)	-10,89797	1,218063	-8,95	<,0001*
	FG (%) × SBR (%)	0,415339	1,572513	0,26	0,7984
ABS_{28}	Intercepts	4,4354915	0,21842	20,31	<,0001*
	FG (%)	0,7849153	0,281979	2,78	0,0238*
	SBR (%)	-2,181034	0,267509	-8,15	<,0001*
	FG (%) × SBR (%)	0,244661	0,345352	0,71	0,4988
SH_{28}	Intercepts	1051,7294	9,891966	106,32	<,0001*
	FG (%)	3,7579802	12,77047	0,29	0,7760
	SBR (%)	-79,86144	12,11513	-6,59	0,0002*
	FG (%) × SBR (%)	9,2068856	15,64057	0,59	0,5723

IV. 2.1.2 Mathematical models

The obtained independent variables, namely [GF (%)] and [SBR (%)], along with the responses [FS28], [CS28], [WA], and [SH], were entered into the JMP 16 software [38]. The developed models are based on a full factorial design approach. It is expected that the mathematical form of these models remains valid for a wide range of mixtures, including glass fiber (GF) values ranging from 0% to 0.5% and SBR contents ranging from 0% to 10% by mass.

Although the developed models are based on a limited dataset, they provide valuable insights into the influence of each term on the behavior of repair mortars. The proposed mathematical models for predicting the responses of CS, FS, WA, and SH are as follows:

valuable insights into the influence of each term, specifically (BSS m^2/kg) and (MP mass%), on the behavior of eco-mortars.

The proposed mathematical models for predicting the responses of CS, FS, ABS and SH are as follows:

$$RF = 10{,}61 + 0.55.\left(\frac{\%GF-0.25}{0.25}\right) + 0.934.\left(\frac{\%SBR-5}{5}\right) + 0.027.\left(\frac{\%GF-0.25}{0.25}\right)\left(\frac{\%SBR-5}{5}\right) \quad (2)$$

$$CS = 30.64 - 0.88.\left(\frac{GF\%-0.25}{0.25}\right) - 10.89.\left(\frac{SBR\%-5}{5}\right) + 0.415.\left(\frac{GF\%-0.25}{0.25}\right)\left(\frac{SBR\%-5}{5}\right) \quad (3)$$

$$ABS(\%) = 4.43 + 0.78.\left(\frac{GF\%-0.25}{0.25}\right) - 2.18.\left(\frac{SBR\%-5}{5}\right) + 0.244.\left(\frac{GF\%-0.25}{0.25}\right)\left(\frac{SBR\%-5}{5}\right) \quad (4)$$

$$SH\left(\frac{ùm}{m}\right) = 1051.71 + 3.75.\left(\frac{GF\%-0.25}{0.25}\right) - 79.86.\left(\frac{SBR\%-5}{5}\right) + 9.2.\left(\frac{GF\%-0.25}{0.25}\right)\left(\frac{SBR\%-5}{5}\right) \quad (5)$$

IV. 2.1.3 Correlation between experimental values and numerical values

Figure IV.1 represents the correlation between experimental and numerical values of various mechanical and physical properties.

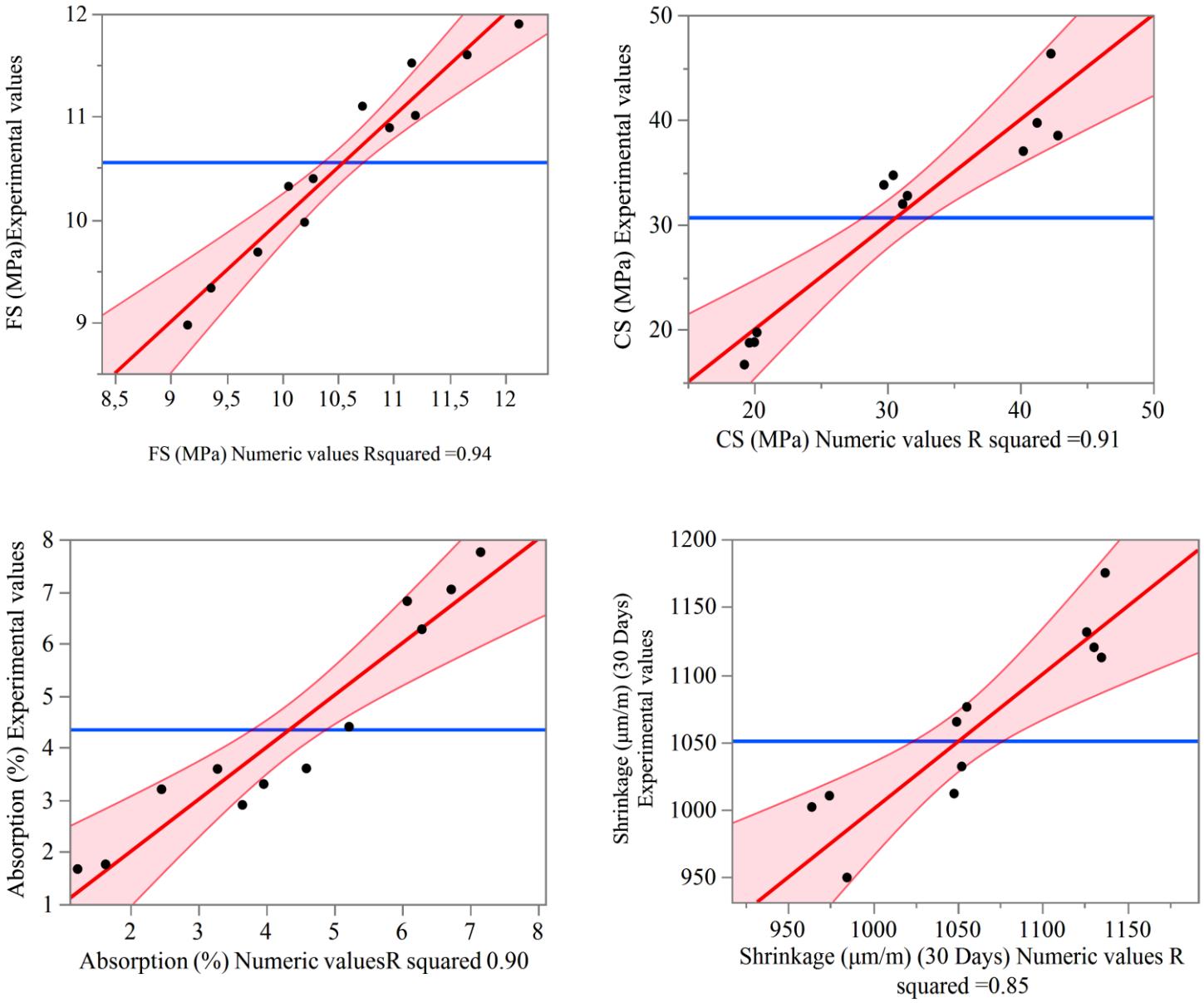

Figure IV. 1 Correlation between experimental values and numerical values of (a) flexural strength, (b) compressive strength, (c) water absorption, and (d) total shrinkage.

Based on the analysis of Figure IV.1, it is evident that there is a correlation between the experimental and numerical values. This correlation indicates an excellent prediction of the numerical model for all properties. The coefficient of correlation, R-squared, reaches a very high level, ranging from 0.85 to 0.94. Furthermore, all the points are located near the mean line, further enhancing the reliability of the model.

IV. 2.1.4 Flexural strength at 28 days

The graphical representation of the analysis results for the flexural strength (FS) at 28 days, considering the factors of fiberglass content (volume %) and SBR content (mass%), can be seen in Figure IV.2 and Figure IV.3.

Figure IV.2 illustrates the iso-response curves and surfaces for the flexural strength at 28 days in mortars with varying percentages of GF (mass%) and SBR contents. The flexural strength at 28 days increases from 10 MPa to 11.5 MPa as the GF percentage goes from 0% to 0.5%. Additionally, an increase in SBR content enhances the strength of GF-containing mortars. Mortars with high GF and SBR contents are identified as the combination that yields good FS28. In Figure IV.3 (a), the main effects plots depict the response of FS at 28 days in the mortar, taking into account the GF and SBR factors. Notably, a significant increase in FS at 28 days, from 10 MPa to 11.5 MPa, is observed with the variation in the GF factor from 0% to 0.5%. This increase can be attributed to the reinforcing effect of fibers, resulting in improved ductility and resistance to rupture. Furthermore, a substantial increase in FS is observed with the variation in the SBR factor from 0 to 10%, indicating a noteworthy influence of SBR on the flexural strength of the mortar at 28 days. These findings align with the estimated coefficients (Table IV.3) and equation (2).

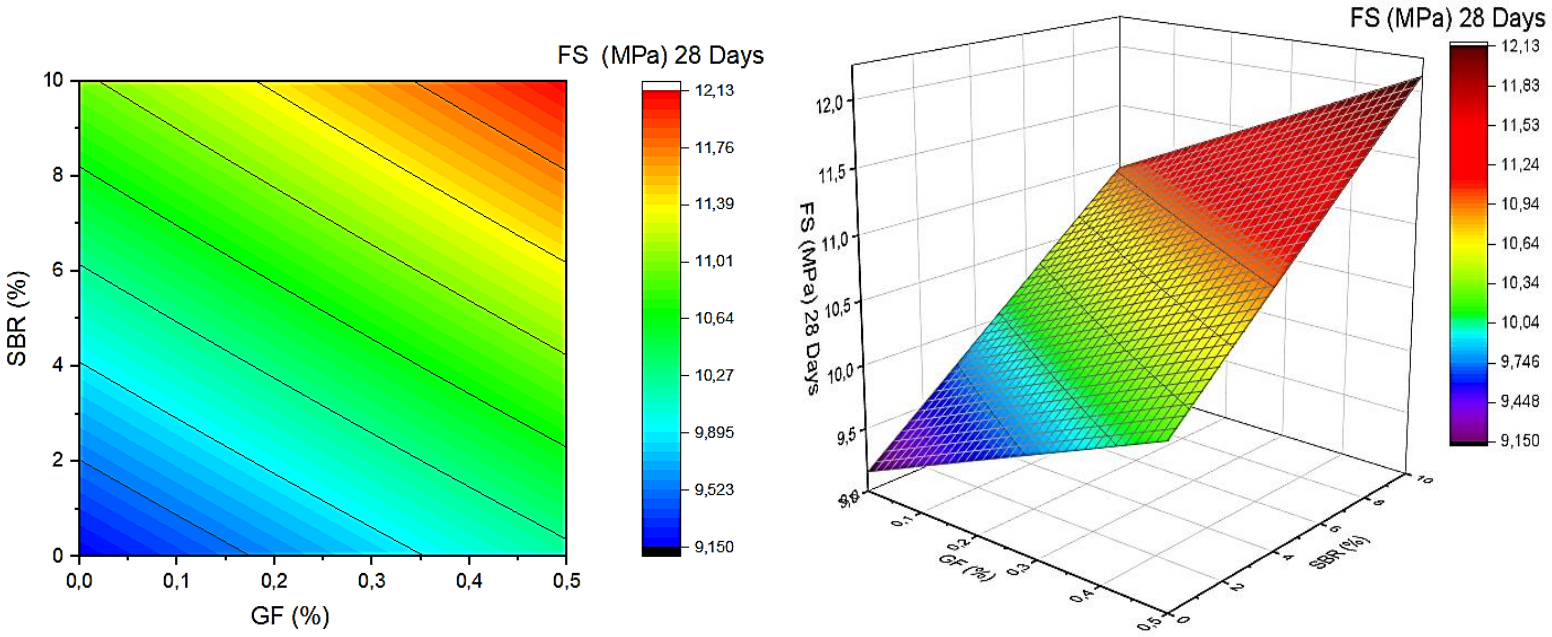

Figure IV. 2 Curves and surfaces of iso-response for the flexural strength at 28 days.

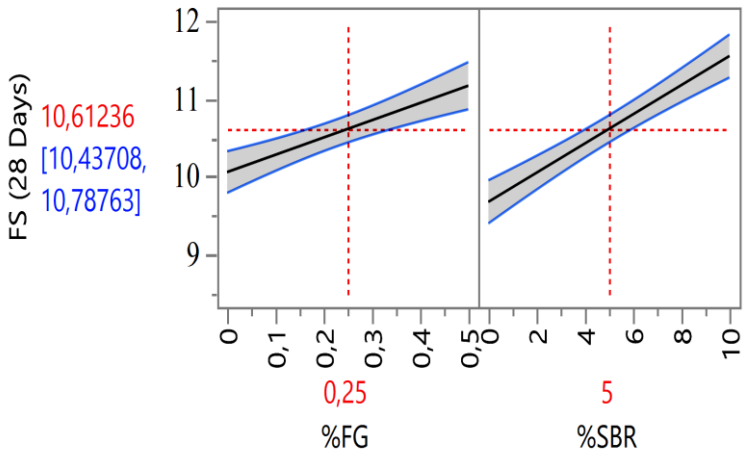

Figure IV. 3 Plot showing the main effects of the flexural strength at 28 days.

IV. 2.1.5 Compressive strength at 28 days

The graphical representation of the analysis results for the compressive strength (CS) at 28 days, considering the factors of fiberglass content (mass%) and SBR content (mass%), can be observed in Figure IV.4 and Figure IV.5. Figure IV.4 depicts the iso-response curves and surfaces that illustrate the compressive strength at 28 days in mortars with varying

percentages of GF (mass%) and different SBR contents. The compressive strength at 28 days shows a slight decrease, ranging from 31 MPa to 29 MPa, as the GF percentage increases from 0% to 0.5%. Furthermore, an increase in SBR content leads to a significant reduction in the strength of mortars, regardless of the presence of GF. In Figure IV.5, the main effects plots demonstrate the response of CS at 28 days in the mortar, considering the GF and SBR factors. Notably, there is a substantial decrease in CS at 28 days, dropping from 42 MPa to 20 MPa, as the SBR factor varies from 0% to 10%, indicating a significant influence of SBR on the compressive strength of the mortar at 28 days. These results are consistent with the estimated coefficients (Table IV.3) and equation (3).

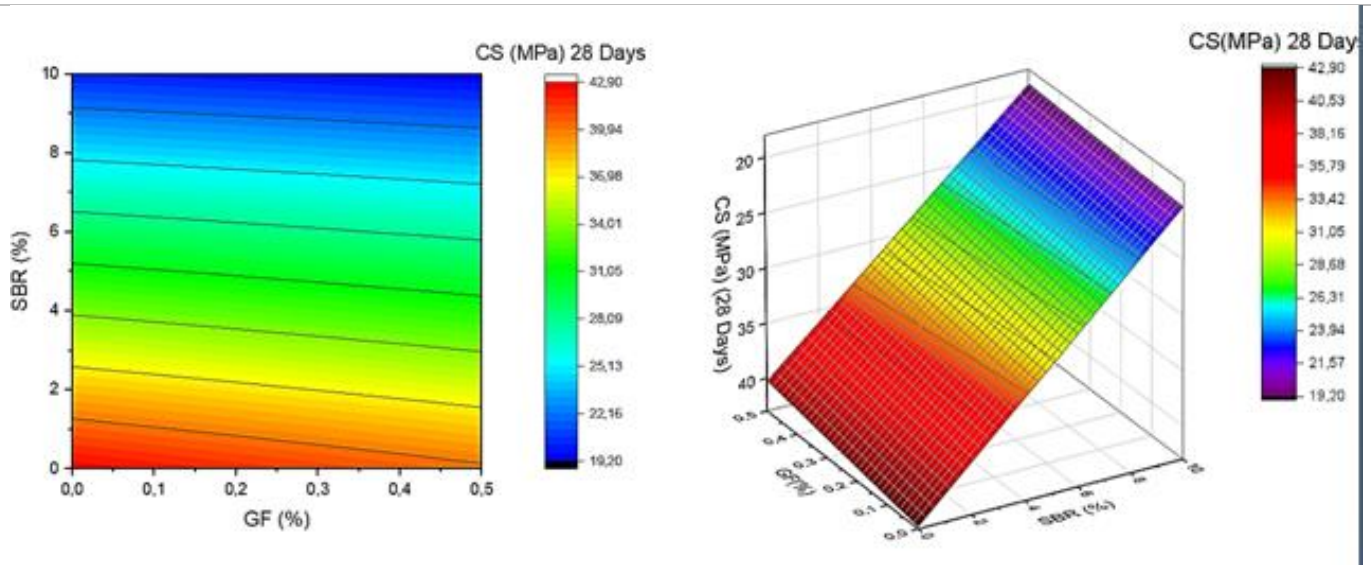

Figure IV. 4 Curves and surfaces of iso-response for the compressive strength at 28 days

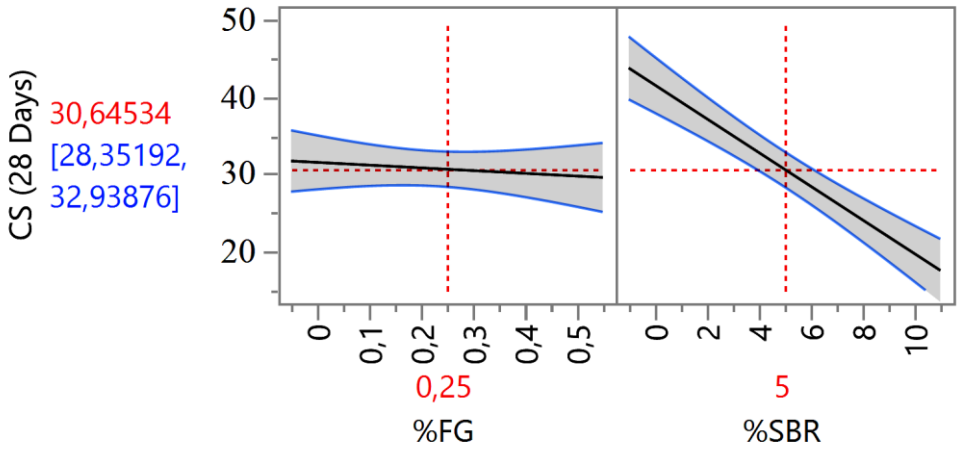

Figure IV. 5 Plot showing the main effects of the compressive strength at 28 days.

IV. 2.1.6Water absorption at 28 days

Figures IV.6 and IV.7 provide insight into the influence of two factors, namely fiberglass content (GF %) and the mass percentage of SBR, on the water absorption response after 28 days.

Figure IV.6 illustrates the iso-response curve and iso-response surfaces depicting water absorption (WA) after 28 days for mortars with varying levels of GF and SBR (%). It is evident that increasing the fiber content from 0% to 0.5% leads to a rise in water absorption. The presence of SBR plays a vital role in the water absorption characteristics of the mortars. For example, a higher SBR content leads to a significant 40% reduction in water absorption for a mortar containing 0.5% GF and 10% SBR, as compared to another sample with the same fiber content.

Figure IV.7(a) displays the main effects graphs representing the 28-day water absorption response of the mortar, considering the factors of fiberglass content and SBR. It can be observed that water absorption after 28 days increases from 10% to 15% due to a change in the level of the GF factor from 0% to 0.5%. Conversely, an increase in water absorption from 10% to 40% is observed due to a change in the level of the SBR factor from 0 to 10%. This indicates that the impact of SBR content on water absorption is more significant when compared to the influence of GF content.

These findings align with the estimated coefficients (Table IV.3) and equation (4)

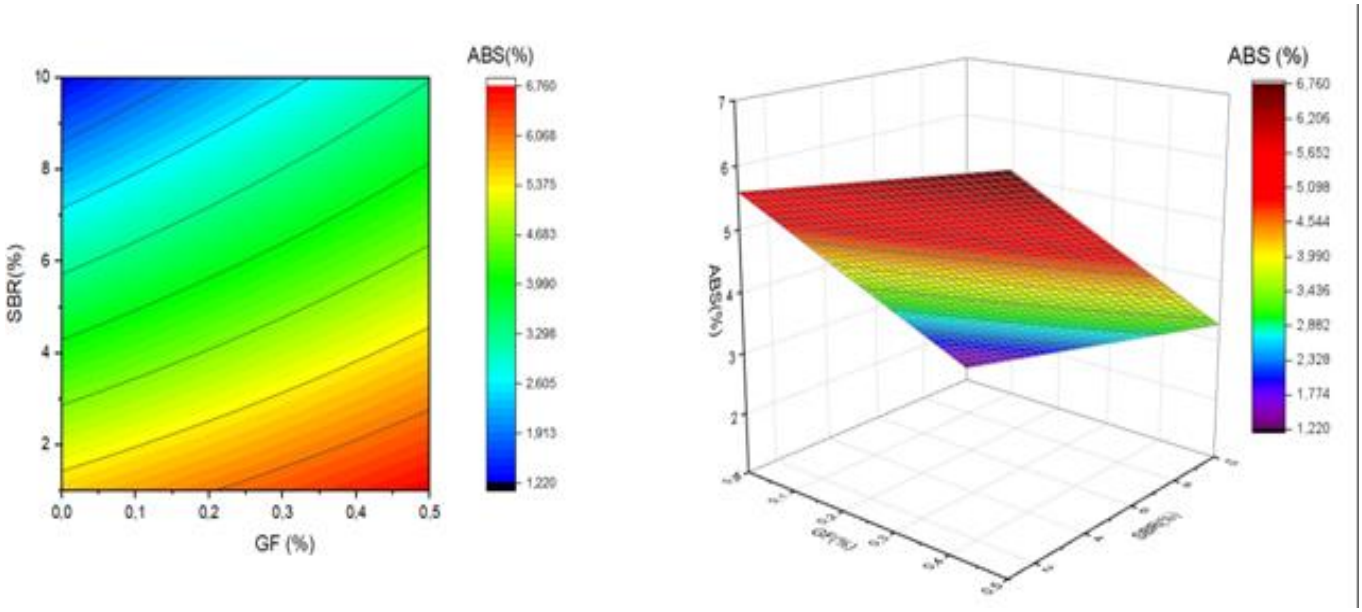

Figure IV. 6 Curves and surfaces of iso-response for the water absorption at 28 days.

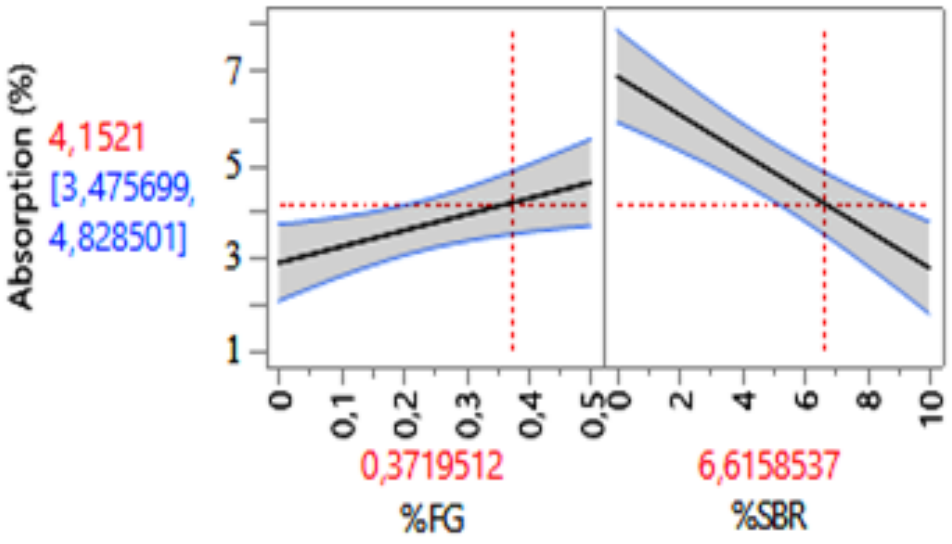

Figure IV. 7 Plot showing the main effects of the water absorption at 28 days.

IV. 2.1.7 Total shrinkage

Figures IV.8 and IV.9 provide a comprehensive overview of how two factors, fiberglass content (GF %) and the mass percentage of SBR, influence the shrinkage response after 30 days.

Figure IV.8 showcases the iso-response curve and iso-response surfaces that depict the overall shrinkage after 30 days for mortars with varying levels of GF and SBR (%). It is clear that increasing the fiber content from 0% to 0.5% leads to a slight rise in shrinkage. The presence of SBR plays a vital role in the total shrinkage of the mortars. For instance, a higher SBR content results in a significant 55% reduction in shrinkage for a mortar containing 0.5% GF and 10% SBR, compared to another sample with the same fiber content.

Figure IV.9(a) displays the main effects graphs illustrating the shrinkage response after 30 days of the mortar, taking into account the factors of fiberglass content and SBR. It is observed that the shrinkage after 30 days increases from 3% to 6% due to a change in the level of the GF factor from 0% to 0.5%. Conversely, a decrease in shrinkage from 5% to 55% is noted due to a change in the level of the SBR factor from 0 to 10%. This indicates that the impact of SBR content on shrinkage is more significant than the influence of GF content.

These findings align with the estimated coefficients (Table IV.3) and equation (4).

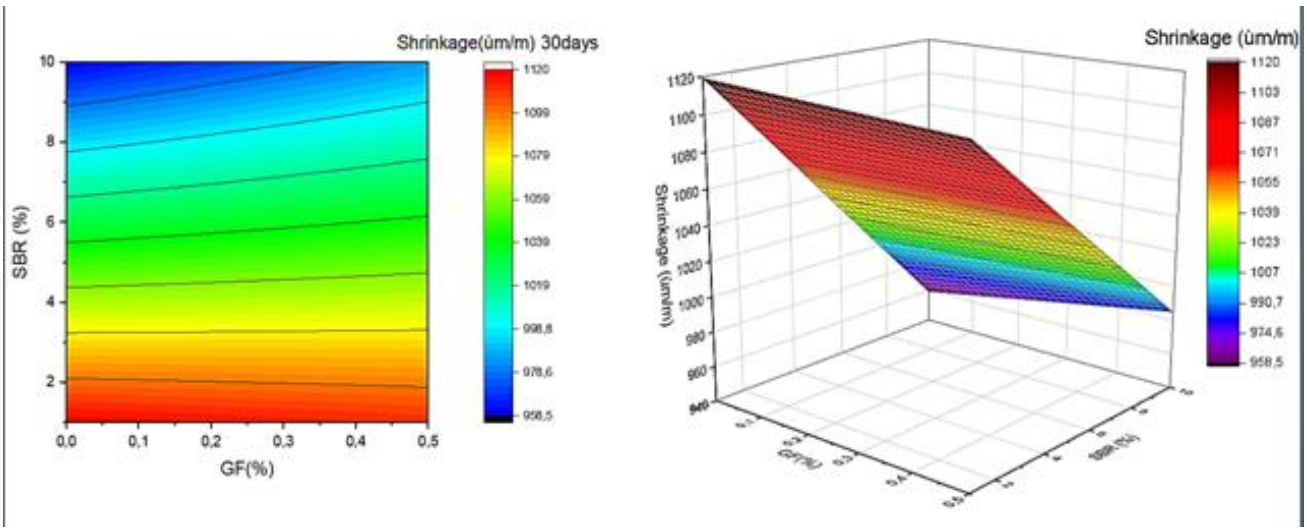

Figure IV. 8 Curves and surfaces of iso-response for the Shrinkage at 30 days.

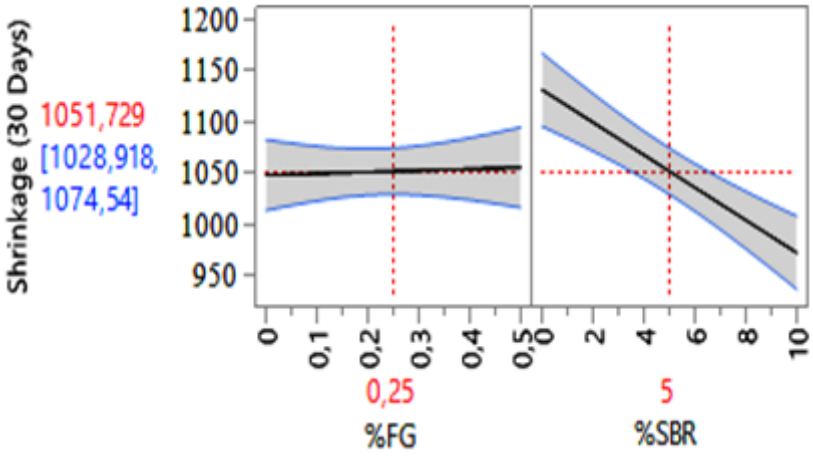

Figure IV. 9 Plot showing the main effects of the Shrinkage at 30 days.

IV.2.2 Microstructural analysis:

Figure IV.10 represents the scanning electron microscopy observation images.

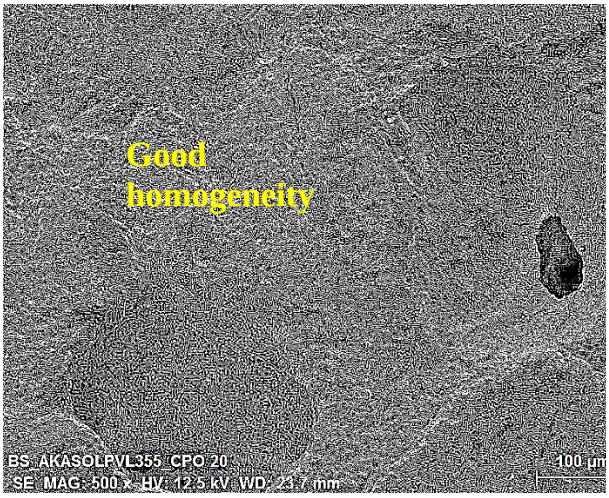

M-C

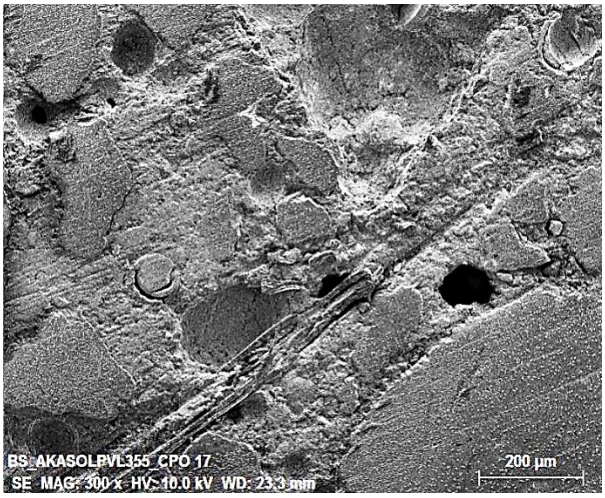

M-0.5G

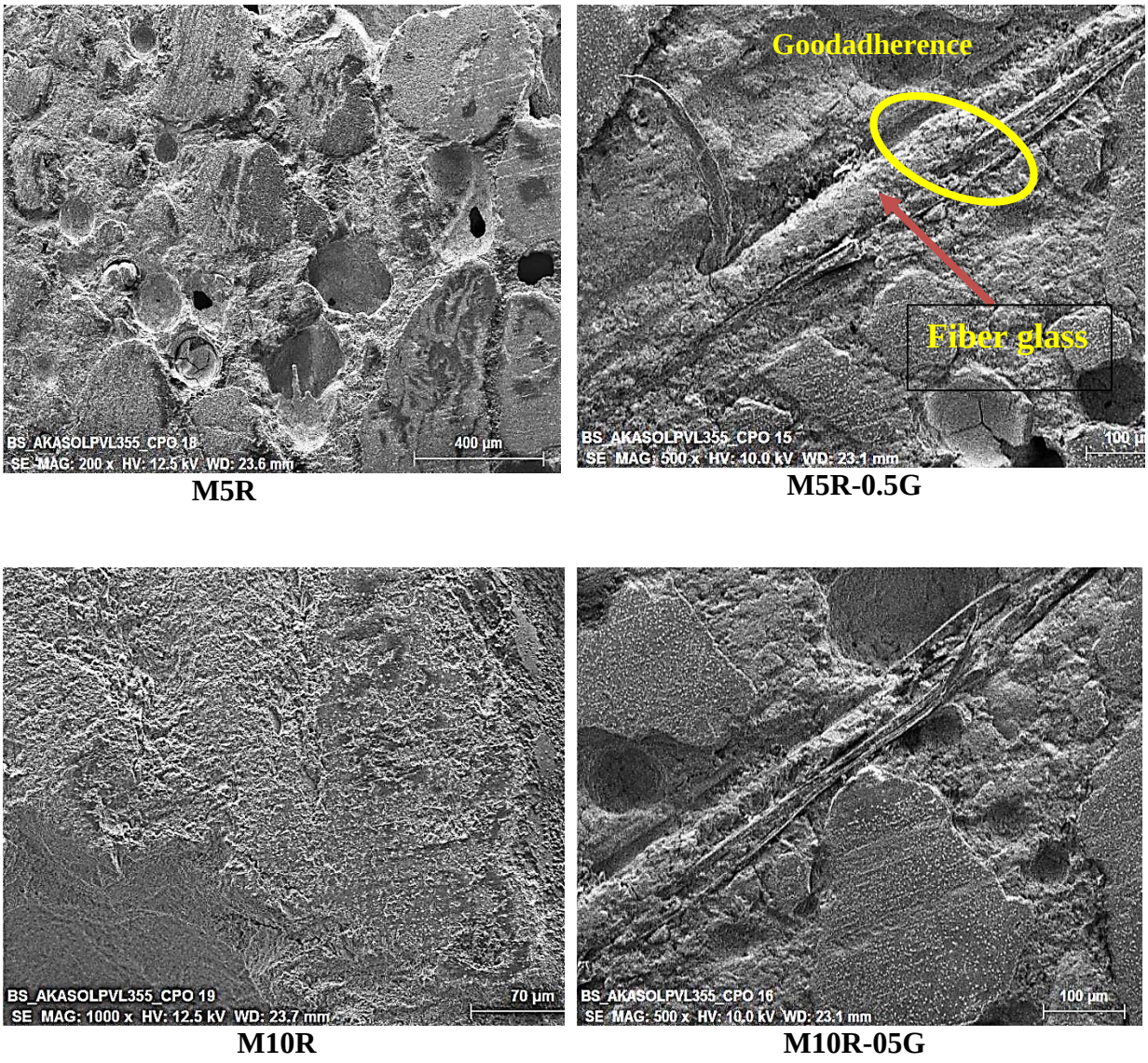

Figure IV. 10 Scanning electron microscope images of different types of mortars.

The results of scanning electron microscopy (SEM) images of different repair mortars can be interpreted as follows: 1- Homogeneity and dense structure: The observation of homogeneity in all the repair mortar mixtures indicates a good quality of mixing and a uniform distribution of components within the matrix, promoting high compactness and low porosity for increased mechanical strength and durability. 2- Good adhesion between glass fibers and the polymer matrix: Effective adhesion between the fibers and the matrix allows for efficient transfer of loads and stresses, thereby enhancing resistance to traction and flexion. This is particularly important in repair applications where resistance to cracking and deformation is crucial. 3- Limitations in visualizing the composition of the paste: The SEM technique does not directly

visualize the chemical composition of the paste, highlighting a limitation. Other analytical techniques such as energy-dispersive spectroscopy (EDS) may be necessary to obtain detailed information about the composition. In summary, scanning electron microscopy images of repair mortars reveal homogeneity and a dense structure, along with good adhesion between glass fibers and the polymer matrix, but do not directly visualize the composition of the paste.

IV.2.3 Results and discussion of fiber polymer mortars

IV.2.3.1 Fresh state

In Figure IV.11 and figure IV.12, the wet density and diameter of spread of the different mixtures are depicted.

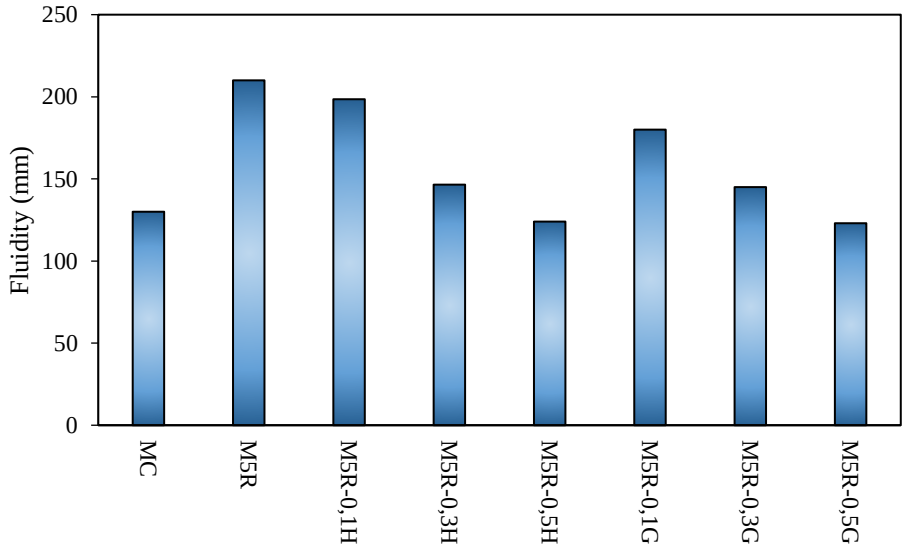

Figure IV. 11 Fluidity of the different mixtures.

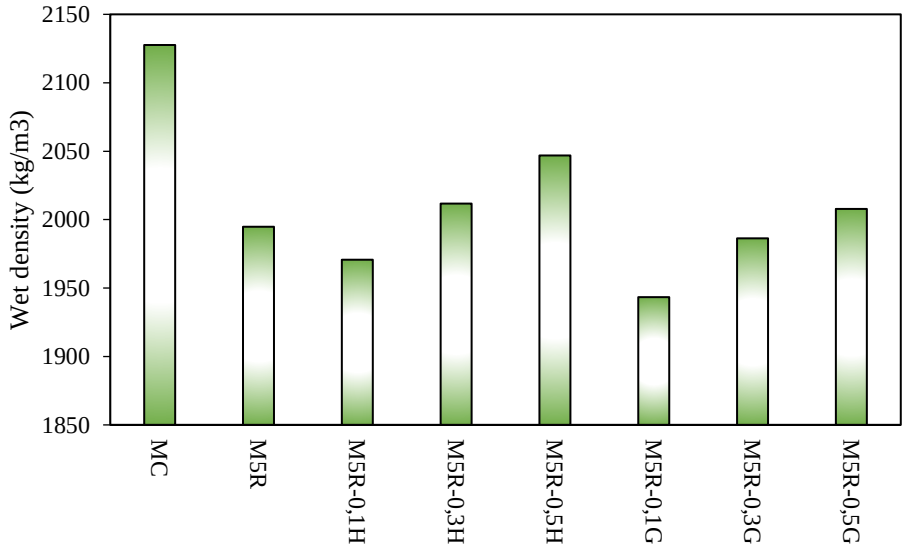

Figure IV. 12 Wet density of the different mixtures.

Various research studies have indicated that incorporating 5% SBR latex content into cement mortar results in a 38% increase in fluidity and a reduction of the water-cement ratio (W/C) from 0.5 to 0.43, when compared to CM without resin. The presence of polymers, especially in the form of latex, has been proven to enhance the workability of cement mortars and concretes with lower water content. [68, 99]. As indicated by Eren, F., et al [102], According to research studies conducted by Eren, F., et al and Felekoğlu, K.T., the presence of SBR resin in cement mortar acts as a lubricant and also retards the setting time of cement. The retardation effect is due to the immobilization of SBR on the surface of cement particles, which creates a physical barrier and inhibits its reaction with water. [102, 164].

The impact of fiber content and type on the fluidity of polymer mortars can vary, as per research studies. For instance, the addition of hemp and glass fibers to polymer mortars may cause a decrease in fluidity. The diameters of M5R-0.1H, M5R-0.3H, and M5R-0.5H mortars were determined to be 198.5 mm, 146.5 mm, and 124 mm, respectively, whereas M5R had a diameter of 210 mm. Likewise, the spreads of M5R-0.1G, M5R-0.3G, and M5R-0.5G mortars were found to be 180 mm, 145 mm, and 123 mm, respectively. The research studies have established that the water absorption capacity of plant fibers has a negligible impact on the fluidity of polymer mortars. The alkaline pre-treatment of hemp fibers and the removal of water-absorbent particles resulted in similar outcomes as those observed in mortars containing fiberglass. The addition of fibers to cementitious materials enhances cohesion and

homogeneity, which can cause a decrease in fluidity. The wet densities of CM and M5R were established to be 2128 kg/m^3 and 1995 kg/m^3, respectively. The addition of 5% SBR latex resulted in a 6% decrease in wet density, attributed to the air-entraining effect of SBR, as depicted in Figure IV.11 and IV.12.[68, 102, 165]. In contrast, an increase in wet density has been observed in fiber-reinforced polymer mortars with increasing fiber content and type, suggesting good compatibility between the fibers and the polymer matrix. For example, the M5R-0.5H mixture exhibited a 3% higher density compared to the M5R. The role of SBR latex in fresh cement mortar has been extensively explained by Sun, K., et al. [84]. The high molecular weight polymer SBR is composed of long chains and a mixture of hydrophilic and hydrophobic groups. When SBR is added to cement paste during mixing, it can entrain air and trapping microscopic air bubbles. It has been discovered that air inclusions have an impact not only on the fluidity of cement pastes, but also on their density. The density of the mixture containing 15% SBR was found to be reduced by 31.1% compared to that of the cement paste alone.

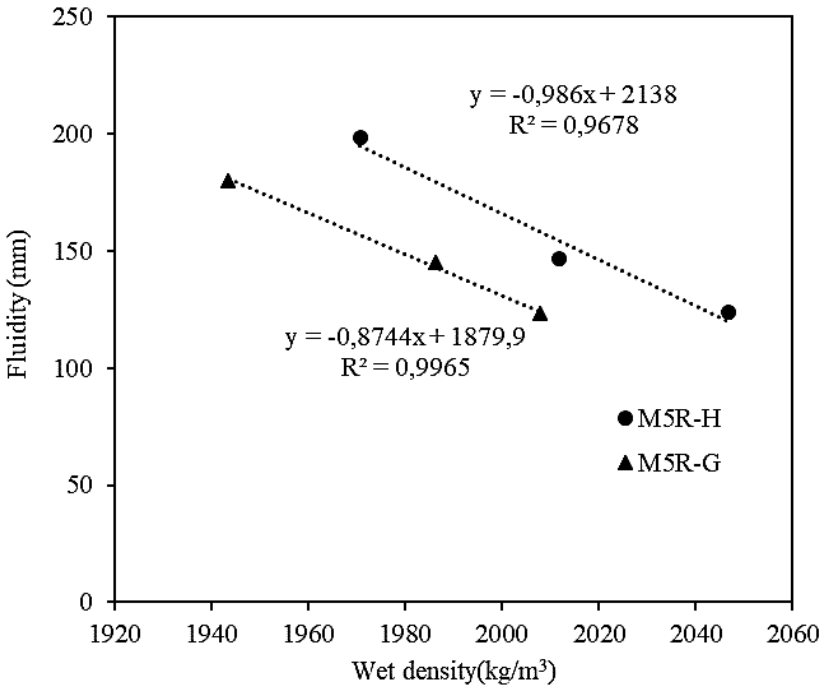

Figure IV. 13 Relationship between wet density and spreading.

A strong correlation has been noted between the wet density and the spread of mixtures containing glass fibers and hemp fibers, with a linear relationship observed between the two

variables. The coefficients for this correlation were determined to be 0.99 and 0.97 for glass fibers and hemp fibers, respectively, indicating a good correlation. Moreover, the results suggest that an increase in wet density results in a corresponding decrease in the fluidity diameter.

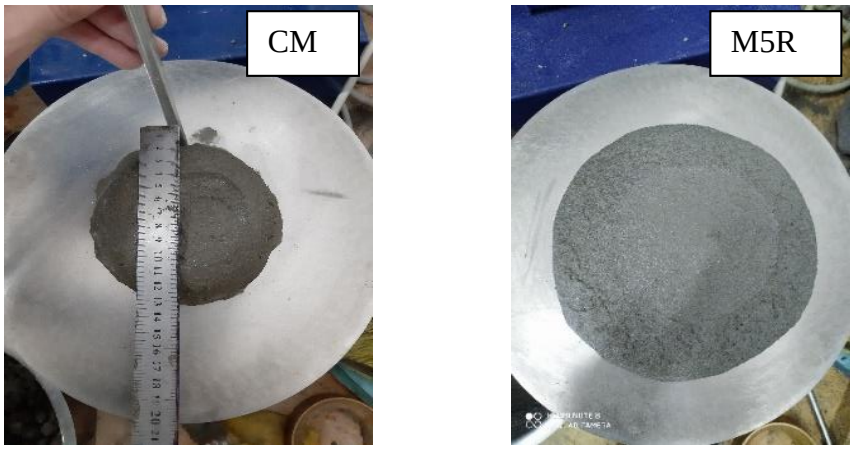

Figure IV. 14 Flow-spread of CM and M5R mortars.

IV.2.3.2 Flexural strength

The results of the flexural strength of the control mortars and their relationship to age and fiber content (glass and hemp) are presented in Figure IV.15.

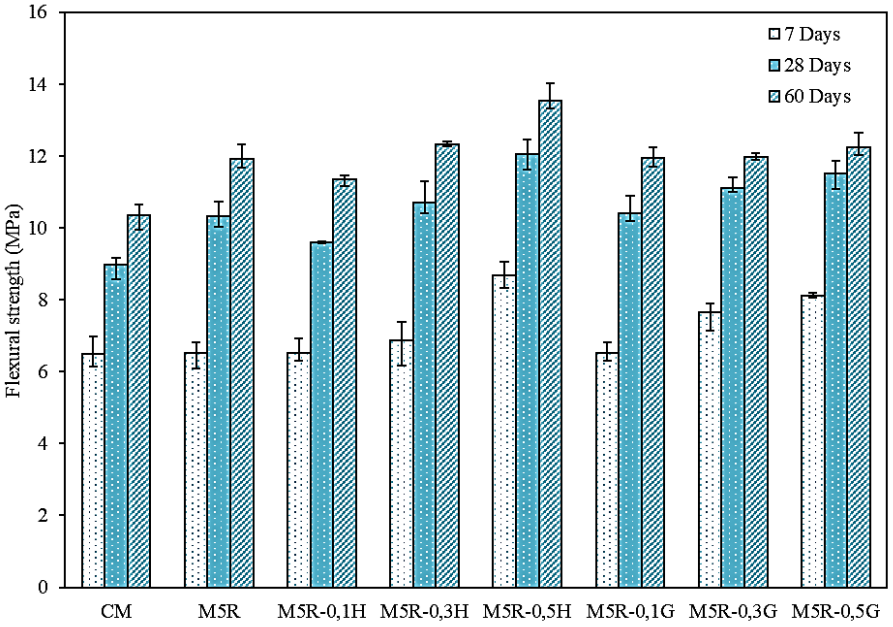

Figure IV. 15 Flexural strength of the different mortars made.

The data presented in Figure IV.15 is the average of four tests carried out on prismatic samples measuring 40x40x160 mm^3, showing the flexural strength of various mortar mixtures. Research studies have indicated that most of the samples tested showed an increase in strength with increased curing time. However, after 7 days, there was no significant improvement in the strength of the mortar containing 5% SBR compared to the control mixture without resin. This is attributed to the delayed formation of the polymer film within the cement matrix. [99, 166]. The bending resistance has been found to increase by 25% and 20% respectively for M5R-0.5H and M5R-0.5G, in contrast. This improvement is attributed to the toughness and ductility of hemp and glass fibers, which enhance the material's ability to withstand cracking caused by stress [96].

After 28 days, the flexural strength of M5R mortar was found to increase by 14% compared to the control CM mortar. This improvement is attributed to the enhanced cohesion between the sand and cement grout, which is a result of the formation of the polymer film and co-matrix [95].

Mortars modified with latex and reinforced with fibers, such as hemp and glass, displayed superior flexural strength compared to CM and M5R mortars. The extent of this improvement is influenced by the dosage and type of fibers, and an optimal fiber content of 0.5% was identified, resulting in a 12% increase in strength over M5R mortar. The application of an alkaline treatment to hemp fibers enhanced the bonding between the fibers and cement by causing cement precipitation on the exposed fiber surfaces, which improved crack resistance and reduced crack propagation. Additionally, the polymer film filling the voids between particles facilitated good adhesion of the polymer matrix to glass fibers, resulting in improved tensile strength and toughness of the polymer-based mortars [126].

After 60 days, the flexural strength of the mortars continued to increase, and those containing hemp fibers showed significant resistance compared to other types of mortars. Specifically, M5R-0.5H showed a 10% increase in flexural strength compared to M5R and an 11% higher resistance compared to CM. This can be attributed to the development of the cement hydrate structure, which forms a continuous polymer film that causes the polymer particles to come together and form a layer of calcium silicate [109, 167]. The polymer film also reduces the formation of Wollaston by absorbing calcium [109]. The decrease in silicates contributes to the improved durability of hemp fibers in modified mortars, as a decrease in silicates leads to a decline in alkalinity [168][137].

The application of soda and polymer treatments to plant fibers leads to an improvement in the tensile strength of modified cement mortars. This is accomplished by removing pectin, wax,

and hemicellulose content in the natural fibers. The high-tenacity SBR polymer network serves as a useful bridge between the different components of the mortar matrix, thereby preventing the formation and propagation of microcracks caused by deflection[165][169][69]. In the case of mortars containing glass fibers, a slight improvement was noted in M5R-0.5G compared to M5R.

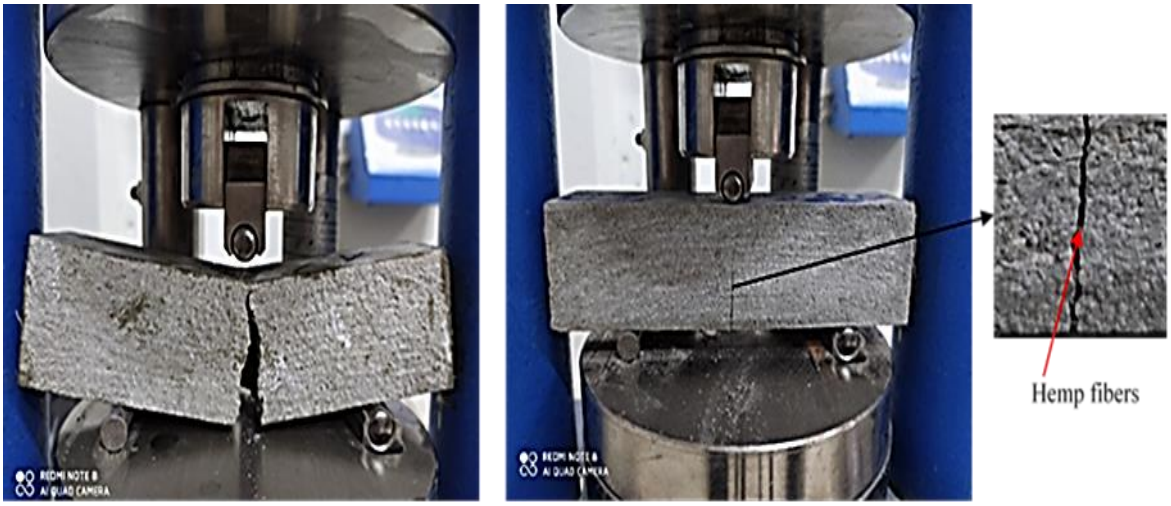

(a) (b)

Figure IV. 16 Analysis of Rupture Mode for M5R (a) and M5R-0.5H (b) Samples Following Flexural Test.

IV.2.3.3 Compressive strength

The compressive strength of the control mortar and the SBR latex modified mortar with glass and hemp fibers at various ages is depicted in Figure IV.17. The data was obtained from six tests carried out on fragments from the flexural strength tests.

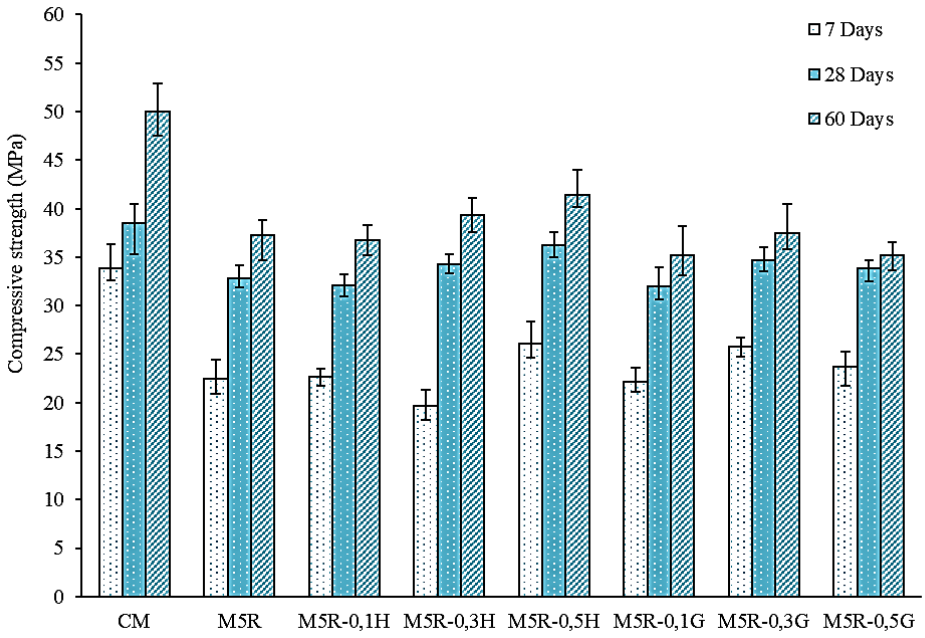

Figure IV. 17 Compressive strength of the various mortars made.

Upon analyzing the results, it was found that the compressive strength of the 5% SBR latex modified mortar decreases by about 21% and 31% at 28 days and 60 days, respectively, compared to the control mortar (CM). This decrease can be attributed to the increased volume of air present in the polymer-modified mortar. Studies have shown that the presence of polymers can have a negative impact on compressive strength[69, 170]. Shi, C., et al [95]explain that the decrease in compressive strength results from the lower mechanical strength of the SBR latex compared to cement mortar [69, 166]. This reduction in strength also lowers the elastic modulus of the polymer molecule compared to the various cement hydration products alone [69].

In contrast, the addition of 0.5% hemp fibers in the modified mortar resulted in an increase of 14.2%, 11%, and 3% in compressive strength at 7, 28, and 60 days respectively, compared to the modified mortar containing 5% SBR latex. Additionally, incorporating 0.3% glass fibers in the modified mortar led to increases of 13.5%, 5%, and 1% after 7, 28, and 60 days respectively. However, beyond this percentage, the resistance of the modified mortar containing 5% SBR latex decreased slightly compared to the hemp and glass fiber modified mortars. This increase in strength is attributed to the latex film formation within the cement structure, which enhances the adhesion between the fibers and the matrix [165, 171].

Fidelis, M.E.A., et al [141]demonstrate that coating jute fabric with polymers enhances the bonding between fibers and matrix [172]. They also find that using pozzolan additives

depletes calcium hydroxide, leading to an increase in matrix density, which protects the plant fibers [173-175]. Candamano, S., et al [139] reveal that chemically treating hemp fibers removes hemicellulose, lignin, and waxes, providing a clean fiber surface [135]. In their conclusion, the authors found that the addition of acrylic latex to the cement matrix fills the pores and enhances the bond between the chemically treated hemp fibers and the matrix. However, they also observed that the compressive strength of other fiber types remains unchanged regardless of their nature. They recommend using 0.5% hemp fibers to effectively increase the compressive strength of SBR latex-based mortars.

IV.2.2.4 Correlation between physical and mechanical properties of mortars modified with fibers

Figure IV.18 illustrates the correlation between the compressive strength and dry density of fiber-modified mortar.

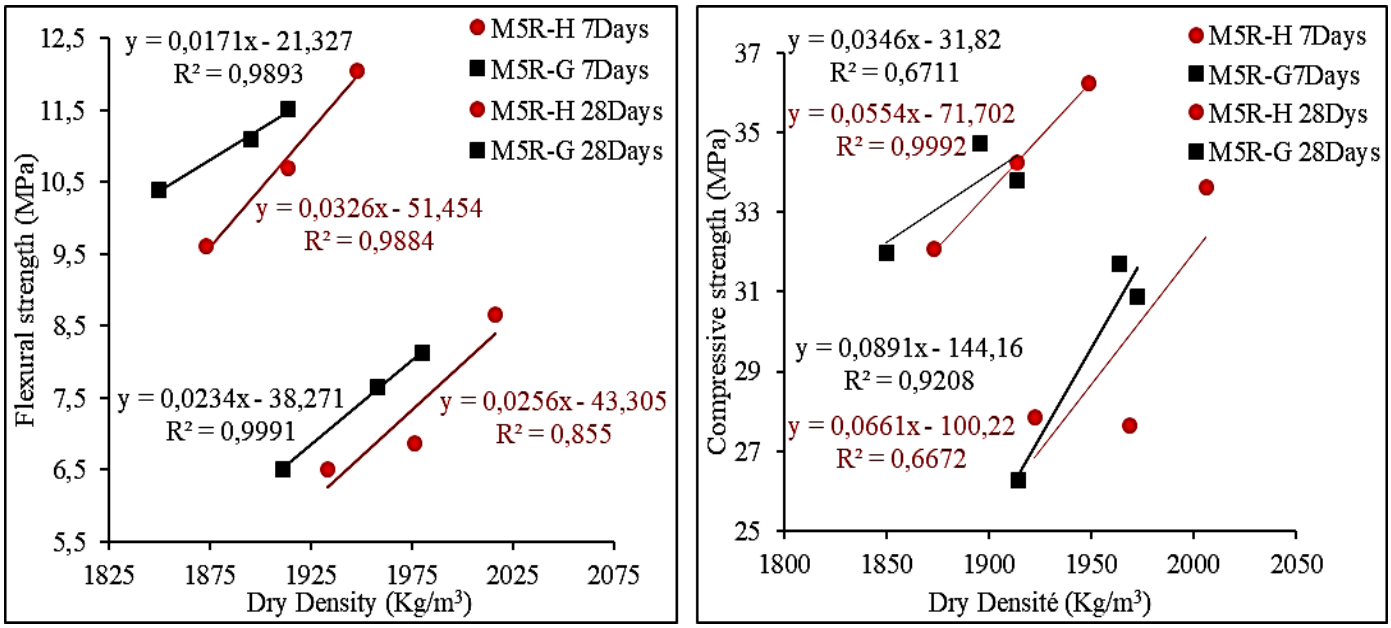

Figure IV. 18 Relationship between dry density, flexural and compressive strength.

Based on the figure presented, it can be observed that the compressive strength of the modified mortar containing hemp or glass fibers is directly proportional to its dry density. This means that an increase in the density of the mortar leads to a linear increase in its strength.

IV.2.3.5 Shrinkage

The property of shrinkage is of utmost importance in determining the dimensional stability of materials, whether they are based on cement or polymer. When shrinkage is not compatible, it can lead to the development of internal stresses, which may cause failure either at the material's interface or within the material itself. Figure IV.19 illustrates the results of shrinkage strain for various samples for 4 days, 30 days, and 60 days.

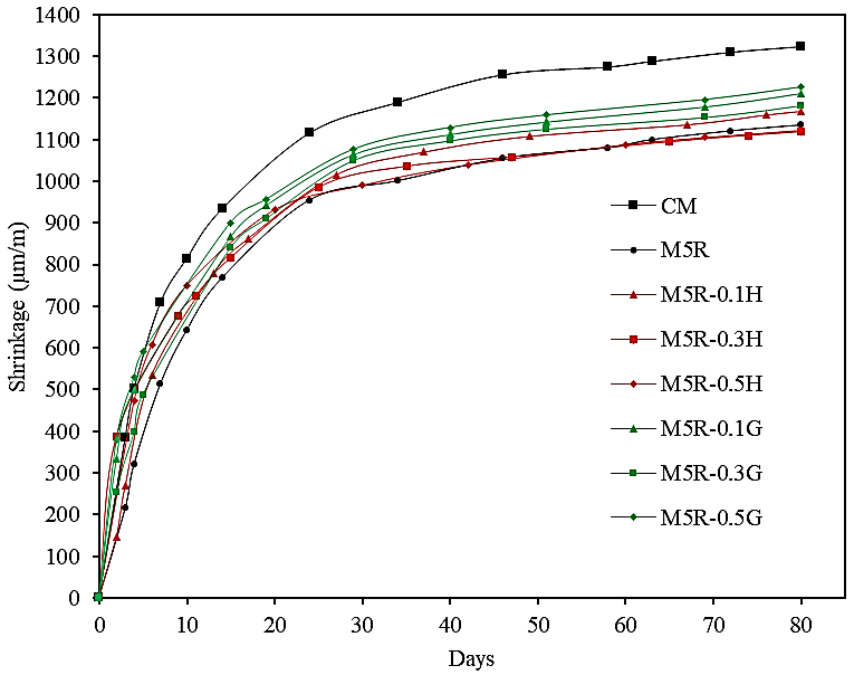

Figure IV. 19 The shrinkage strain results of different samples.

According to Figure IV.19, the inclusion of 5% SBR has resulted in a 20% decrease in the shrinkage rate when compared to CM. This decrease in shrinkage is believed to be due to the existence of resin particles or films that partially occupy the pores, leading to a reduction in drying shrinkage. This was demonstrated by Guo, S.-Y. et al. [69]and Parhizkar, T. and A. Ramezanianpour [176]. Ribeiro, M. et al. have explained the reduction in shrinkage observed in polymer mortars compared to pure cement-based mortars [68]. Their findings indicate that the presence of polymers reduces the density of microcracks at the surface of the paste-

aggregate interface. Additionally, the polymer film increases the capacity of the wet-hardening paste to retain water, leading to a decrease in drying shrinkage [94].

The initial 10-day period in polymer mortars is characterized by increased shrinkage and deformation, which is attributed to the high humidity gradient between the material and its surroundings. Furthermore, the presence of fibers in the mortar creates additional porosity, which facilitates the movement of water out of the material, leading to significant shrinkage.Ban, Y et al [177] found that the porosity of natural fibers like bamboo contributes to greater drying shrinkage due to their fibrous structure and interconnected pores. De Andrade Silva, F. et al [178] observed a 40% increase in shrinkage in the presence of sisal fibers compared to a cement matrix without fibers, which was linked to the size, shape, and continuity of capillary pores in hydrated cement-based pastes. At the microstructural level, fiber porosity creates more water channels in the matrix, leading to increased drying shrinkage [179]. Shafei, B. et al [132] found that the low stiffness of the glass fibers increases the shrinkage of glass fiber mortars. The shrinkage values of fiber mortars vary depending on the speed and type of fibers. After 60 days, the shrinkage values of M-5R-0.5H, M-5R-0.3H, M-5R-0.3G, and M-5R-0.5G mortars were found to be similar to that of M5R, as shown in Figure IV.17.

According to Liuquan, Q., L. Dongxu, and L. Zongjin, the addition of 10% fumed silica is a contributing factor to the decrease in shrinkage observed in polymer-modified cement mortar. This is because fumed silica induces a pozzolanic reaction in the long-term, leading to an increase in the amount of C-S-H gels[180, 181]. Liuquan, Q., L. Dongxu, and L. Zongjin[181] found that the presence of C-S-H gels in the cementitious material helps to decrease its porosity, ultimately leading to a decrease in shrinkage. Additionally, the encapsulation of lignocellulose by cement hydration products on day 14 has been shown to play a role in controlling both shrinkage and expansion in mortar through the cohesive stress between cellulosic lignin and cement hydrate. The control of mortar shrinkage and expansion is achieved through the cohesive stress present between the cellulosic lignin and cement hydrate. According to a study conducted by Benali and Ghomari, [99]after ten days of curing, the formation of a polymer film integrated into the pores of fibers, particularly the hemp fibers treated with NaOH, results in improved adhesion between the fiber and matrix, leading to a decrease in porosity and shrinkage of the polymer mortar. Another study by Afroughsabet et al [180] found that the inclusion of fibers in cementitious composites prevented cracking caused by drying shrinkage. The addition of 10% fumed silica and 5% SBR latex to cement

mortars containing 0.5% hemp fibers treated in 5% NaOH was found to result in composites with desirable properties. Therefore, it can be concluded that this formulation effectively reduces the adverse impact of plant fibers on the shrinkage of the cementitious matrix.

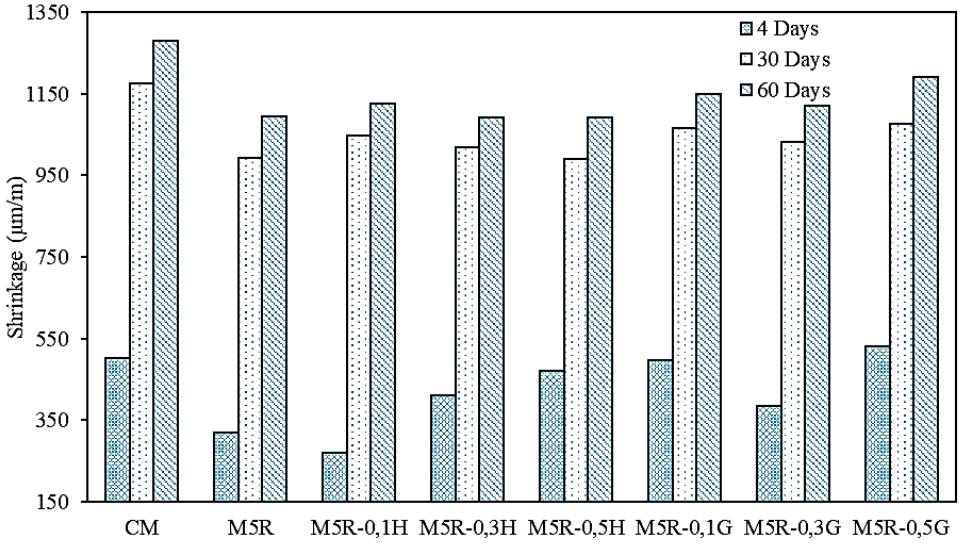

Figure IV. 20 Total shrinkage for different deadlines of the mixes made.

IV.2.3.6 Water absorption

The evolution of capillary water absorption and total immersion water absorption for various mixtures is depicted in Figures IV.21 and IV.22, respectively.

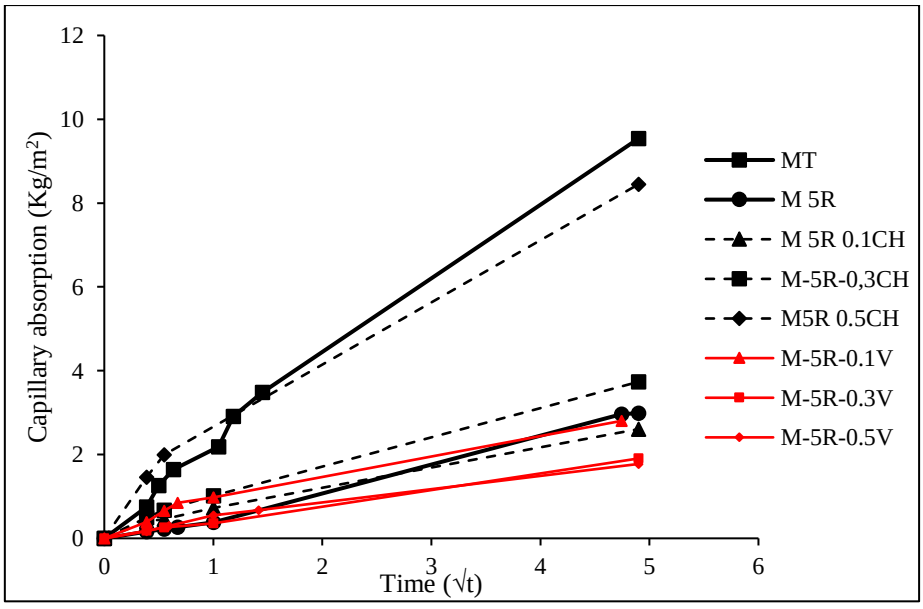

Figure IV. 21 Absorption of water by capillarity.

Unlike drying shrinkage, capillary water absorption tests measure the water absorption of a sample when it is in contact with external water. The results are frequently used to assess the material's durability [177]. According to Figure IV.21, a decrease of 68% in capillary absorption after 24 hours compared to the mortar without CM resin is observed as a result of the addition of 5% SBR latex. This decrease is attributed to the filling of pores by polymer, which leads to a reduction in open porosity and the bridging of microcracks within the matrix [166]. An increase in capillary absorption after 24 hours of testing is shown by mortars containing hemp fibers, specifically M5R-0.3H and M5R-0.5H, with increases of 20% and 60% respectively compared to M5R. This increase is due to the high water absorption of natural fibers, which exceeds 90% and results in an increase in porosity in the transition zone, as reported by deAzevedo et al [138]. The high absorption of samples containing plant fibers is attributed by Booya et al [136] to the shrinkage of plant fibers during kiln drying, which creates a space between the fiber and the cementitious matrix. Upon contact with water, these samples absorb more water than before. In contrast, a reduction in water absorption of 13% after 24 hours is shown by M5R-0.1H due to the small amount of added fiber. Glass fiber mortars exhibit low capillary water absorption compared to M5R, which may be due to the better microstructural behavior of the glass fibers in the interfacial zone and refinement of pores, resulting in a decrease in water absorption. Additionally, the cementitious composite is prevented from rising through capillaries by the fibers within it.

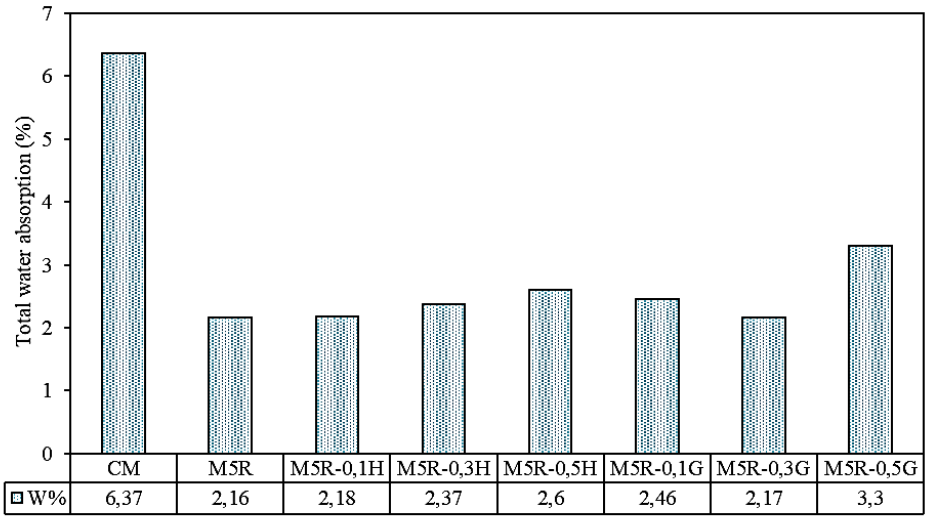

Figure IV. 22 Water absorption by total immersion.

The total water absorption provides an estimate of the total number of pores in the material that can be reached by water [136]. The lowest absorption was observed in the M5R-0.3G mixture, although the addition of hemp fibers slightly increased the porosity of the mortar, resulting in a higher absorption rate. Natural fibers have significantly increased water absorption and are more easily saturated than the hardened cementitious matrix, as stated by de Azevedo et al [138]. A strong correlation was found between the results of total absorption and capillary absorption.

IV.2.3.7Adhesion resistance

Figure IV.23 illustrates the results of the adhesion strength of two-component mortars based on the fiber content and type after 28 days of dry curing. The average results are based on three experiments.

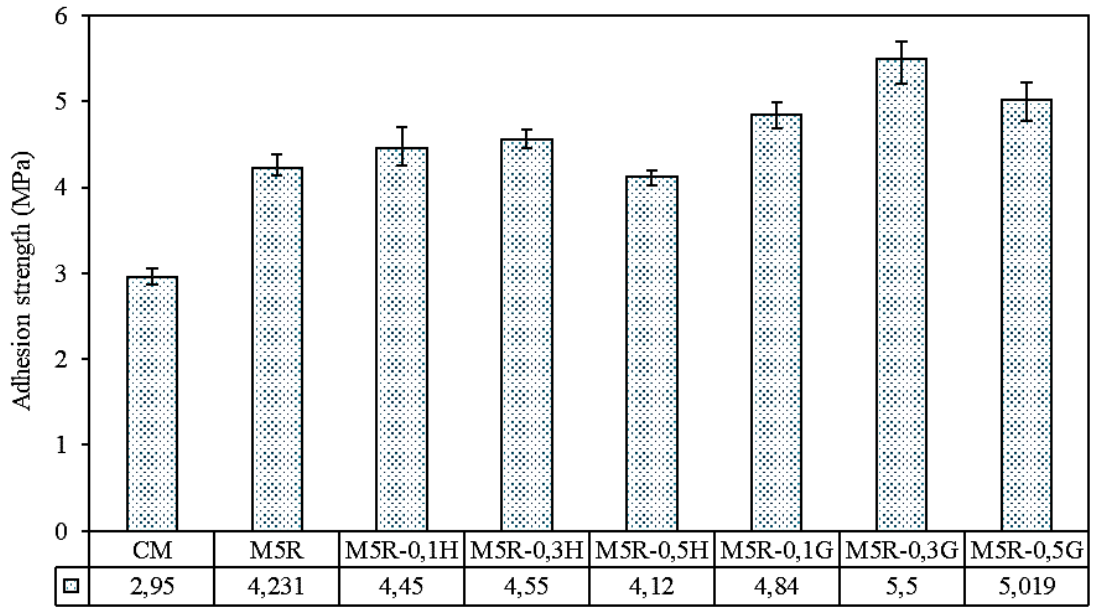

Figure IV. 23 Adhesion of mortars to cementitious supports.

Adding 5% SBR latex improved adhesion by 30%, as demonstrated in the results. Various studies have investigated the effect of polymer addition on mortar adhesion to different substrates. For example, Jo, Y.-K [104] reported that adding polymers such as SBR, EVA, and PAE could increase mortar substrate adhesion by 2-3 times. Benali, Y. and F. Ghomari [99] conducted adhesion tests on mortar substrates and found that adding SBR latex in powder or emulsion form in the range of 0-20% proportion increased adhesion. Jo, Y.-K [104] also observed, using SEM, that the polymer film was uniformly distributed and adhered to the substrate's concrete aggregate. The bond between the polymer film and the hydrated cement

and aggregates was found to be strong, especially with the silica produced from cement hydration. For regular cement mortars, bonding surface adhesion is solely accomplished through cement hydration. The glass fiber-based polymer mortar (M5R-0.3G) showed superior adhesion compared to CM and M5R-H.

Figure IV. 24 Two-component mortar after rupture.

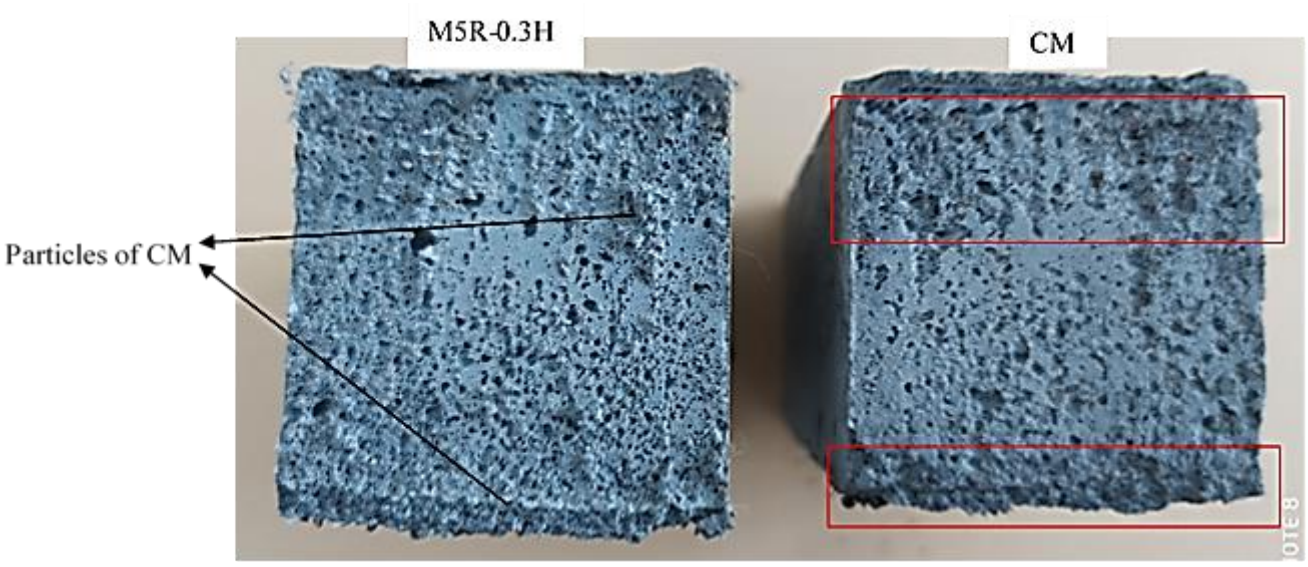

Figure IV. 25 Failure mode of M5R-0.3H sample under bending test.

IV.2.3.8 The thermogravimetric Derivatives (DTG) of mixtures

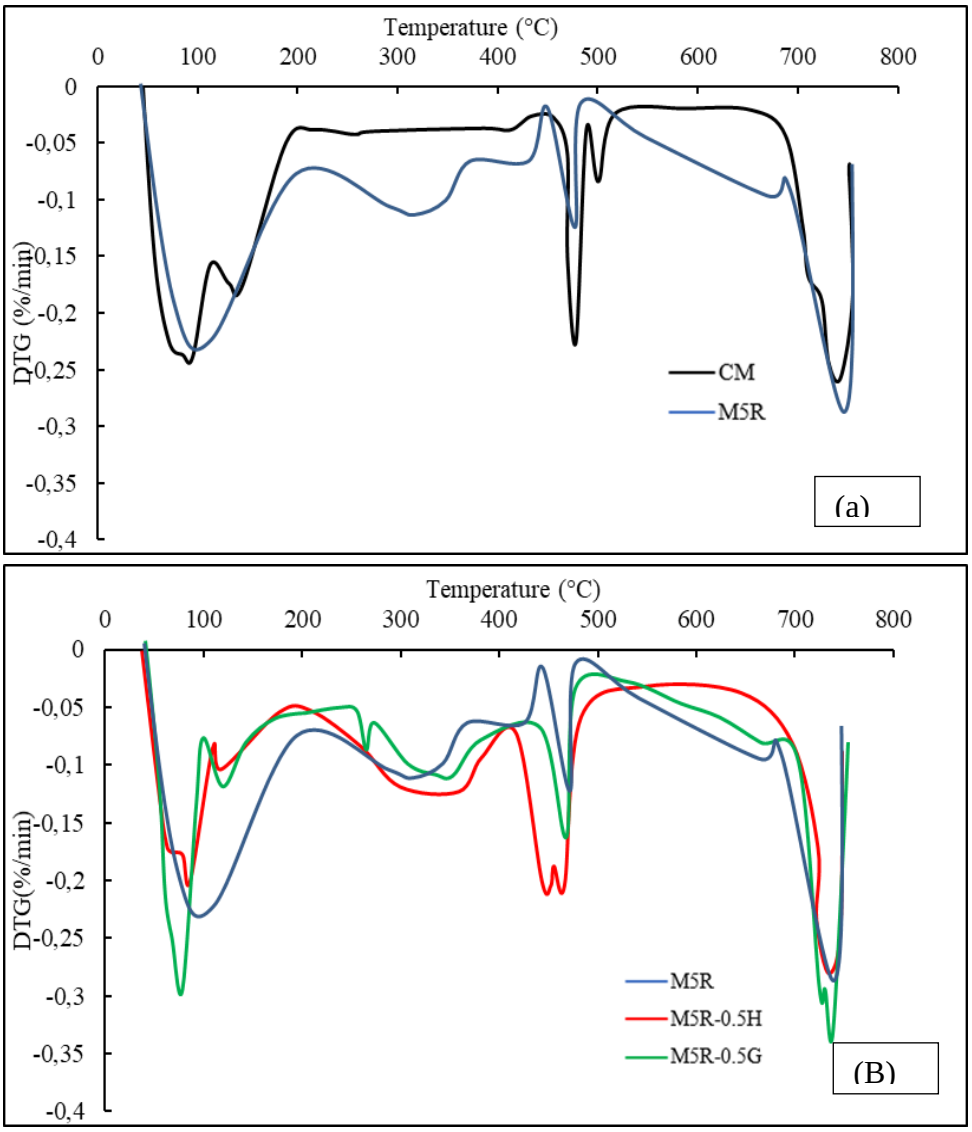

Figure IV. 26 Thermogravimetric analysis (DTG) results: (a) CM and M5R, (b) M5R, M5R-0.5H, and M5R-0.5G at 60 days.

The significance of Thermogravimetric Derivatives (DTG) in evaluating hydration product properties and identifying different phases is emphasized [182]. The DTG curves for CM and M5R samples at 60 days are presented in Figure IV. 26. a. The DTG curve of the cement mortar (CM) showed three regions with 68-120°C corresponding to the dehydration of calcium silicate hydrate (CSH), 460-480°C consisting of calcium hydroxide calcium and 700-750°C for the decarbonation of calcium carbonate $CaCO_3$ [183]. Examination of the M5R

DTG curve revealed that the presence of the polymer had a minimal effect on the formation of CSH but resulted in the formation of carbonates, with the carbonate decomposition peak (700-750°C) of M5R broadened. These findings are consistent with those of Betioli et al. [184]. Additionally, M5R displayed a weaker peak at 440-470°C than CM, which is associated with the degradation of polymers and silicate solids [185].

The reduction in compressive strength of polymer mortars can be attributed to the adsorption of polymers on the surface of cement particles, limiting contact with water and inhibiting the growth of hydrates, forming a film that makes it difficult to access water. This is accompanied by slower silicate hydrate formation than that of CM. Furthermore, the complexation of SBR with the calcium ions in the interstitial solution leads to a decrease in the formation of portlandite and ettringite [186].

As seen in Figure IV.26. b, the DTG curves of M5R, M5R-0.5H, and M5R-0.5G revealed that the presence of hemp fibers in the PM increased the peak between 400 and 480°C, which corresponds to the decomposition of portlandite and SBR. This increase is believed to be due to the absorption of Ca^{2+} and OH^- from the cement by the fibers and the polymer. As a result, the CSH of the M5R-0.5H mixture was reduced compared to M5R. Sedan et al. [156] demonstrated that hemp fibers with high pectin content bind Ca^{2+} calcium ions and OH^- hydroxide ions to their surface, resulting in a lack of hydroxide and calcium ions in the interstitial phase and a delay in setting due to the inhibition of calcium silicate hydrate (CSH). However, M5R-0.5G displayed a distinct CSH peak, which could result from a reaction between the glass fibers and the initial calcium, explaining the increased bond strength of the glass fibers-containing M5R due to the increase in C-S-H.

IV.2.4 Ultrasonic Pulse Velocity, dynamic modulus and damage coefficient

The Ultra Pulse Velocity (UPV), the dynamic modulus and damage coefficient of concrete at both room temperature and high temperature are presented in table IV.4.

Table IV. 4 Results from non-destructive testing.

Temperature	V^T(m/s)	$\rho^T(\frac{t}{m^3})$	D_V^T	E_d (GPa)
20°C	4350	2354	0,58	9.21
750°C	2900	2199		5.71

According to the data presented in Table IV.4 a clear observation emerges: the dynamic modulus of concretes undergoes a significant decrease after being subjected to a temperature of 750°C. Indeed, it can be observed that the initial value of this modulus is 9.21 GPa, whereas after exposure to heat, this value decreases considerably to reach 5.71 GPa.

This significant reduction in the dynamic modulus can be interpreted as an indicator of the impact of high temperature on the mechanical properties of the material. When concretes are subjected to intense heat, the chemical bonds and internal structure of the material can be altered, resulting in a decrease in its rigidity.

Furthermore, the mention of a "damage rate equal to 0.58" suggests a relationship between the decrease in the dynamic modulus and the damage suffered by the concretes because of exposure to 750°C. This damage rate of 0.58 can be understood as a quantitative measure of the extent of the damage suffered by the material.

In summary, the data from Table IV.4 reveal a significant reduction in the dynamic modulus of concretes after exposure to 750°C, thus reflecting the damage caused by heat. The damage rate of 0.58 emphasizes the importance of these damages and can serve as a reference for evaluating the performance and resistance of concretes under similar conditions in the future.

IV.2.5 Concrete after heating

The degradation of the concrete structure can be roughly identified by observing the surface of the concrete following exposure to high temperatures, as illustrated in figure IV.27. The test results reveal that, following the heating-cooling cycle at 750°C, all specimens exhibited obvious damage in the structure.

Figure IV. 27 Concrete specimens after the heating-cooling cycle to 750°C.

The interior morphologies of concrete after the 750°C heating-cooling cycle are depicted in figure IV.28. As the temperature rises, the aggregate volume expands, while the cement paste undergoes shrinkage. Consequently, cracks form along the interface of the aggregate-cement matrix. This occurrence may be attributed to the thermal incompatibility between the aggregates and cement matrix.

Figure IV. 28 Internal damage of specimens following the 750°C heating-cooling cycle.

IV.2.5.1 Repair of concrete subjected to high temperature

Fire is a crucial phenomenon that can have a profound effect on concrete. In many cases, it causes enormous degradation, which can weaken the structure and put it at risk of collapse. In our study, we tested the effects of fire on concrete specimens by placing 10x10x10 cm^3 concrete blocks in an oven and exposing them to a temperature of 750°C for 1 hour. The

results showed a dramatic decrease in the residual compressive strength of the concrete, which was measured to be 18 MPa after heating (C-F), representing a great decrease from the initial strength of 43 MPa measured at 365 days. The photos taken during the experiment clearly illustrate the severe degradation caused by the fire, which highlights the need for effective fire protection measures in concrete structures. Given the risks posed by fire degradation in concrete structures, such as tunnels and major building structures, our goal in this research was to develop a low-cost and highly effective method for repairing degraded concrete. To that end, we used polymer concrete containing 0.3% fiberglass and 5% SBR latex, and compared the results with commercially available mortars.

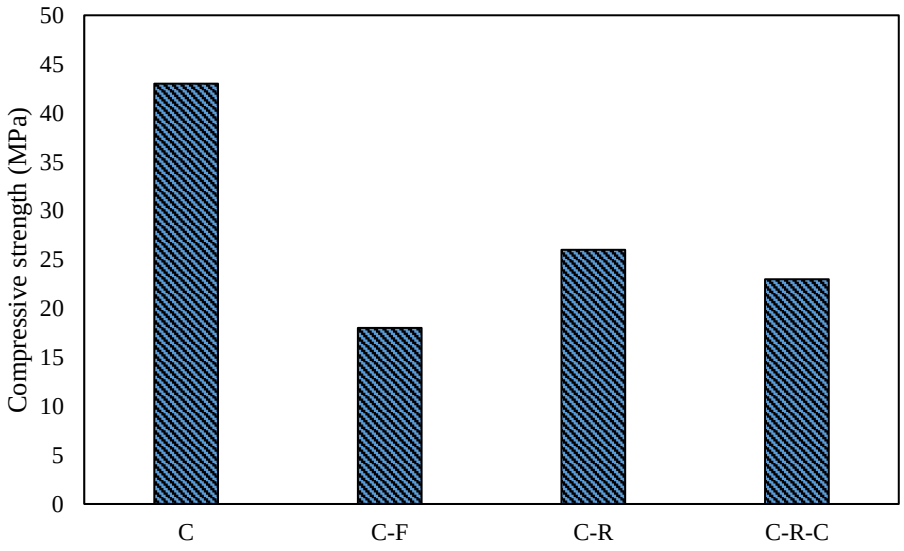

C: The control concrete before heating.
C-F: Concrete after heating.
C-R: The concrete specimens repaired using the repair concrete of our study
C-R-C: The concrete specimens repaired using a commercial reparation mortar.

Figure IV. 29 Comparison between concrete that was heated and repaired using two different types of materials.

According to Figure IV.29, it can be observed that (C-R) exhibits a remarkable improvement in resistance, with an increase of 35%. This is a significant result and demonstrates the effectiveness of the repair concrete in strengthening the damaged concrete structures. Additionally, the adhesion of the repaired concrete is very good, which ensures that the repair remains stable and secure over time. Furthermore, the new mortar-based concrete developed

in our research delivers comparable results to commercially available mortar. This implies that the mortar-based concrete developed in our study can be a viable alternative to commercial products(C-R-C), offering similar levels of performance and durability. In conclusion, our study provides evidence of the effectiveness of the repair concrete and the new mortar-based concrete, making them suitable options for repairing and restoring concrete structures.

Figure IV. 30 Photo of test specimens repaired after crushing.

IV.2.5.2 Adhesion between damaged concrete and repair concrete

According to figure IV.31, it is evident that there is a good bond between the degraded concrete and the chosen laboratory-level repair mortar. This indicates the effectiveness of our repair product for concrete subjected to high temperatures. The strong bond between the two materials is essential for ensuring a solid and durable repair of damaged concrete surfaces. This finding reinforces confidence in our repair product and suggests that it is capable of repairing concrete exposed to extreme conditions, such as high temperatures, providing a reliable solution for concrete repair in such situations.

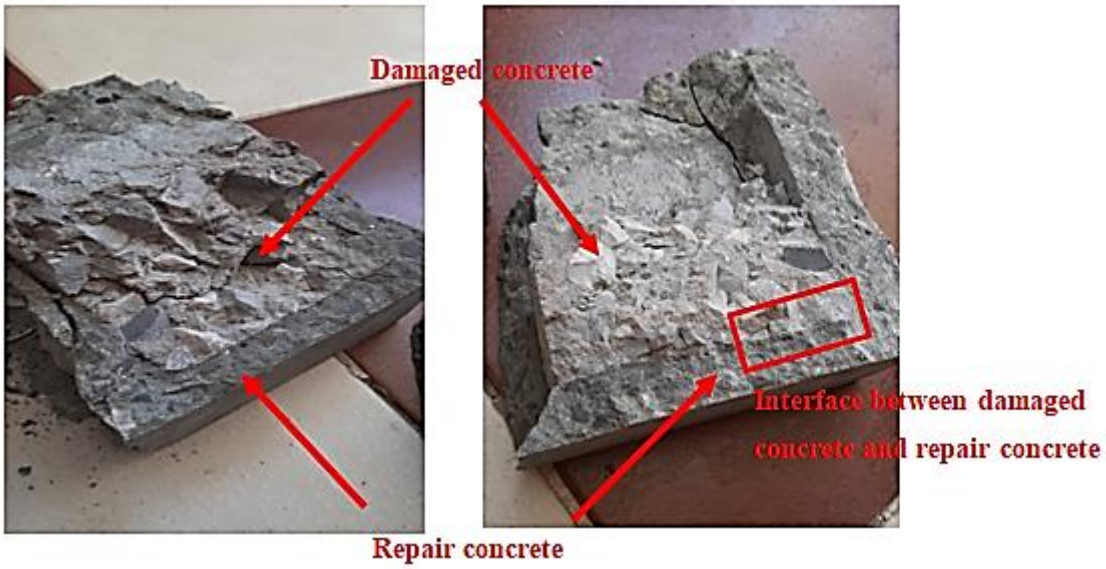

Figure IV. 31 The adhesion between heated concrete specimens and the repair concrete.

IV.2.5.3 Image analysis (digital modeling)

The figure III.32 presents the deformation response in relation to the applied compressive load on the repaired test specimens.

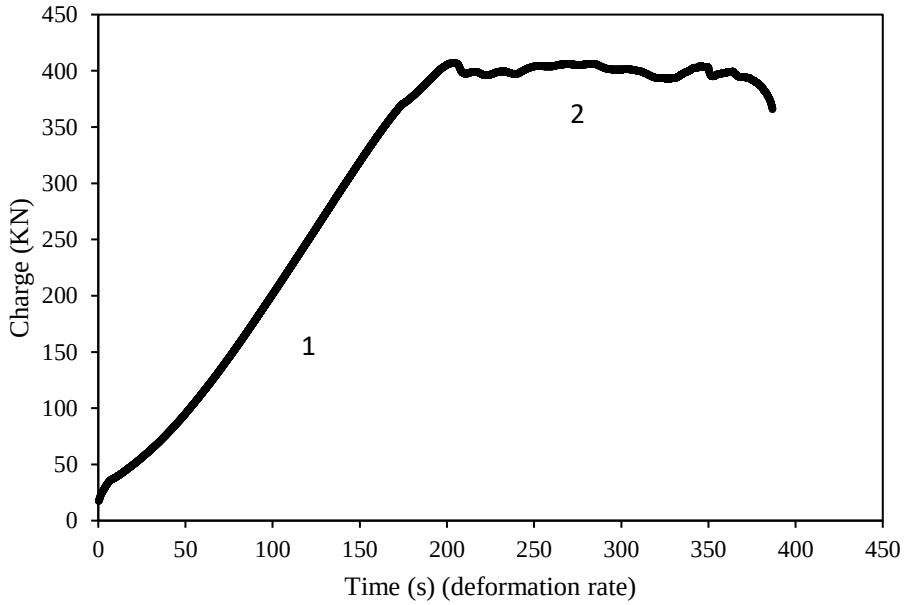

Figure IV. 32 load deformation curve.

In phase 2, a ductile portion is observed, indicating the effect of fibers and polymers present in the repair concrete.

The appearance of a ductile portion in the deformation curve suggests that the repair concrete has improved ductility properties due to the incorporation of fibers and polymers. Fibers, such as glass fibers, enhance the strength and toughness of the concrete by preventing crack propagation and absorbing deformation energy. Polymers, on the other hand, can contribute to improving the flexibility and resistance of the material.

This observation highlights the effectiveness of the repair techniques employed, which result in repair concrete exhibiting higher ductile properties compared to the original concrete. This can be beneficial for enhancing resistance to compressive loads and the material's ability to absorb stresses without fracturing.

In summary, the presence of a ductile portion in the deformation curve of the repaired test specimens indicates that the incorporation of fibers and polymers in the repair concrete helps improve its ductility and resistance to compressive loads. These characteristics are essential in ensuring the durability and performance of the repaired concrete under structural demands.

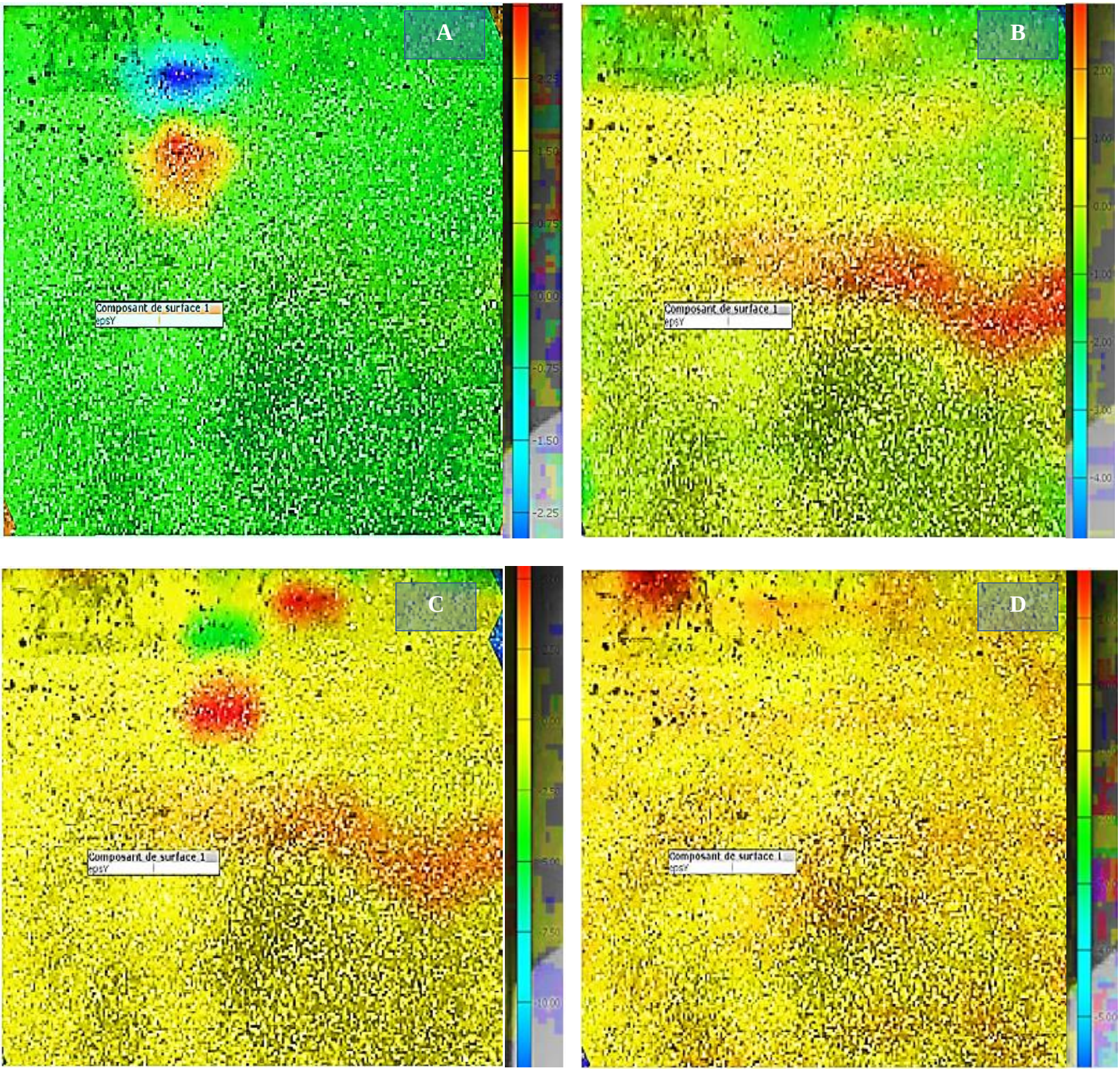

Figure IV. 33 Evolution of the deformations of the specimen.

The figure represents an analysis of images of repaired concretes using Gom software, showing different states of damage. At the beginning of the crushing zone (Phase A), the

majority of the surface appears glassy, suggesting a relatively low stress. This indicates a moderate compressive stress on this part of the concrete. However, a small portion of the surface is represented in blue, suggesting a tensile stress. This area may experience deformation due to tensile forces, which could be the result of structural weakness or external loading.

Additionally, a small yellow-colored area is present, indicating a compressive stress. This zone may be subjected to significant pressure, possibly due to additional loading or locally applied stress.

In Phase B, a yellow band with red is observed on the surface of the specimen. This indicates a very high compressive stress in the middle of the specimen, while the other parts are predominantly glassy with some yellow. It can be concluded that the central part of the repaired specimen experiences the highest stress and requires particular attention.

In Phase C, it is observed that the yellow area expands and occupies the majority of the surface, indicating a higher compressive stress. This suggests that this specific zone of the concrete is subjected to significant pressure, possibly due to additional loading or locally applied stress. Furthermore, a red band appears in the middle of the specimen, indicating very high stress. This highlights the importance of adhesion between the repair materials and the concrete exposed to fire, as it is more heavily stressed compared to other parts.

In Phase D, the entire surface of the specimen is yellow, indicating a homogeneous distribution of compressive stresses. This observation suggests that the repair concrete has successfully absorbed and evenly distributed the stresses exerted on the entire surface, demonstrating enhanced overall strength.

In summary, the image analysis reveals different zones of damage in the repaired concrete. The presence of specific colors such as glassy, blue, and yellow helps identify the different stresses to which these zones are subjected, including low stress, tension, and compression. This interpretation aids in understanding the strengths and weaknesses of the material, guiding appropriate repair and reinforcement measures.

This comprehensive interpretation contributes to guiding appropriate repair and reinforcement measures, focusing on areas with higher stresses. By considering this information, targeted repair strategies can be implemented to strengthen the most vulnerable parts of the repaired concrete, ensuring long-term durability and structural resistance.

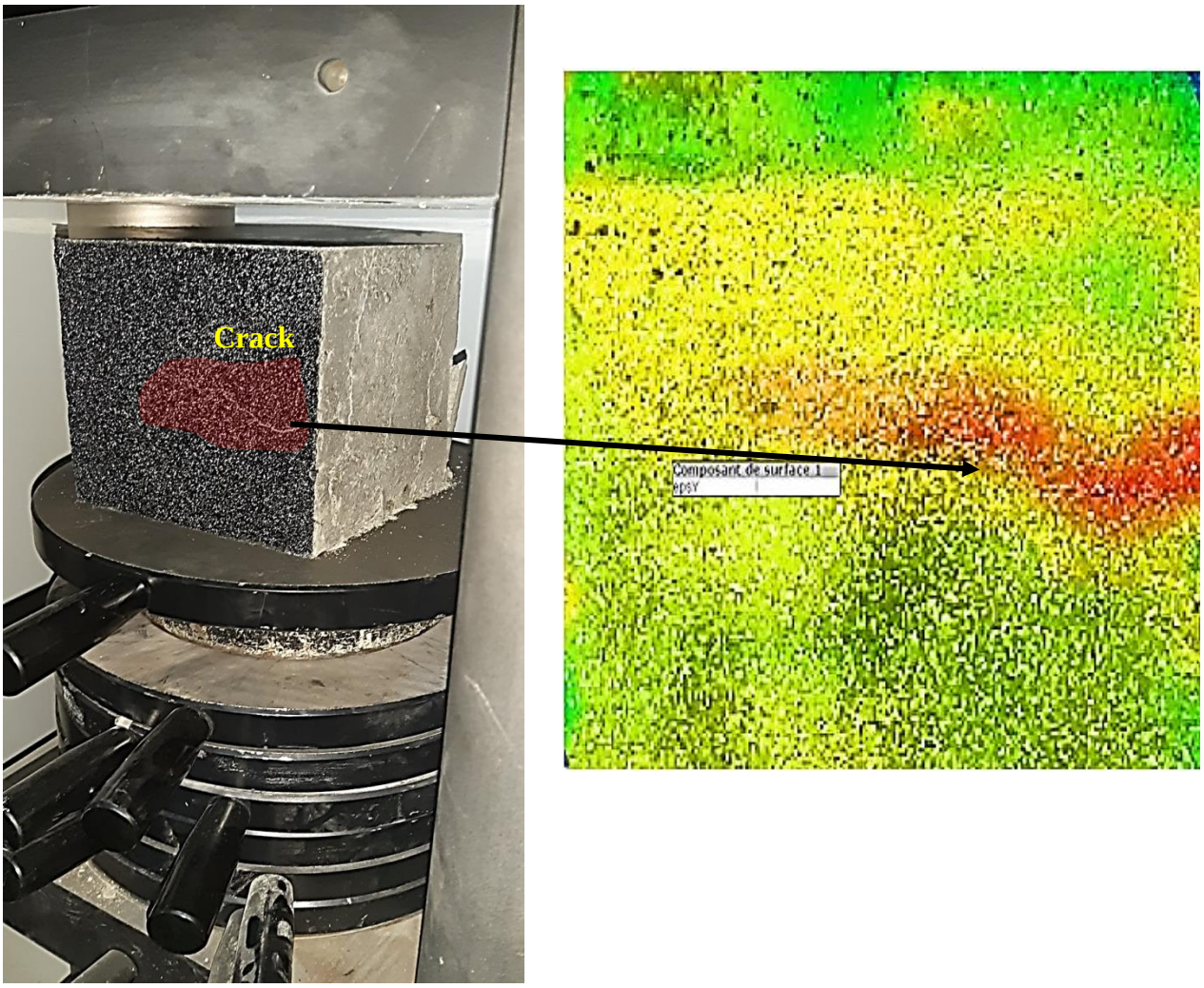

Figure IV. 34 Specimen after crushing.

IV.3 Conclusion

The properties of mortar-polymer composites containing different fibers were studied in this chapter. Spreading, resistance to compression and bending, shrinkage adhesion, absorption, and thermogravimetric analysis were conducted for this purpose. The following conclusions have been drawn from the results obtained in the study:

- The numerical modeling based on the factorial design demonstrates its effectiveness by providing mathematical laws for accurate prediction of various observed phenomena.
- The microstructural analysis conducted using a scanning electron microscope reveals excellent compatibility between the fibers and the polymer matrix."
- A 38% increase in fluidity and a decrease in the W/C ratio from 0.5 to 0.43 were noted in cement mortar upon the addition of 5% SBR latex.
- Fluidity was found to be poor in polymer mortars containing hemp and glass fibers, depending on the content and type of fibers, due to the increased cohesion and homogeneity of the fiber-based mixture.
- A 6% decrease in wet density was observed upon the addition of 5% SBR latex, due to the air-entraining effect of the SBR latex. Conversely, the wet density of fibrous polymer mortars increased based on the proportion and nature of the fibers, indicating good cohesion between the fibers and the polymer matrix. M5R-0.5H was found to be 3% denser than M5R.
- According to the results of the tests, a positive effect on most of the samples was noted for cure time. After 7 days, a 25% increase in flexural strength was recorded for M5R-0.5H mortars and a 20% increase in flexural strength was recorded for M5R-0.5G mortars in comparison to M5R and CM. This is due to the ductility and toughness of hemp and glass fibers, which leads to greater resistance to cracking from stress transfer from the fibrous matrix. The best flexural strength after 28 days was found to be in the latex-modified mortar containing hemp and glass fibers, dependent on the dosage and nature of the fiber. The optimum fiber content for hemp and fiberglass was determined to be 0.5%, with increases of 14% and 10% respectively over M5R.
- An increase of 14%, 9.5% and 10% in compressive strength after 7, 28 and 60 days respectively was observed upon the incorporation of 0.5% hemp fiber in PM compared to M5R. Similarly, the presence of 0.3% glass fibers in PM resulted in increases of 13.5%, 6% and 0.6% after 7, 28 and 60 days respectively.

- Good long-term shrinkage properties were noted in cement mortars containing 0.5% or 0.3% hemp fiber soaked in 5% NaOH, upon the addition of 10% silica fume and 5% SBR latex.
- An increase in adhesion was observed for fiberglass-based polymer mortars, particularly M5R-0.3G, with a 23% increase compared to M5R. Slight increases in adhesion were noted for M5R-0.1H and M5R-0.3H compared to M5R, while a slight decrease in adhesion was observed for M5R-0.5H. Further study is required for these results.
- A decrease in CSH and a slight increase in portlandite were indicated in PM upon the presence of hemp fibers, according to the DTG curves.

The image analysis using GOM software provides valuable insights into the condition of the repaired concrete. The identification of different zones of damage and the analysis of specific colors indicative of different stresses offer a comprehensive understanding of the material's strengths and weaknesses. This knowledge allows for targeted repair and reinforcement measures to be implemented, focusing on areas experiencing higher stresses.

By utilizing this comprehensive interpretation, repair strategies can be tailored to strengthen the most vulnerable parts of the repaired concrete. This approach ensures long-term durability and structural resistance, as the repairs are specifically designed to address the identified areas of concrete. Ultimately, the image analysis and its resulting insights contribute significantly to guiding appropriate repair and reinforcement measures, promoting the overall integrity and longevity of the concrete structure.

General conclusion

GENERAL CONCLUSION

The degradation of concrete due to fire is a common problem in buildings, which has motivated research on the behavior of ordinary and high-performance concrete during fires. Theoretical and experimental studies have been conducted to better understand the observed phenomena and identify the key factors influencing the fire performance of concrete. However, limited research has been done on the repair of concrete damaged by thermal shock. Polymer-mortar composites are commonly used materials for protecting and repairing concrete surfaces. While previous studies have explored the use of polymer mortars to repair chemical and mechanical degradation, none have specifically examined the repair of concrete exposed to high temperatures. This study chose to use a single type of polymer, styrene-butadiene rubber (SBR), and incorporated two types of fibers: glass fiber and hemp fiber.

The study was composed of three distinct parts. The first part involved numerical modeling based on a full factorial design to study the influence of the presence or absence of polymer and glass fibers. The results showed that the addition of a high dosage of SBR resulted in increased flexural strength, reduced water absorption and shrinkage. Furthermore, a microstructural analysis conducted using a scanning electron microscope revealed good adhesion between the polymer matrix and the glass fibers, thus explaining the increased flexural strength.

The second part of the study focused on comparing the effect of vegetable fibers and glass fiber on the performance of repair mortars. The objective was to introduce vegetable fibers to reduce environmental impact and costs while maintaining or improving the same mechanical performance as polymer mortars. The results showed that after 7 days, a 25% increase in flexural strength was recorded for M5R-0.5H mortars, and a 20% increase was recorded for M5R-0.5G mortars compared to M5R and CM mortars. This is due to the ductility and toughness of hemp and glass fibers, which provide greater resistance to cracking caused by stress transfer from the fibrous matrix. The best flexural strength after 28 days was achieved in the latex-modified mortar containing hemp and glass fibers, depending on the dosage and nature of the fiber. The optimal fiber content for hemp and glass fiber was determined to be 0.5%, resulting in respective increases of 14% and 10% over M5R mortars.

Furthermore, an increase of 14%, 9.5%, and 10% in compressive strength after 7, 28, and 60 days, respectively, was observed upon the incorporation of 0.5% hemp fiber in the polymer mortar compared to M5R mortar. Similarly, the presence of 0.3% glass fibers in the polymer mortar resulted in increases of 13.5%, 6%, and 0.6% after 7, 28, and 60 days, respectively. Good long-term shrinkage properties were noted in cement mortars containing 0.5% or 0.3%

hemp fiber soaked in a 5% NaOH solution, with the addition of 10% silica fume and 5% SBR latex.

In summary, the results of the second part of the study showed that the addition of fibers significantly improves the mechanical and physical performance of polymer mortars. The presence of hemp and glass fibers in polymer mortars reduces their fluidity, increases cohesion and homogeneity, and leads to a decrease in spread ability. However, the adhesion strength of mortars containing hemp fibers showed a slight increase, except for M5R-0.5H mortar, which showed a slight decrease. Further studies are needed to fully understand these results.

Finally, the study of repairing concrete exposed to high temperatures has revealed that the materials developed in this study exhibit superior behavior compared to commercially available mortars. This suggests that the repair concrete and the new mortar-based concrete developed in this study could be a viable option as substitutes for commercial products, offering equivalent or even better levels of performance and durability. In conclusion, this study demonstrates the effectiveness of repair concrete and the new mortar-based concrete, making them appropriate choices for the repair and restoration of concrete structures, while providing significant environmental and economic benefits. Future research can further explore these findings and investigate other types of fibers and polymers for optimal use in high temperature concrete repair applications.

Image analysis using GOM software is a powerful tool for assessing the condition of concrete structures and guiding appropriate repair and reinforcement measures. By analyzing different zones of damage and identifying specific colors associated with varying stresses, the analysis provides a comprehensive understanding of the material's behavior and vulnerabilities.

This comprehensive interpretation enables targeted repair strategies to be implemented, focusing on areas experiencing higher stresses. By strengthening the most vulnerable parts of the structure, long-term durability and structural resistance can be ensured.

The use of image analysis in concrete assessment contributes significantly to the overall integrity and longevity of structures. It allows for informed decision-making regarding repair and reinforcement, leading to improved structural performance and reduced maintenance costs.

Overall, image analysis using GOM software plays a crucial role in the field of concrete engineering, providing valuable insights for efficient and effective repair and reinforcement strategies. It is a valuable tool for engineers and professionals involved in the maintenance

and preservation of concrete structures, promoting their safety and longevity in various industries such as construction, infrastructure, and beyond.

References

1. Dreux, G. and J. Festa, *Nouveau guide du béton et de ses constitutants*. 1998: Eyrolles.
2. Mehta, P.K. and P.J. Monteiro, *Concrete: microstructure, properties, and materials*. 2014: McGraw-Hill Education.
3. Feldman, R.F. and P.J. Sereda, *A model for hydrated Portland cement paste as deduced from sorption-length change and mechanical properties.* Matériaux et Construction, 1968. **1**(6): p. 509-520.
4. Badmann, R., N. Stockhausen, and M.J. Setzer, *The statistical thickness and the chemical potential of adsorbed water films.* Journal of Colloid and Interface science, 1981. **82**(2): p. 534-542.
5. Aïtcin, P.-C., *Binders for durable and sustainable concrete*. 2007: CRC Press.
6. Hagymassy Jr, J., S. Brunauer, and R.S. Mikhail, *Pore structure analysis by water vapor adsorption: I. t-curves for water vapor.*Journal of Colloid and Interface Science, 1969. **29**(3): p. 485-491.
7. Sierra, R., *CONTRIBUTION A L'ETUDE DE L'HYDRATATION DES SILICATES CALCIQUES HYDRAULIQUES.* Rapport de recherche, 1974(39).
8. Tsimbrovska, M., *Dégradation des bétons à hautes performances soumis à des températures élevées: évolution de la perméabilité en liaison avec la microstructure*. 1998, Grenoble 1.
9. Canonico, F., et al. *Microstructural investigations on hydrated high-performance cements based on calcium sulfoaluminate*. in *12th International Congress on the Chemistry of Cement. Montreal, Canada*. 2007.
10. Stark, J. and B. Wicht, *Dauerhaftigkeit von Beton der Baustoffals Werkstoff*. 2001, Springer Berlin.
11. Reynouard, J.M. and G. Pijaudier-Cabot, *Comportement mécanique du béton*. 2005, Hermès Sciences.
12. Noumowe, A., *Effet de hautes températures (20-600 C) sur le béton: cas particulier du béton a hautes performances*. 1995, Lyon, INSA.
13. Hachemi, S., *Etude du Comportement du béton soumis à haute température: Influence du type de béton et de la nature des constituants*. 2015, Université Mohamed Khider-Biskra.
14. Alonso, C. and L. Fernandez, *Dehydration and rehydration processes of cement paste exposed to high temperature environments.* Journal of materials science, 2004. **39**(9): p. 3015-3024.
15. Wetzig, V. *Destruction mechanisms in concrete material in case of fire, and protection systems*. in *PROCEEDINGS OF THE FOURTH INTERNATIONAL CONFERENCE ON SAFETY IN ROAD AND RAIL TUNNELS, HELD MADRID, SPAIN, 2-6 APRIL 2001*. 2001.
16. Castellote, M., et al., *Composition and microstructural changes of cement pastes upon heating, as studied by neutron diffraction.*Cement and concrete research, 2004. **34**(9): p. 1633-1644.
17. Hager, I., *Comportement à haute température des bétons à haute performance: évolution des principales propriétés mécaniques*. 2004, Marne-la-vallée, ENPC.
18. Kodur, V.K.R. and M.A. Sultan, *Structural behaviour of high strength concrete columns exposed to fire.* 1998.
19. Khoury, G., et al., *Fire Design of Concrete Structures—Materials, Structures and Modelling.* Fib Bull, 2007. **38**: p. 6245.

20. Rodovalho, F.d.S. and M.R.S. Corrêa, *Thermal simulation of prisms with concrete blocks in a fire situation.* Revista IBRACON de Estruturas e Materiais, 2019. **12**: p. 638-657.
21. Matesová, D., D. Bonen, and S.P. Shah, *Factors affecting the resistance of cementitious materials at high temperatures and medium [0] heating rates.*Materials and structures, 2006. **39**(4): p. 455-469.
22. Hachemi, S. and A. Ounis, *L'influence de la nature du sable sur les proprietes physiques et mecaniques du beton soumis a haute temperature.*Courrier du Savoir, 2017. **24**.
23. Khoury, G., *Compressive strength of concrete at high temperatures: a reassessment.* Magazine of concrete Research, 1992. **44**(161): p. 291-309.
24. Rafi, M.M., T. Aziz, and S.H. Lodi, *Mechanical properties of low-strength concrete at exposure to elevated temperatures.*Journal of Structural Fire Engineering, 2017.
25. Razafinjato, R.N. *Comportement à haute température des granulats naturels siliceux et calcaires et leur influence sur celui du béton*. in *Rencontres Universitaires de Génie Civil*. 2015.
26. Tshimanga, M.K., *Influence des paramètres de formulation et microstructuraux sur le comportement à haute température des bétons.* Revue Européenne de Génie Civil, 2006. **10**(8): p. 1011-1011.
27. Fares, H., *Propriétés mécaniques et physico-chimiques de bétons autoplaçants exposés à une température élevée*. 2009, Université de Cergy Pontoise.
28. Haniche, R., *Contribution à l'étude des bétons portés en température/Evolution des propriétés de transfert: Etude de l'éclatement*. 2011, Lyon, INSA.
29. Hachemi, S. and A. Ounis, *Performance of concrete containing crushed brick aggregate exposed to different fire temperatures.* European Journal of Environmental and Civil Engineering, 2015. **19**(7): p. 805-824.
30. Chen, B., C. Li, and L. Chen, *Experimental study of mechanical properties of normal-strength concrete exposed to high temperatures at an early age.* Fire Safety Journal, 2009. **44**(7): p. 997-1002.
31. Tufail, M., et al., *Effect of elevated temperature on mechanical properties of limestone, quartzite and granite concrete.*International Journal of Concrete Structures and Materials, 2017. **11**(1): p. 17-28.
32. Xing, Z., *Influence de la nature minéralogique des granulats sur leur comportement et celui du béton à haute température*. 2011, Université de Cergy Pontoise.
33. Amen prosper Pliya, B., *Contribution des fibres de polypropylène et métalliques à l'amélioration du comportement du béton soumis à une température élevée*. 2010, Cergy-Pontoise.
34. Mindeguia, J.-C., *Contribution expérimentale à la compréhension des risques d'instabilité thermique des bétons*. 2009, Université de Pau et des Pays de l'Adour.
35. Nguyen, h., *Comportement des bétons ordinaire et à hautes performances soumis à haute température: application à des éprouvettes de grandes dimensions*. 2013, Cergy-Pontoise.
36. Hager, I. and P. Pimienta, *Déformation thermique transitoire des bétons à haute performance: Etude expérimentale.*Revue européenne de génie civil, 2005. **9**(3): p. 373-383.
37. Castillo, C., *Effect of transient high temperature on high-strength concrete*. 1987: Rice University.
38. Ulrich, S., *Concrete at high temperatures—A general review.*Fire Safety Journal, 1988. **13**(1): p. 55-68.

39. Kanema Tshimanga, M., *Influence des paramètres de formulation sur le comportement à haute température des bétons*. 2007, Cergy-Pontoise.
40. Anand, N. and G.P. Arulraj, *Effect of grade of concrete on the performance of self-compacting concrete beams subjected to elevated temperatures.* Fire Technology, 2014. **50**(5): p. 1269-1284.
41. Al razib, M.S., F.I. Rahman, and M. Hussain, *Elevating the Effect of Temperature on Compressive and Tensile Strength of Concrete with Admixture.*2017.
42. BELARIBI, H., *L'influence des types de fibres sur le comportement du béton à haute température*. 2019, Université Mohamed Khider-Biskra.
43. Yermak, N., *Comportement à hautes températures des bétons additionnés de fibres*. 2015, Cergy-Pontoise.
44. ArupFire, H., *Fire resistance of concrete enclosures, Work package 1: data collection, work package 2: spalling categories.* Rev B, 2005.
45. Jansson, R., *Material properties related to fire spalling of concrete*. 2008: Division of Building Materials, Lund Institute of Technology, Lund University.
46. Ho, D. and R. Lewis, *Carbonation of concrete and its prediction.* Cement and Concrete Research, 1987. **17**(3): p. 489-504.
47. Ekolu, S., *A review on effects of curing, sheltering, and CO2 concentration upon natural carbonation of concrete.* Construction and Building Materials, 2016. **127**: p. 306-320.
48. Stanish, K., R. Hooton, and M. Thomas, *Testing the chloride penetration resistance of concrete: a literature review.* 1997.
49. Stanish, K., R.D. Hooton, and M.D. Thomas, *Testing the chloride penetration resistance of concrete: a literature review.* 2001.
50. CURRIE, R., et al., *Corrosion of reinforcement in concrete construction*. 1983.
51. Lawrence, C., *Sulphate attack on concrete.* Magazine of concrete Research, 1990. **42**(153): p. 249-264.
52. Piasta, W., *Analysis of carbonate and sulphate attack on concrete structures.* Engineering Failure Analysis, 2017. **79**: p. 606-614.
53. Suleiman, A.R., *Physical sulphate attack on concrete.* 2014.
54. Bazant, Z.P. and F.H. Wittmann, *Creep and shrinkage in concrete structures.* 1982.
55. Cai, H. and X. Liu, *Freeze-thaw durability of concrete: ice formation process in pores.* Cement and concrete research, 1998. **28**(9): p. 1281-1287.
56. Sun, W., et al., *Damage and damage resistance of high strength concrete under the action of load and freeze-thaw cycles.* Cement and Concrete Research, 1999. **29**(9): p. 1519-1523.
57. Wang, R., et al., *Review on the deterioration and approaches to enhance the durability of concrete in the freeze–thaw environment.* Construction and Building Materials, 2022. **321**: p. 126371.
58. Khoury, G.A., *Effect of fire on concrete and concrete structures.* Progress in structural engineering and materials, 2000. **2**(4): p. 429-447.
59. Georgali, B. and P. Tsakiridis, *Microstructure of fire-damaged concrete. A case study.* Cement and Concrete composites, 2005. **27**(2): p. 255-259.
60. Chabbi, R., N. Ferhoune, and F. Bouabdallah, *Pathologies, diagnostic à l'aide de CND et techniques de réparation et protection des ouvrages en béton armé: état de l'art.*
61. Song, H.-W., et al., *Service life prediction of repaired concrete structures under chloride environment using finite difference method.*Cement and concrete composites, 2009. **31**(2): p. 120-127.

62. Mirouzi, G., B. Redjel, and R. Jauberthie, *Formulation et comportement mécanique de micro-bétons à matrice de résine polyester.*Nature & Technology, 2013(9): p. 19.
63. Iskhakov, I., et al., *High performance repairing of reinforced concrete structures.* Materials & Design, 2013. **44**: p. 216-222.
64. Garbacz, A., L. Courard, and K. Kostana, *Characterization of concrete surface roughness and its relation to adhesion in repair systems.* Materials characterization, 2006. **56**(4-5): p. 281-289.
65. Kay, T., *Assessment and renovation of concrete structures*. 1992.
66. Tiberti, G., F. Minelli, and G. Plizzari, *Reinforcement optimization of fiber reinforced concrete linings for conventional tunnels.* Composites Part B: Engineering, 2014. **58**: p. 199-207.
67. Chiaia, B., A.P. Fantilli, and P. Vallini, *Combining fiber-reinforced concrete with traditional reinforcement in tunnel linings.* Engineering Structures, 2009. **31**(7): p. 1600-1606.
68. Ribeiro, M.S.S., A.F. Gonçalves, and F.A.B. Branco, *Styrene-butadiene polymer action on compressive and tensile strengths of cement mortars.* Materials and Structures, 2008. **41**(7): p. 1263-1273.
69. Guo, S.-Y., et al., *Mechanical and interface bonding properties of epoxy resin reinforced Portland cement repairing mortar.* Construction and Building Materials, 2020. **264**: p. 120715.
70. Monteiro, F., L. Trautwein, and L. Almeida, *The importance of the European standard EN 1504, on the protection and repair of concrete structures.* Journal of Building Pathology and Rehabilitation, 2017. **2**(1): p. 1-12.
71. Ohama, Y. *Recent progress in research and development activities of concrete-polymer composites in Japan*. in *Proc. of 11th International Congress on Polymers in Concrete, Berlin, Germany, 2004*. 2004.
72. Ribeiro, M.C.d.S., *New polymer mortar formulations: development, characterization and application forms.* 2006.
73. Ohama, Y. *Concrete-polymer composites–The past, present and future*. in *Key Engineering Materials*. 2011. Trans Tech Publ.
74. Dhir, R., et al., *An investigation into the feasibility of formulating 'self-cure'concrete.* Materials and structures, 1994. **27**(10): p. 606-615.
75. Rixom, R. and N. Mailvaganam, *Chemical admixtures for concrete', E &FN SPON, Ltd*. 1999, London.
76. Day, R.J., P.A. Lovell, and D. Pierre, *Toughening of epoxy resins using particles prepared by emulsion polymerization: effects of particle surface functionality, size and morphology on impact fracture properties.* Polymer international, 1997. **44**(3): p. 288-299.
77. Fowler, D.W. *State of the art in concrete polymer materials in the US*. in *International Congress on Polymers in Concrete, Chuncheon, Korea*. 2007. Citeseer.
78. Van Gemert, D., et al. *Cement concrete and concrete Polymer composites: two merging worlds. A report from 11th ICPIC Congress in Berlin, 2004*. in *Proceedings of the International Symposium Polymers in Concrete. ISPIC*. 2006.
79. Benosman, A.S., *Performances mécaniques et durabilité des matériaux cimentaires modifiés par ajout de polymére (PET)*. 2010, Université d'Oran1-Ahmed Ben Bella.
80. Ohama, Y., *Recent progress in concrete-polymer composites.* Advanced Cement Based Materials, 1997. **5**(2): p. 31-40.
81. Czarnecki, L., *Concrete-polymer composites: trends shaping the future.* International journal of the Society of Materials Engineering for Resources, 2007. **15**(1): p. 1-5.

82. Haidar, M., *Optimisation et durabilité des micro-bétons à base d'époxyde*. 2011, Cergy-Pontoise.
83. Wang, R. and P. Wang, *Physical properties of SBR latex-modified mortar under different curing conditions.* Journal of the Chinese Ceramic Society, 2009. **37**(12): p. 2118-2123.
84. Sun, K., et al., *Effect of styrene-butadiene rubber latex on the rheological behavior and pore structure of cement paste.* Composites Part B: Engineering, 2019. **163**: p. 282-289.
85. Barluenga, G. and F. Hernández-Olivares, *SBR latex modified mortar rheology and mechanical behaviour.* Cement and Concrete Research, 2004. **34**(3): p. 527-535.
86. Ohama, Y., *Handbook of polymer-modified concrete and mortars: properties and process technology*. 1995: William Andrew.
87. Ohama, Y., D. Van Gemert, and M. Ota, *Introducing process technology and applications of polymer-modified mortar and concrete in construction.*Restoration of Buildings and Monuments, 2013. **19**(6): p. 369-392.
88. Goto, T., *Influence des paramètres moléculaires du latex sur l'hydratation, la rhéologie et les propriétés mécaniques des composites ciment/latex*. 2006, Université Pierre et Marie Curie-Paris VI.
89. Ramli, M., A.A. Tabassi, and K.W. Hoe, *Porosity, pore structure and water absorption of polymer-modified mortars: An experimental study under different curing conditions.* Composites Part B: Engineering, 2013. **55**: p. 221-233.
90. Wang, P., Q. Xu, and J. Stark, *Mechanical properties of styrene–butadiene emulsion modified cement mortar used for repair of bridge surface.* J. Build. Mater, 2001. **4**(1): p. 1-6.
91. Ngassam, I.L.T., S. Marceau, and T. Chaussadent. *Durabilité des réparations des ouvrages en béton armé avec des mortiers modifiés par des polymères*. in *Annales du Bâtiment et des Travaux Publics*. 2013. Editions ESKA.
92. Metalssi, O.O., *Étude des couplages hydratation-échanges hydriquescarbonatation dans les mortiers modifiés polymères.*Université de La Rochelle, 2006.
93. Dridi, M., S. Hachemi, and A.A. Belkadi, *Influence of styrene-butadiene rubber and pretreated hemp fibers on the properties of cement-based repair mortars.* European Journal of Environmental and Civil Engineering, 2022: p. 1-20.
94. Li, L., R. Wang, and Q. Lu, *Influence of polymer latex on the setting time, mechanical properties and durability of calcium sulfoaluminate cement mortar.* Construction and Building Materials, 2018. **169**: p. 911-922.
95. Shi, C., et al., *Influence of humidity on the mechanical properties of polymer-modified cement-based repair materials.* Construction and Building Materials, 2020. **261**: p. 119928.
96. Akinyemi, B. and T. Omoniyi, *Properties of latex polymer modified mortars reinforced with waste bamboo fibers from construction waste.* Buildings, 2018. **8**(11): p. 149.
97. Huang, H., et al., *Synthesis and characterization of ground glass fiber reinforced polyurethane-based polymer concrete as a cementitious runway repair material.* Construction and Building Materials, 2020. **242**: p. 117221.
98. Kwiecień, A., M. Gruszczyński, and B. Zajac. *Tests of flexible polymer joints repairing of concrete pavements and of polymer modified concretes influenced by high deformations*. in *Key Engineering Materials*. 2011. Trans Tech Publ.
99. Benali, Y. and F. Ghomari, *Latex influence on the mechanical behavior and durability of cementitious materials.* Journal of adhesion science and Technology, 2017. **31**(3): p. 219-241.

100. Wong, W., P. Fang, and J. Pan, *Dynamic properties impact toughness and abrasiveness of polymer-modified pastes by using nondestructive tests.* Cement and concrete research, 2003. **33**(9): p. 1371-1374.
101. Ma, H. and Z. Li, *Microstructures and mechanical properties of polymer modified mortars under distinct mechanisms.* Construction and Building Materials, 2013. **47**: p. 579-587.
102. Eren, F., et al., *Effects of latex modification on fresh state consistency, short term strength and long term transport properties of cement mortars.* Construction and Building Materials, 2017. **133**: p. 226-233.
103. Kim, J.-H. and R.E. Robertson, *Prevention of air void formation in polymer-modified cement mortar by pre-wetting.* Cement and Concrete Research, 1997. **27**(2): p. 171-176.
104. Jo, Y.-K., *Adhesion in tension of polymer cement mortar by curing conditions using polymer dispersions as cement modifier.* Construction and Building Materials, 2020. **242**: p. 118134.
105. Jo, Y., Y. Ohama, and K. Demura. *Strength, adhesion and chemical resistance of epoxy-modified mortars without hardener*. in *Proceedings of the First East Asia Symposium on Polymers in Concrete, Kangwon National University, Korea*. 1994.
106. Van den Heede, P., et al. *Screening of different encapsulated polymer-based healing agents for chloride exposed self-healing concrete using chloride migration tests*. in *Key Engineering Materials*. 2018. Trans Tech Publ.
107. Belbachir, B., et al. *Durability of mortars modified by the effect of combining SPA polymers and supplementary cementitious materials*. in *MATEC Web of Conferences*. 2018. EDP Sciences.
108. Rossignolo, J.A. and M.V. Agnesini, *Durability of polymer-modified lightweight aggregate concrete.* Cement and Concrete Composites, 2004. **26**(4): p. 375-380.
109. Yang, Z., et al., *Effect of styrene–butadiene rubber latex on the chloride permeability and microstructure of Portland cement mortar.* Construction and Building Materials, 2009. **23**(6): p. 2283-2290.
110. Koleva, D., et al., *Microstructural analysis of plain and reinforced mortars under chloride-induced deterioration.* Cement and concrete research, 2007. **37**(4): p. 604-617.
111. Beeldens, A., et al., *From microstructure to macrostructure: an integrated model of structure formation in polymer-modified concrete.* Materials and structures, 2005. **38**(6): p. 601-607.
112. Zeng, S., *Polymer modified cement: hydration microstructure and diffusion properties*. 1996, Aston University.
113. Baueregger, S., M. Perello, and J. Plank, *On the role of colloidal crystal-like domains in the film forming process of a carboxylated styrene-butadiene latex copolymer.* Progress in Organic Coatings, 2014. **77**(3): p. 685-690.
114. Ramli, M. and A.A. Tabassi, *Effects of polymer modification on the permeability of cement mortars under different curing conditions: a correlational study that includes pore distributions, water absorption and compressive strength.* Construction and Building Materials, 2012. **28**(1): p. 561-570.
115. Ohama, Y., *Polymer-based admixtures.* Cement and concrete composites, 1998. **20**(2-3): p. 189-212.
116. Bansal, P.P. and R. Sidhu, *Mechanical and durability properties of fluoropolymer modified cement mortar.* Structural engineering and mechanics: An international journal, 2017. **63**(3): p. 317-327.

117. Rozenbaum, O., R.-M. Pellenq, and H. Van Damme, *An experimental and mesoscopic lattice simulation study of styrene-butadiene latex-cement composites properties.* Materials and structures, 2005. **38**(4): p. 467-478.
118. Aggarwal, L., P. Thapliyal, and S. Karade, *Properties of polymer-modified mortars using epoxy and acrylic emulsions.* Construction and Building Materials, 2007. **21**(2): p. 379-383.
119. Li, Y.C., et al. *Study on Impermeability and Resistance to Sulfate Attack of Polymeric Sulphoaluminate Cement*. in *Key Engineering Materials*. 2009. Trans Tech Publ.
120. Luyckx, J., *Composites à fibres de carbone dans le génie civil*. 1999: Ed. Techniques Ingénieur.
121. Gherdaoui, M., *RENFORCEMENT DES OUVRAGES EN BETON ARME SOUMIS AUX ACTIONS GRAVITAIRES AVEC MATERIAUX COMPOSITES*. 2018.
122. Foo, S., N. Naumoski, and M. Saatcioglu, *Aléas sismiques, codes du bâtiment et opinions d'atténuation des risques pour les immeubles canadiens*. 2001: Bureau de la protection des infrastructures essentielles et de la protection ….
123. Elgabbas, F., et al., *Different CFRP strengthening techniques for prestressed hollow core concrete slabs: Experimental study and analytical investigation.* Composite Structures, 2010. **92**(2): p. 401-411.
124. Mosallam, A., *Strength and ductility of reinforced concrete moment frame connections strengthened with quasi-isotropic laminates.* Composites Part B: Engineering, 2000. **31**(6-7): p. 481-497.
125. Khalil, N. and J.J. Assaad, *Bond properties between smooth carbon fibre-reinforced polymer bars and ultra-high performance concrete modified with polymeric latexes and fibres.* European Journal of Environmental and Civil Engineering, 2021: p. 1-18.
126. Xu, F., et al., *Influences of polypropylene fiber and SBR polymer latex on abrasion resistance of cement mortar.* Journal of Wuhan University of Technology-Mater. Sci. Ed., 2010. **25**(4): p. 624-627.
127. Yang, J., R. Wang, and Y. Zhang, *Influence of dually mixing with latex powder and polypropylene fiber on toughness and shrinkage performance of overlay repair mortar.* Construction and Building Materials, 2020. **261**: p. 120521.
128. Cakir, F., *Evaluation of mechanical properties of chopped glass/basalt fibers reinforced polymer mortars.* Case Studies in Construction Materials, 2021. **15**: p. e00612.
129. Moreira, G., et al., *Effect of fiber reinforcement on mixed-mode fracture of polymer mortars.* Composite Structures, 2016. **141**: p. 179-183.
130. Reis, J., *Sisal fiber polymer mortar composites: Introductory fracture mechanics approach.* Construction and Building Materials, 2012. **37**: p. 177-180.
131. Nunes, L. and J. Reis, *Estimation of crack-tip-opening displacement and crack extension of glass fiber reinforced polymer mortars using digital image correlation method.* Materials & Design, 2012. **33**: p. 248-253.
132. Shafei, B., et al., *State-of-the-Art Review of Capabilities and Limitations of Polymer and Glass Fibers Used for Fiber-Reinforced Concrete.* Materials, 2021. **14**(2): p. 409.
133. Denzin Tonoli, G.H., et al., *Surface properties of eucalyptus pulp fibres as reinforcement of cement-based composites.* 2010.
134. Chiker, T., A.A. Belkadi, and S. Aggoun, *Physico-chemical and microstructural fire-induced alterations into metakaolin-based vegetable and polypropylene fibred mortars.* Construction and Building Materials, 2021. **276**: p. 122225.
135. Belkadi, A.A., et al., *Effect of vegetable and synthetic fibers on mechanical performance and durability of Metakaolin-based mortars.* Journal of adhesion science and Technology, 2018. **32**(15): p. 1670-1686.

136. Booya, E., et al., *Durability of cementitious materials reinforced with various Kraft pulp fibers.* Construction and Building Materials, 2018. **191**: p. 1191-1200.
137. Akinyemi, B.A. and A. Adesina, *Utilization of polymer chemical admixtures for surface treatment and modification of cellulose fibres in cement-based composites: a review.* Cellulose, 2021: p. 1-26.
138. De Azevedo, A.R., et al., *Technological Perspective for Use the Natural Pineapple Fiber in Mortar to Repair Structures.* Waste and Biomass Valorization, 2021: p. 1-15.
139. Candamano, S., et al., *Influence of acrylic latex and pre-treated hemp fibers on cement based mortar properties.* Construction and Building Materials, 2021. **273**: p. 121720.
140. Ferreira, S.R., et al., *The influence of carboxylated styrene butadiene rubber coating on the mechanical performance of vegetable fibers and on their interface with a cement matrix.* Construction and Building Materials, 2020. **262**: p. 120770.
141. Fidelis, M.E.A., et al., *The effect of accelerated aging on the interface of jute textile reinforced concrete.* Cement and Concrete Composites, 2016. **74**: p. 7-15.
142. Gallego, J.M., et al., *Fatigue behaviour at elevated temperature of RC slabs strengthened with EB CFRP strips.* Composites Part B: Engineering, 2018. **141**: p. 37-49.
143. Ahmed, A. and V. Kodur, *Effect of bond degradation on fire resistance of FRP-strengthened reinforced concrete beams.* Composites Part B: Engineering, 2011. **42**(2): p. 226-237.
144. Hajiloo, H., et al., *Fire tests on full-scale FRP reinforced concrete slabs.* Composite Structures, 2017. **179**: p. 705-719.
145. Yaqub, M. and C. Bailey, *Seismic performance of shear critical post-heated reinforced concrete square columns wrapped with FRP composites.* Construction and Building Materials, 2012. **34**: p. 457-469.
146. Yaqub, M. and C. Bailey, *Cross sectional shape effects on the performance of post-heated reinforced concrete columns wrapped with FRP composites.* Composite Structures, 2011. **93**(3): p. 1103-1117.
147. Roy, A., U. Sharma, and P. Bhargava, *Strengthening of heat damaged reinforced concrete short columns.* Journal of Structural Fire Engineering, 2014.
148. Haddad, R., N. Al-Mekhlafy, and A. Ashteyat, *Repair of heat-damaged reinforced concrete slabs using fibrous composite materials.* Construction and Building Materials, 2011. **25**(3): p. 1213-1221.
149. Haddad, R.H., R. Al-Rousan, and A. Almasry, *Bond-slip behavior between carbon fiber reinforced polymer sheets and heat-damaged concrete.* Composites Part B: Engineering, 2013. **45**(1): p. 1049-1060.
150. Danie Roy, A., U. Sharma, and P. Bhargava, *Bond properties of GFRP laminate with heat-damaged concrete.* Journal of Composites for Construction, 2016. **20**(2): p. 04015053.
151. Jadooe, A., R. Al-Mahaidi, and K. Abdouka, *Bond behavior between NSM CFRP strips and concrete exposed to elevated temperature using cement-based and epoxy adhesives.* Journal of Composites for Construction, 2017. **21**(5): p. 04017033.
152. Tajmir-Riahi, A., N. Moshiri, and D. Mostofinejad, *Inquiry into bond behavior of CFRP sheets to concrete exposed to elevated temperatures–Experimental & analytical evaluation.* Composites Part B: Engineering, 2019. **173**: p. 106897.
153. Nimafar, M., et al., *Use of bacteria externally for repairing cracks and improving properties of concrete exposed to high temperatures.* Crystals, 2021. **11**(12): p. 1503.
154. Santos-Ribeiro, D., et al., *Pulmonary arterial hypertension: Basic knowledge for clinicians.* Archives of cardiovascular diseases, 2016. **109**(10): p. 550-561.

155. Ardanuy, M., J. Claramunt, and R.D. Toledo Filho, *Cellulosic fiber reinforced cement-based composites: a review of recent research.*Construction and Building Materials, 2015. **79**: p. 115-128.
156. Sedan, D., et al., *Propriétés mécaniques de matériaux enchevêtrés à base de fibre de chanvre et matrice cimentaire.* 18ème Congrès Français de Mécanique (Grenoble 2007), 2007.
157. ASTM.C1437-20, *Standard Test Method for Flow of Hydraulic Cement Mortar,*. 2020, ASTM International, West Conshohocken, PA.
158. EN.196-1, *Methods of testing cement - Part 1: Determination of strength*. 2018.
159. Czarnecki, L. *Polymer-Concrete Composites for the repair of concrete structures*. in *MATEC Web of Conferences*. 2018. EDP Sciences.
160. Tchetgnia Ngassam, I.L., P. Arito, and H. Beushausen, *A new approach for the mix design of (patch) repair mortars.* African Journal of Science, Technology, Innovation and Development, 2018. **10**(3): p. 259-265.
161. Mirza, J., et al., *Preferred test methods to select suitable surface repair materials in severe climates.* Construction and Building Materials, 2014. **50**: p. 692-698.
162. Makani, J., et al., *Mortality in sickle cell anemia in Africa: a prospective cohort study in Tanzania.* PloS one, 2011. **6**(2): p. e14699.
163. EN.1015-18, *Methods of test for mortar for masonry : Determination of water absorption coefficient due to capillary action of hardened mortar*. 2002.
164. Felekoğlu, K.T., et al. *Influence of Styrene Acrylate and Styrene Butadiene Rubber on Fresh and Mechanical Properties of Cement Paste and Mortars*. in *7th Asian Symposium on Polymers in Concrete, ITU, İstanbul, Turkey*. 2012.
165. Chakraborty, S., et al., *Polymer modified jute fibre as reinforcing agent controlling the physical and mechanical characteristics of cement mortar.* Construction and Building Materials, 2013. **49**: p. 214-222.
166. Ukrainczyk, N. and A. Rogina, *Styrene–butadiene latex modified calcium aluminate cement mortar.*Cement and Concrete Composites, 2013. **41**: p. 16-23.
167. Soufi, A., *Etude de la durabilité des systèmes béton armé: mortiers de réparation en milieu marin*. 2013, Université de La Rochelle.
168. Baueregger, S., M. Perello, and J. Plank, *Impact of carboxylated styrene–butadiene copolymer on the hydration kinetics of OPC and OPC/CAC/AH: The effect of Ca2+ sequestration from pore solution.* Cement and Concrete Research, 2015. **73**: p. 184-189.
169. C1437-20, A., *Standard Test Method for Flow of Hydraulic Cement Mortar,*. 2020, ASTM International, West Conshohocken, PA.
170. Barluenga, G. and F. Hernandez-Olivares, *SBR latex modified mortar rheology and mechanical behaviour.* Cement and Concrete Research, 2004. **34**(3): p. 527-535.
171. Akinyemi, B., et al., *Innovative husk-crete building materials from rice chaff and modified cement mortars.* Acta Technol. Agric., 2020. **2**: p. 67-72.
172. Li, Q., et al., *Treatment methods for plant fibers for use as reinforcement in cement-based materials.* Cellulose, 2021: p. 1-12.
173. Wei, J. and C. Meyer, *Utilization of rice husk ash in green natural fiber-reinforced cement composites: Mitigating degradation of sisal fiber.* Cement and Concrete Research, 2016. **81**: p. 94-111.
174. Mármol, G., et al., *Portland cement, gypsum and fly ash binder systems characterization for lignocellulosic fiber-cement.* Construction and Building Materials, 2016. **124**: p. 208-218.

175. Wei, J., S. Ma, and G.T. D'Shawn, *Correlation between hydration of cement and durability of natural fiber-reinforced cement composites.* Corrosion Science, 2016. **106**: p. 1-15.
176. Parhizkar, T. and A. RAMEZANIANPOUR, *COMPARATIVE STUDY OF SEVERAL REPAIR MORTARS IN SIMULATED PERSIAN GULF CONDITIONS.*32 .2004 ,(2): p. 12-12.
177. Ban, Y., et al., *Preparation and Performance of Cement Mortar Reinforced by Modified Bamboo Fibers.* Polymers, 2020. **12**(11): p. 2650.
178. de Andrade Silva, F., et al., *Physical and mechanical properties of durable sisal fiber–cement composites.* Construction and building materials, 2010. **24**(5): p. 777-785.
179. Onuaguluchi, O. and N. Banthia, *Plant-based natural fibre reinforced cement composites: A review.* Cement and Concrete Composites, 2016. **68**: p. 96-108.
180. Afroughsabet, V., L. Biolzi, and P.J. Monteiro, *The effect of steel and polypropylene fibers on the chloride diffusivity and drying shrinkage of high-strength concrete.* Composites Part B: Engineering, 2018. **139**: p. 84-96.
181. Liuquan, Q., L. Dongxu, and L. Zongjin, *Effects of lignin cellulose and expansive agent on microstructure and macro-property of polymer-modified mortar containing fly ash.* Construction and Building Materials, 2009. **23**(6): p. 2467-2471.
182. Boondamnoen, O., et al., *EFFECT of blend ratio and compatibilizer on solution casted treated waste natural rubber latex/polystyrene blends.* Songklanakarin Journal of Science & Technology, 2013. **35**(5).
183. Biricik, H. and N. Sarier, *Comparative study of the characteristics of nano silica-, silica fume-and fly ash-incorporated cement mortars.* Materials Research, 2014. **17**: p. 570-582.
184. Betioli, A., et al., *Chemical interaction between EVA and Portland cement hydration at early-age.* Construction and Building Materials, 2009. **23**(11): p. 3332-3336.
185. Choi, S.-S. and C.E. Son, *Influence of silane coupling agent on bound rubber formation of NR/SBR blend compounds reinforced with carbon black.* Polymer Bulletin, 2016. **73**(12): p. 3453-3464.
186. Plank, J. and M. Gretz, *Study on the interaction between anionic and cationic latex particles and Portland cement.* Colloids and Surfaces A: Physicochemical and Engineering Aspects, 2008. **330**(2-3): p. 227-233.

BUILDING TRUST

NOTICE PRODUIT

SikaLatex®

Résine à mélanger à l'eau de gâchage des mortiers

INFORMATIONS SUR LE PRODUIT

SikaLatex® est une dispersion aqueuse de résine synthétique qui se présente sous la forme d'un liquide laiteux concentré.
Parfaitement miscible, il s'ajoute directement à l'eau de gâchage des mortiers de ciment.

DOMAINES D'APPLICATION

Enduits et chapes
- Barbotines pour accrochage des enduits et chapes de ciment.
- Enduits imperméables pour réservoirs et piscines d'eau douce et d'eau de mer.
- Chapes de haute résistance à l'usure même en présence d'eau : seuils sous vanne, radiers soumis à des efforts d'érosion.

Jointoiements
- Joints de maçonnerie durables et étanches.
- Joints de prédalles et de panneaux préfabriqués.

Rejointoiements et réparations
- Reprofilages et réparations d'épaufrures de béton, béton armé ou précontraint.

Travaux de finition de couverture
- Emburrures et crêtes de tuiles faîtières.
- Raccords d'enduits des maçonneries et solins de rives.
- Enduits de souches et solins.

Collages et durcissement des plâtres
- Collage par barbotine conformément au DTU 25.1
- Réalisation de plâtres durs et étanches.

Reprises de bétonnage
- Reprises entre coulées successives de béton par incorporation de SikaLatex® dans un mortier de liaison.

CARACTÉRISTIQUES / AVANTAGES

- Améliore fortement l'adhérence du mortier sur tout support, même lisse (béton, pierre, brique, métaux ferreux, verre et céramique),
- Rend le mortier plastique et facile à mettre en œuvre,
- Augmente les résistances à la traction,
- Limite le risque de fissuration,
- Améliore l'imperméabilisation,
- Améliore la dureté de surface,
- Réduit l'usure et le poussiérage.

SikaLatex® conserve ses qualités, même en milieu humide ou en immersion.
SikaLatex® est compatible avec tous les ciments, la chaux et le plâtre.

AGRÉMENTS / NORMES

PV CNEBB DTEM: 157/2016.

DESCRIPTION DU PRODUIT

Conditionnement	Bidons de 1 kg, 5 kg et 10 kg Fût de 210 kg
Aspect / Couleur	Liquide laiteux
Durée de Conservation	Dans son emballage d'origine intact : • 12 mois pour les sachets et les bidons • 18 mois pour les cartons
Conditions de Stockage	A l'abri du gel et d'une chaleur excessive.

BUILDING TRUST

NOTICE PRODUIT

Sika MonoTop® SF-126

Mortier de réparation fibré prêt à gâcher à base de fumée de silice

INFORMATIONS SUR LE PRODUIT

Sika MonoTop® SF-126 est mortier hydraulique monocomposant fibré à base de ciment, charges spéciales, fumée de silice et adjuvants pour la réparation des bétons soumis à des atmosphères agressives avec inhibiteurs de corrosion.
Après gâchage à l'eau, on obtient un mortier de couleur gris clair.
Épaisseur d'application par couche varie de 3 à 100 mm.

DOMAINES D'APPLICATION

- Réparation des bétons armés exposés à des milieux agressifs (sites industriels, bord de mer, montagne).
- Réparation d'épaufrures d'ouvrages d'art (ponts, barrages, etc).
- Réparation d'épaufrures d'ouvrages de génie civil (silos, réservoirs, écluses, etc).
- Réparation d'épaufrures de bâtiments.
- Réparation de nids de poule (sols industriels, ateliers, garages).
- Pour la remise en état du béton, comme mortier de réparation, sur supports en béton, en pierre et en mortier. Spécialement indiqué pour l'application en surplomb et sur les surfaces verticales pour la réparation d'éléments sous charges statiques et dynamiques.

CARACTÉRISTIQUES / AVANTAGES

- Mise en oeuvre simple et aisée.
- Bonne adhérence sur béton, mortier, brique, pierre.
- Applicable sur des épaisseurs de 3 à 100 mm par passe.
- Excellente imperméabilité.
- Excellent comportement au retrait.
- Excellente tenue au gel et aux sels de déverglaçage.
- Excellente résistance aux sulfates et aux eaux de mer.
- Très bonne protection du béton armé contre les environnements agressifs.
- Contient des inhibiteurs de corrosion.

AGRÉMENTS / NORMES

Classe R4 selon la norme EN NF 1504-3.
PV CNERIB: DTEM: 187/2015.

DESCRIPTION DU PRODUIT

Conditionnement	Sac de 25 kg
Durée de Conservation	12 mois
Conditions de Stockage	En emballage d'origine non entamé, stocké à des températures entre +5 °C et +25 °C. Protéger de l'humidité.
Aspect / Couleur	Gris
Granulométrie maximale	0 à 1,6 mm

INFORMATIONS TECHNIQUES